REPORT DOCUMENTATION PAGE

1. Recipient's Reference	2. Originator's Reference	3. Further Reference	4. Security Classification of Document
	AGARD-R-745	ISBN 92-835-0346-4	UNCLASSIFIED

5. Originator Advisory Group for Aerospace Research and Development
North Atlantic Treaty Organization
7 rue Ancelle, 92200 Neuilly sur Seine, France

6. Title APPLICATION OF MODIFIED LOSS AND DEVIATION CORRELATIONS TO TRANSONIC AXIAL COMPRESSORS

7. Presented at

8. Author(s)/Editor(s) M.Çetin, A.Ş.Üçer, Ch.Hirsch and G.K.Serovy

9. Date November 1987

10. Author's/Editor's Address Various

11. Pages 74

13. Keywords/Descriptors

Axial flow compressors
Transonic flow
Performance tests
Prediction
Correlation

14. Abstract

This report is the outcome of the AGARD Project of Support to Turkey No.T15, on 'Losses and Deviation in Turbomachines', performed in 1982—1986, in which Belgium, the United States and Turkey were involved. The project was initiated from the work of the AGARD Propulsion and Energetics Panel Working Group 12 on 'Through Flow Calculations in Axial Turbomachines', which resulted in the AGARD Advisory Report AR 175, published in October 1981.

The goal of this report was to analyse the transonic compressor tests available in the open literature and to propose possible improvements in total loss and turning correlations From the work performed six conclusions could be drawn for the achievement of better loss predictions. A comparison with results of a two-stage compressor showed that the results of the new correlation set were satisfactory. For more accurate predictions a consistent end-wall boundary layer and secondary loss calculation method must be applied; in multi-stage compressors, spanwise loss mixing procedures must be used.

AGARD Report No.745
Advisory Group for Aerospace Research and Development, NATO
APPLICATION OF MODIFIED LOSS AND DEVIATION CORRELATIONS TO TRANSONIC AXIAL COMPRESSORS
by M.Çetin, A.Ş.Üçer, Ch.Hirsch and G.K.Serovy
Published November 1987
74 pages

This report is the outcome of the AGARD Project of Support to Turkey No.T15, on 'Losses and Deviation in Turbomachines', performed in 1982—1986, in which Belgium, the United States and Turkey were involved. The project was initiated from the work of the AGARD Propulsion and Energetics Panel Working Group 12 on

P.T.O.

AGARD-R-745

Axial flow compressors
Transonic flow
Performance tests
Prediction
Correlation

AGARD Report No.745
Advisory Group for Aerospace Research and Development, NATO
APPLICATION OF MODIFIED LOSS AND DEVIATION CORRELATIONS TO TRANSONIC AXIAL COMPRESSORS
by M.Çetin, A.Ş.Üçer, Ch.Hirsch and G.K.Serovy
Published November 1987
74 pages

This report is the outcome of the AGARD Project of Support to Turkey No.T15, on 'Losses and Deviation in Turbomachines', performed in 1982—1986, in which Belgium, the United States and Turkey were involved. The project was initiated from the work of the AGARD Propulsion and Energetics Panel Working Group 12 on

P.T.O.

AGARD-R-745

Axial flow compressors
Transonic flow
Performance tests
Prediction
Correlation

AGARD Report No.745
Advisory Group for Aerospace Research and Development, NATO
APPLICATION OF MODIFIED LOSS AND DEVIATION CORRELATIONS TO TRANSONIC AXIAL COMPRESSORS
by M.Çetin, A.Ş.Üçer, Ch.Hirsch and G.K.Serovy
Published November 1987
74 pages

This report is the outcome of the AGARD Project of Support to Turkey No.T15, on 'Losses and Deviation in Turbomachines', performed in 1982—1986, in which Belgium, the United States and Turkey were involved. The project was initiated from the work of the AGARD Propulsion and Energetics Panel Working Group 12 on

P.T.O.

AGARD-R-745

Axial flow compressors
Transonic flow
Performance tests
Prediction
Correlation

AGARD Report No.745
Advisory Group for Aerospace Research and Development, NATO
APPLICATION OF MODIFIED LOSS AND DEVIATION CORRELATIONS TO TRANSONIC AXIAL COMPRESSORS
by M.Çetin, A.Ş.Üçer, Ch.Hirsch and G.K.Serovy
Published November 1987
74 pages

This report is the outcome of the AGARD Project of Support to Turkey No.T15, on 'Losses and Deviation in Turbomachines', performed in 1982—1986, in which Belgium, the United States and Turkey were involved. The project was initiated from the work of the AGARD Propulsion and Energetics Panel Working Group 12 on

P.T.O.

AGARD-R-745

Axial flow compressors
Transonic flow
Performance tests
Prediction
Correlation

'Through Flow Calculations in Axial Turbomachines', which resulted in the AGARD Advisory Report AR 175, published in October 1981.

The goal of this report was to analyse the transonic compressor tests available in the open literature and to propose possible improvements in total loss and turning correlations. From the work performed six conclusions could be drawn for the achievement of better loss predictions. A comparison with results of a two-stage compressor showed that the results of the new correlation set were satisfactory. For more accurate predictions a consistent end-wall boundary layer and secondary loss calculation method must be applied; in multi-stage compressors, spanwise loss mixing procedures must be used.

ISBN 92-835-0346-4

'Through Flow Calculations in Axial Turbomachines', which resulted in the AGARD Advisory Report AR 175, published in October 1981.

The goal of this report was to analyse the transonic compressor tests available in the open literature and to propose possible improvements in total loss and turning correlations. From the work performed six conclusions could be drawn for the achievement of better loss predictions. A comparison with results of a two-stage compressor showed that the results of the new correlation set were satisfactory. For more accurate predictions a consistent end-wall boundary layer and secondary loss calculation method must be applied; in multi-stage compressors, spanwise loss mixing procedures must be used.

ISBN 92-835-0346-4

'Through Flow Calculations in Axial Turbomachines', which resulted in the AGARD Advisory Report AR 175, published in October 1981.

The goal of this report was to analyse the transonic compressor tests available in the open literature and to propose possible improvements in total loss and turning correlations. From the work performed six conclusions could be drawn for the achievement of better loss predictions. A comparison with results of a two-stage compressor showed that the results of the new correlation set were satisfactory. For more accurate predictions a consistent end-wall boundary layer and secondary loss calculation method must be applied; in multi-stage compressors, spanwise loss mixing procedures must be used.

ISBN 92-835-0346-4

'Through Flow Calculations in Axial Turbomachines', which resulted in the AGARD Advisory Report AR 175, published in October 1981.

The goal of this report was to analyse the transonic compressor tests available in the open literature and to propose possible improvements in total loss and turning correlations. From the work performed six conclusions could be drawn for the achievement of better loss predictions. A comparison with results of a two-stage compressor showed that the results of the new correlation set were satisfactory. For more accurate predictions a consistent end-wall boundary layer and secondary loss calculation method must be applied; in multi-stage compressors, spanwise loss mixing procedures must be used.

ISBN 92-835-0346-4

ERRATUM

Page iv

The reference number of the AGARD Lecture Series entitled "Engine Airframe Integration for Rotorcraft" (June 1986) should be LS 148 and not as printed.

AGARD-R-745

AGARD

ADVISORY GROUP FOR AEROSPACE RESEARCH & DEVELOPMENT

7 RUE ANCELLE 92200 NEUILLY SUR SEINE FRANCE

AGARD REPORT No.745

Application of Modified Loss and Deviation Correlations to Transonic Axial Compressors

NORTH ATLANTIC TREATY ORGANIZATION

DISTRIBUTION AND AVAILABILITY
ON BACK COVER

AGARD-R-745

NORTH ATLANTIC TREATY ORGANIZATION

ADVISORY GROUP FOR AEROSPACE RESEARCH AND DEVELOPMENT, Paris.

(ORGANISATION DU TRAITE DE L'ATLANTIQUE NORD)

AGARD Report No.745

APPLICATION OF MODIFIED LOSS AND DEVIATION CORRELATIONS TO TRANSONIC AXIAL COMPRESSORS

by

M.Çetin, A.Ş.Üçer, Ch.Hirsch and G.K.Serovy

This Report was sponsored by the Propulsion and Energetics Panel of AGARD.

THE MISSION OF AGARD

According to its Charter, the mission of AGARD is to bring together the leading personalities of the NATO nations in the fields of science and technology relating to aerospace for the following purposes:

— Recommending effective ways for the member nations to use their research and development capabilities for the common benefit of the NATO community;

— Providing scientific and technical advice and assistance to the Military Committee in the field of aerospace research and development (with particular regard to its military application);

— Continuously stimulating advances in the aerospace sciences relevant to strengthening the common defence posture;

— Improving the co-operation among member nations in aerospace research and development;

— Exchange of scientific and technical information;

— Providing assistance to member nations for the purpose of increasing their scientific and technical potential;

— Rendering scientific and technical assistance, as requested, to other NATO bodies and to member nations in connection with research and development problems in the aerospace field.

The highest authority within AGARD is the National Delegates Board consisting of officially appointed senior representatives from each member nation. The mission of AGARD is carried out through the Panels which are composed of experts appointed by the National Delegates, the Consultant and Exchange Programme and the Aerospace Applications Studies Programme. The results of AGARD work are reported to the member nations and the NATO Authorities through the AGARD series of publications of which this is one.

Participation in AGARD activities is by invitation only and is normally limited to citizens of the NATO nations.

Published November 1987

ISBN 92-835-0346-4

Set and printed by Specialised Printing Services Limited
40 Chigwell Lane, Loughton, Essex IG10 3TZ

RECENT PUBLICATIONS OF THE PROPULSION AND ENERGETICS PANEL

Conference Proceedings

Testing and Measurement Techniques in Heat Transfer and Combustion
AGARD Conference Proceedings No.281, 55th *A* Meeting, May 1980

Centrifugal Compressors, Flow Phenomena and Performance
AGARD Conference Proceedings No.282, 55th *B* Meeting, May 1980

Turbine Engine Testing
AGARD Conference Proceedings No.293, 56th Meeting, Sep/October 1980

Helicopter Propulsion Systems
AGARD Conference Proceedings No.302, 57th Meeting, May 1981

Ramjets and Ramrockets for Military Applications
AGARD Conference Proceedings No.307, 58th Meeting, October 1981

Problems in Bearings and Lubrication
AGARD Conference Proceedings No.323, 59th Meeting, May/June 1982

Engine Handling
AGARD Conference Proceedings No.324, 60th Meeting, October 1982

Viscous Effects in Turbomachines
AGARD Conference Proceedings No.351, 61st *A* Meeting, June 1983

Auxiliary Power Systems
AGARD Conference Proceedings No.352, 61st *B* Meeting, May 1983

Combustion Problems in Turbine Engines
AGARD Conference Proceedings No.353, 62nd Meeting, October 1983

Hazard Studies for Solid Propellant Rocket Motors
AGARD Conference Proceedings No.367, 63rd *A* Meeting, May/June 1984

Engine Cyclic Durability by Analysis and Testing
AGARD Conference Proceedings No.368, 63rd *B* Meeting, May/June 1984

Gears and Power Transmission Systems for Helicopters and Turboprops
AGARD Conference Proceedings No.369, 64th Meeting October 1984

Heat Transfer and Cooling in Gas Turbines
AGARD Conference Proceedings No.390, 65th Meeting, May 1985

Smokeless Propellants
AGARD Conference Proceedings No.391, 66th *A* Meeting, September 1985

Interior Ballistics of Guns
AGARD Conference Proceedings No.392, 66th *B* Meeting, September 1985

Advanced Instrumentation for Aero Engine Components
AGARD Conference Proceedings No.399, 67th Meeting, May 1986

Engine Response to Distorted Inflow Conditions
AGARD Conference Proceedings No.400, 68th *A* Meeting, September 1986

Transonic and Supersonic Phenomena in Turbomachines
AGARD Conference Proceedings No.401, 68th *B* Meeting, September 1986

Advanced Technology for Aero Engine Components
AGARD Conference Proceedings No.421, 69th Meeting, September 1987

Working Group Reports

Aircraft Fire Safety
AGARD Advisory Report 132, Vol.1 and Vol.2. Results of WG11 (September and November 1979)

Turbulent Transport Phenomena (in English and French)
AGARD Advisory Report 150. Results of WG 09 (February 1980)

Through Flow Calculations in Axial Turbomachines
AGARD Advisory Report 175. Results of WG 12 (October 1981)

Alternative Jet Engine Fuels
AGARD Advisory Report 181. Vol.1 and Vol.2. Results of WG 13 (July 1982)

Suitable Averaging Techniques in Non-Uniform Internal Flows
AGARD Advisory Report 182 (in English and French). Results of WG 14 (June/August 1983)

Producibility and Cost Studies of Aviation Kerosines
AGARD Advisory Report 227. Results of WG 16 (June 1985)

Performance of Rocket Motors with Metallized Propellants
AGARD Advisory Report 230. Results of WG 17 (September 1986)

Lecture Series

Non-Destructive Inspection Methods for Propulsion Systems and Components
AGARD LS 103 (April 1979)

The Application of Design to Cost and Life Cycle Cost to Aircraft Engines
AGARD LS 107 (May 1980)

Microcomputer Applications in Power and Propulsion Systems
AGARD LS 113 (April 1981)

Aircraft Fire Safety
AGARD LS 123 (June 1982)

Operation and Performance Measurement of Engines in Sea Level Test Facilities
AGARD LS 132 (April 1984)

Ramjet and Ramrocket Propulsion Systems for Missiles
AGARD LS 136 (September 1984)

3-D Computation Techniques Applied to Internal Flows in Propulsion Systems
AGARD LS 140 (June 1985)

Engine Airframe Integration for Rotorcraft
AGARD LS ~~150~~ 148 (June 1986)

Design Methods Used in Solid Rocket Motors
AGARD LS 150 (April 1987)

Other Publications

Airbreathing Engine Test Facility Register
AGARD AG 269 (July 1981)

Rocket Altitude Test Facility Register
AGARD AG 297 (March 1987)

Manual for Aeroelasticity in Turbomachines
AGARD AG 298/1 (March 1987)

PREFACE

This report is the outcome of AGARD Support Project T15. The support programme of AGARD to Southern Flank Nations started in 1981, its purpose being to set-up cooperation among member nations and thereby improve the capabilities of Southern Flank Countries in the field of aerospace research and development. The programme is intended to provide assistance to member nations for the purpose of increasing their scientific and technical potential.

Project T15 was initiated from the work of Working Group 12 of the AGARD Propulsion and Energetics Panel (PEP). The work was mainly conducted in the Mechanical Engineering Department of the Middle East Technical University (METU), with the technical support of Vrije Universiteit Brussel, Belgium and Iowa State University, USA.

The authors would like to thank the National Delegates of the countries involved, the members of the Propulsion and Energetics Panel, the Turkish Aircraft Industries (TUSAŞ) for their support in the initial phase of the project, and the Turkish Scientific and Technical Research Council. The members of the Fluid Mechanics Group (METU, Mech. Eng. Dept.) who took part in this project on various occasions are acknowledged.

* * *

Le présent rapport s'inscrit dans la suite logique du Projet de Support T15 de l'AGARD. Le programme de support AGARD aux Nations du Flanc Sud date de 1981. Le but du programme est de promouvoir une coopération parmi les nations membres de l'OTAN et d'améliorer les potentialités des Pays du Flanc Sud dans le domaine de la recherche et des réalisations aérospatiales. Le programme doit servir d'aide aux nations membres de l'OTAN, et leur permettre d'accroître leurs capacités scientifiques et techniques.

Le projet T15 résulte des travaux du Panel de Propulsion et d'Energétique de l'AGARD (PEP). L'essentiel du travail s'est effectué au sein de la Faculté de Génie Mécanique du Middle East Technical University (METU), avec le support technique du Vrije Universiteit, Bruxelles, Belgique et du Iowa State University, USA.

Les auteurs tiennent à remercier les Délégués Nationaux des différents pays concernés, les membres du Panel de Propulsion et d'Energétique, et les Industries turques de l'Aéronautique (TUSAŞ) pour leur support lors de la phase initiale du projet, ainsi que le Conseil National de la Recherche Scientifique et Technique de la Turquie.

La contribution des membres du Groupe de la Dynamique des Fluides (METU Mech. Eng. Dept,) qui ont participé au projet à plusieurs reprises est également très appréciée.

PROPULSION AND ENERGETICS PANEL

Chairman: Dr William L.MacMillan
Project Manager
EHF Communication Satellite
Defence Research Establishment
Ottawa, Ontario K1A 0Z4
Canada

Deputy Chairman: Ing. Principal de l'Armement Philippe Ramette
Direction des Recherches, Etudes et
Techniques — Pièce 512
26 Boulevard Victor
75996 Paris Armées
France

EDITORS

M.Çetin
Turkish Scientific and Research Council
(TUBITAK-BAE)
Atatürk Bulvarı 221
Ankara, Turkey

A.Ş.Üçer
Middle East Technical University
O D T Ü
Makina Muh. Bölümü
Ankara, Turkey

Ch.Hirsch
Vrije Universiteit Brussel
Dienst Stromingsmechanica
Pleinlaan 2
1050 Brussel, Belgium

G.K.Serovy
Anson Marston Distinguished Professor
Dept. of Mechanical Engineering
3038 ME/ESM
Iowa State University
Ames, Iowa 50011, United States

PANEL EXECUTIVE

Dr-Ing. E.Riester
AGARD-NATO
7 rue Ancelle
92200 Neuilly sur Seine
France

CONTENTS

APPLICATION OF MODIFIED LOSS AND DEVIATION CORRELATIONS TO TRANSONIC AXIAL COMPRESSORS

by

M.Çetin, A.Ş.Üçer, Ch.Hirsch and G.K.Serovy

1. INTRODUCTION

Throughflow calculation programs are probably the most important tool of the compressor aerodynamic designer. The main objective of a throughflow calculation is to provide a spanwise prediction of thermodynamic and other flow variables so that suitable blade profiles can be selected to cope with the variations of inlet angle, turning, Mach number, etc. Throughflow programs may be either of analysis or design type. In the former, which is more extensively used, the blade geometry is specified and solutions are sought for the resulting flow pattern. The design method, which is less commonly available, requires enthalpy variations and obtains solutions for meridional velocity and hence flow angles. To determine realistic solutions with both techniques it is necessary to provide reasonably well predicted entropy gradients resulting from viscous effects. Similarly, the solution obtained from an analysis program is very dependent upon the predicted values of blade exit flow angles. Once loss and deviation models have been incorporated into a program it can be used to predict overall machine performance.

Continuation of improvements in throughflow analysis programs and in the empirical correlations necessary for them has become one of the interests of the AGARD Propulsion and Energetics Panel. The Panel organized a Specialist Meeting in 1977 on "Throughflow Calculations in Axial Turbomachinery". A Working Group (WG 12) was subsequently formed on "Throughflow Calculations in Turbomachinery". This group started work in January 1978 and published its report in 1981. A part of this report is devoted to the work of the WG 12 compressor subgroup. The task of the compressor subgroup was to review many aspects of compressor correlations. As a result of this work it was concluded that no set of correlations has general validity, and this was especially emphasized for the validity of off-design correlations. This conclusion was reached for both loss and deviation correlation. As general recommendations of the Working Group it was stated that:

(a) Care should be taken to define a constant set of relations within the correlations in order to avoid the duplication of effects and influence of parameters.

(b) Notwithstanding the continuous development of three dimensional viscous flow calculations and the increase of computing power of digital computers, it is not likely that through flow calculations in multistage machines will be replaced by full viscous calculations in the near future. Therefore the need for reliable correlations will continue to be of great importance.

(c) The general trends with regard to the influence of parameters (such as Mach number) are of particular interest. A particular effort in this direction should be made, especially for off-design cases.

It was with the above conclusions and recommendations that further work on loss and deviation correlations was proposed. The purpose was to use transonic compressor test results of the 1970s for reassessing the loss and deviation correlations. Comparison of the experimental results with the existing correlations was foreseen. It was expected either to correct or modify the existing correlations or to develop new correlations for the off-design prediction.

As the first step of the present investigation, existing loss correlations were reviewed and put into table form, which it is hoped will be useful for users. In the table a consistent set of notation is used and the relevant tables and figures are listed with their number as stated in the reference from which the correlation is adopted. The table is given in Appendix II with the notation used in the table of Appendix I, together with cascade terminology. Appendix II lists the equations used in different correlations together with the calculation procedure. The range of applicability of each correlation is also stated in the remarks section.

Suitable data reported in a number of NASA and Pratt & Whitney compressor tests were analysed to obtain consistent trends which might result in new correlations. During this process an off-design loss correlation was obtained for transonic upstream Mach numbers. Design incidence correlation by NASA for plane cascades was modified for transonic upstream conditions and design deviation angle prediction of Carter's was corrected. More successful comparisons were obtained from modified and new correlations when their results were compared with those of the other loss and deviation methods. No consistent experimental data was found at the transonic upstream conditions for off-design deviation angle assessment. Hence several off-design deviation correlations were examined and it is concluded that the correlation given by Creveling is most successful.

Section 3 of this report discusses the methodology used in data analysis and comparison. The set of correlations which was set up during the course of this study is programmed and fed into a finite-element throughflow code. The correlations were tested by predicting the details of the spanwise variation of total loss, deviation angle, axial velocity and density. The test case

used for this purpose was a two-stage fan. A listing of the loss and deviation subroutine which may be adapted to other throughflow programs is given in Appendix IV.

It must be noted that in all multi-stage performance prediction calculations the computation goes off-design if an inaccurate prediction of deviation for an upstream blade row is made. Therefore, a computer code should calculate design and off-design loss and deviations simultaneously at all times.

2. TEST DATA USED FOR CORRELATION STUDIES

2.1 General

The search for test data of transonic compressor stages which might be used for loss and deviation assessment work revealed eight useful data sets (references [1] to [8]). These tests were carried out in the test facilities of the NASA Lewis Research Center and the Pratt & Whitney Aircraft Company. Test reports include aerodynamic design parameters, blade element geometry, and blade element performance as well as overall performance of blade rows. Some of the necessary blade element data was lacking in the test reports prepared by Pratt & Whitney Aircraft Company. The first five test reports were the results of a research program on axial flow fans conducted by NASA Lewis Research Center. All data which was used in this work was obtained from compressor stages designed using 1970's technology. The annulus areas of these compressors varied over a large range, with tip diameters ranging between 0.25 m and 0.41 m and hub diameters ranging between 0.125 m and 0.15 m. Blade elements used were either Multiple-Circular-Arc (MCA) or Double-Circular-Arc (DCA) type. All rotors were equipped with part-span vibration dampers. For more information the reader can refer to references [1] to [8].

2.2 Test Procedure and Data Uncertainty

Since the main objective of the work was to investigate off-design behaviour, blade element performance data from stall to choke conditions should be available.

The details of the test facilities are given in references [1] to [8]. In all tests from which the experimental data had been obtained and used in this investigation, the following test procedure was employed.

The compressor rotor was set to a predetermined rotational speed, which corresponds to the required blade velocity Mach number component. The sleeve valve located in the collector at the downstream of the compressor stage was then adjusted. Each flow condition created by closing the sleeve valve (increase of back pressure) established a new flow field within the compressor, and hence it was possible to obtain incidence angle changes with the associated changes in total pressure loss coefficient and deviation angle. This procedure was repeated in the unchoked region until the stall point was reached. The sleeve valve adjustment was repeated for several rotational speed settings. Passage survey measurements were made at 9, 11 or 16 radial positions, depending on the test, ranging from 5% ro 95% span, for a number of rotational speeds and back pressures. Data were recorded downstream of rotor and stator blade rows and upstream from the stage.

At each radial position total pressure, static pressure, total temperature, and flow angle were measured. At the downstream of the stator circumferential measurements of total pressure, temperature and flow angle were performed. Mass and energy averaging procedures were applied to these circumferential measurements. Axial and radial velocities and flow angles were obtained from the mass-averaged properties. Data recorded at the measuring stations were modified to give blade leading and trailing edge conditions using theoretical considerations. More information on the analysis procedures can be obtained from the relevant references [1] to [8].

The calculation of total loss coefficient in references [1] to [8] is accomplished through the equation below

$$\bar{\omega}_T = \frac{(P_{02})_{id} - P_{02}}{P_{01} - P_1} \tag{2.1}$$

$(P_{02})_{id}$ is equal to P_{01} in the case of stator blade rows, and total loss coefficient can readily be calculated from the averaged values of the measured data. However, for rotors $(P_{02})_{id}$ is the summation of P_{01} and the stagnation pressure rise due to the radius change along the streamline. Thus equation 2.1 is modified to

$$\bar{\omega}_T = \left\{\left(\frac{P_{02}}{P_{01}}\right) - \left(\frac{P_{02}}{P_{01}}\right)\right\} \left\{\frac{1}{1 - \left[1 \Big/ \left(1 + \frac{\gamma - 1}{2}(M_{01})^2\right)\right]^{\gamma/\gamma - 1}}\right\} \tag{2.2}$$

where

$$\left(\frac{P_{02}}{P_{01}}\right)_{id} = \left\{1 + \frac{\gamma + 1}{2} \frac{(\omega r_2)^2}{\gamma g R T_{01}}\left[1 - \left(\frac{r_1}{r_2}\right)^2\right]\right\}^{\gamma/\gamma - 1} \tag{2.3}$$

Equation 2.3 implies that rothalpy remains constant along a streamline. In calculating the rotor total loss, equation 2.2 is used and it is assumed that the real streamlines coincide with the design streamlines. Measured properties P_{01}, P_{02}, T_{01} and ω together with the approximated value of r_2 are used to calculate $\bar{\omega}_T$. The error made in the calculation of $\bar{\omega}_T$ largely depends on how well the value of r_2 is approximated. The effect of the measurement uncertainties on P_{01}, P_{02}, T_{01}, which are tabulated in Appendix II, are used and propagated through equation 2.2 for calculating the amount of percentage uncertainty on $\bar{\omega}_T$. In this calculation it is assumed that the streamline is exactly passing through the radii tabulated in the test reports. The uncertainty in the radii is estimated as $\pm$ 0.33 mm from reference [40]. As the next step the uncertainty in the value of r_2 is sought. It is concluded that including the bias error corresponding to $\pm$ 0.5 mm probe mispositioning relative to the actual streamline a total uncertainty interval of $\pm$ 1.86% is expected on $\bar{\omega}_T$. Although streamline mispositioning error should be more of a bias type this cannot be detected in the experimental minimum total losses, since the minimum total loss values do not show a distinct bias when compared with Koch and Smith results (Fig. 3.10). As for the off-design total loss variations a consistent expected trend is detected with angle of incidence. Thus it is concluded that the error imposed on $\bar{\omega}_T$ due to streamline mislocation is not of serious order. The details of the calculations are given in Appendix III. Due to the lack of data used in averaging procedures, the uncertainty analysis for data reduction was not possible. The uncertainties in the angle measurements are tabulated in Appendix III.

3. METHODOLOGY OF DATA ANALYSIS

3.1 Overall Loss Correlation

Transonic decelerating flow in the turbomachine is one of the most complex flows which can be found in fluid mechanics. This is because a large number of factors affect the flow regime and therefore influence the magnitude of losses. The complexity is overwhelming because of the fact that the effects of several loss producing factors are not independent, but are cumulative and interrelated. A well known example is the shock-boundary layer interaction. In the presence of such an interaction the order of magnitude of profile loss is closely related to the strength of the shock wave as well as its location on the blade surface. The losses at the end walls are due to the interactive phenomena between blade boundary layers, end-wall boundary layers, passage shock-waves, leakage flow and secondary flow effects. It may be quite unrealistic to single out a loss source, find a loss coefficient for it from experimental work, and then add these linearly for sections along the blade span where the particular loss under consideration is of importance. The equations which govern the entropy accumulation are highly nonlinear, thus loss assessment using superposition is not likely to be realistic.

In the present study, due to the difficulties arising from accurate assessment of interaction of loss factors, loss sources are not separately identified. Instead, the data is analysed so as to determine whether there are some meaningful trends in the variation of total loss coefficients with flow and cascade geometry parameters. Losses are considered as a whole and expressed by a total pressure loss coefficient which accounts for all types of losses except the blockage effects of end wall boundary layers and clearance flows. This approach is advantageous for performance estimation because the combined effect of profile, shock and secondary flow losses are accounted for simultaneously whereas assessment of loss sources separately leads to a superposition type of synthesis which is in many cases unrealistic and imposes some unverified assumptions.

In this work total losses are considered in two parts. The first part is the minimum loss produced in the blade row, which corresponds to the minimum loss incidence; the second part being the loss increase when angle of incidence is not equal to the value of minimum loss incidence.

3.2 Variation of Total Loss with Angle of Incidence

The first step was to plot the data as the total loss versus incidence, and seek a variation of total loss with incidence which has a detectable minimum near the zero incidence. This kind of curve, which is referred to as loss characteristic of a blade section, can only be obtained if the incidence is changed over a wide range, so that a meaningful variation of total loss can be detected. A variation in angle of incidence can only be obtained if the test compressor back pressure is changed at constant speed. The number of tests that are available in the open literature having data suitable for off-design analysis is limited. Although a variation of weight flow is expected with a change of back pressure at unchoked flow, this variation is quite small. Thus it is possible to obtain different flow regimes by changing the rotational speed and back pressure independently. The plots of total loss with angle of incidence for stator blade rows exhibit results similar to the sample given in figure 3.1. As it is clearly seen it is rather difficult to indicate the minimum loss point from such data. The test reports also mention as a conclusion that for stator the minimum loss range extends 8° around the minimum loss point which is rather a large range. Thus the flatness of the loss characteristic around the minimum loss directly affects the process of determining the minimum loss incidence. Therefore all stator data were excluded from the analysis and rotor data were used for the basis of design and off-design total loss analysis. Some of the loss characteristics of the rotors also exhibited variations of $\bar{\omega}_T$ with i which does not allow definition of a rational minimum loss point. In these circumstances the data were not used.

Six sample loss characteristic are given in figures 3.2 to 3.7. The samples are chosen from three different spanwise locations. The first three samples are for DCA blading and the remainder are for MCA blading. The blade element section parameters and cascade geometry are given in each figure. There was difficulty in finding the variation of total loss with incidence for a given blade and cascade geometry at a single constant inlet mach number. Therefore, as is seen in the sample figures, inlet Mach numbers corresponding to the data points are presented as intervals. The Mach number range for each curve is narrow enough to assign an arithmetic mean Mach number value for each curve.

It was a formidable task requiring careful observation of the curve trend and engineering intuition to fit curves to the data points and fix the minimum loss point of each curve. This process gave the minimum loss incidence i^*_{exp} and $\bar{\omega}^*_{exp}$ values. Since the main objective was to find off-design correlation for transonic blade sections, it was decided to check whether both experimental minimum loss and experimental minimum loss incidence can or can not be determined using existing correlations.

3.3 Minimum Loss Incidence Prediction

It is well known and can be seen very clearly from figures 3.2 to 3.7 that minimum loss incidence angle prediction is one of the most important issues for the assessment of off-design performance. It is essential to predict an accurate value for this incidence.

The incidence angle can be measured from blade suction surface or from mean camber line (see Appendix I). It was found convenient to use incidence angle definition referenced to the mean camber line, in accordance with NASA incidence angle correlations. However, it is always possible to convert the angle of incidence based on suction surface i_{ss} into the one based on mean camber line i, if the geometry of the leading edge is known.

The minimum loss design incidence angle correlation presented in NASA SP-36 [9] covers a wide range of parameters which were carefully examined for subsonic flow regimes in two dimensional cascades. NASA minimum loss incidence angle correlations also cover corrections for three-dimensional rotor cascades against relative inlet Mach number for DCA and NACA 65-(A10) series blade profiles.

Since the compressor test data used in this investigation included 3-D effects it was decided to compare the NASA-2D prediction with the experimentally determined i^*_{exp} values. Figure 3.8 shows the variation of $i^*_{exp} - i^*_{2D\text{-}NASA}$ with inlet Mach number. The figure shows that $i^*_{exp} - i^*_{2D\text{-}NASA}$ is less for MCA blades than for DCA blades. The other observation from the figure is that, for both types of blade profiles, the difference increases with inlet Mach number. Straight lines are fitted separately through the data points of DCA and MCA blades. The following equations are obtained for correcting the NASA-2D minimum loss incidence prediction.

For DCA blade profiles

$$i^*_{COR} - i^*_{2D} = 0.7238M_1 + 7.5481 \tag{3.1}$$

For MCA blade profiles

$$i^*_{COR} - i^*_{2D} = 1.3026M_1 + 5.7380 \tag{3.2}$$

where i^*_{COR} in the above equations is the corrected value of minimum loss incidence. Figure 3.9 shows a comparison of NASA-3D minimum loss incidence angle prediction method and the presently modified NASA-2D method. A random sampling of a number of DCA profiles operating at different flow conditions have shown that the NASA 3-D prediction is close to the present prediction around inlet Mach number 1.0. However, at low and high Mach numbers, the discrepancy between the present prediction method and NASA-3D predictions increases to as much as 60%. The correction applied to NASA-2D correlation in reference [9] for 3-D effects and inlet Mach number exhibits no Mach number influence between inlet Mach number 0.25 and 0.55. The correction then increased with inlet Mach number. This increase continues approximately between inlet Mach numbers 0.55 and 0.95. The 3-D cascades used to derive the NASA-3D correlation were probably choked at inlet Mach number 0.95. Thus, a constant value of correction is indicated. It can therefore be argued that the variation of correction between inlet Mach numbers ~ 0.6 and ~ 1.0 is not the same as it is established in this work. This leads to a discrepancy in i* predictions for M_1 values less than 1.0 in Figure 3.9. For inlet Mach numbers greater than 1.0, the NASA correction is no longer valid. In the present analysis 3-D and Mach number effects cannot be separated.

3.4 Design Total Loss Prediction

As it is mentioned above, the minimum loss points of the experimental loss characteristics are fixed by fitting curves to the available test points present at an approximately constant inlet Mach number. These fixed minimum loss values are then compared with the existing design loss prediction methods which include corrections for transonic effects. The comparison between experimental and calculated total losses using different prediction methods can be seen in Figure 3.10. Four different design loss prediction methods are used. Koch and Smith [17], Swan [16], Dettmering [34], Jansen and Moffatt [18]. A number of calculations have suggested that the method proposed by Koch and Smith is the most satisfactory one in determining the design loss for transonic cascades. This method in fact is the most complete one, accounting for many parameters such as stream tube contraction, blade surface roughness, etc. The method uses an equivalent sand roughness term in the calculation of profile losses which affects the profile loss magnitude. It is concluded in [17] that an accurate assessment of profile loss can only be obtained by the evaluation of surface roughness with utmost care.

3.5 Off-Design Total Loss Prediction

The work described above on the prediction of minimum total loss $\bar{\omega}^*_T$ and minimum loss incident i* showed that the experimentally obtained values of these quantities can be determined with less error using the correct form of NASA-2D correlation for minimum loss incidence angle Koch and Smith correlation for minimum total loss.

The experimental loss characteristics were then replotted as $(\bar{\omega}_T - \bar{\omega}^*_T)$ v. $(i - i^*)$, keeping in mind that i^* and $\bar{\omega}^*_T$ can be determined from the above mentioned correlations. Initially the loss characteristics for MCA and DCA blade profiles were replotted on the same $(\bar{\omega}_T - \bar{\omega}^*_T)$ v. $(i - i^*)$ plane. It was then realised that there are observable differences in the slopes of the characteristics for MCA and DCA blades. It was therefore concluded that the magnitude of losses depends on the profile shape. The plots are repeated separately in Figures 3.11 and 3.12 for MCA and DCA blade profiles respectively. The origin in these figures, $(\bar{\omega}_T - \bar{\omega}^*_T) = 0$ and $(i - i^*) = 0$, corresponds to experimentally determined values of minimum loss and minimum loss incidence.

The figures show that at off-design incidences the total loss parameter $\bar{\omega}^*_T$ depends largely on the inlet Mach number. Although cascade geometrical variables such as solidity, camber angle, maximum thickness, etc., influence to a large extent the minimum loss $\bar{\omega}^*_T$, no systematic influence of the cascade geometrical parameters on the off-design loss can be detected.

A comparison between the off-design losses for DCA and MCA blades showed that the losses produced by DCA type of blading are higher compared to MCA type of blading. This is because, for MCA type of blading, camber angle and blade thickness are smaller at the enterence region, thus providing lower suction surface Mach numbers just ahead of the passage shock for a given range of Mach number.

A careful examination of the data points shows a very consistent inlet Mach number dependence at the negative values of $(i - i^*)$. As the inlet Mach number increases at a constant negative value of $(i - i^*)$ the total off-design loss increases. On the right hand side of $(i - i^*) = 0$, Mach number dependence is not very distinct because of the large scatter of data points. However, the increase of off-design loss with inlet Mach number can still be detected if least square fits are applied to data points.

It should once more be strongly emphasised that the experimental data points in Figures 3.11 and 3.12 are for MCA and DCA airfoil sections with a large range of cascade geometries. The ranges of solidity, camber angle, stagger angle, and maximum thickness to chord ratio are indicated in the figures. This indeed shows that the inlet Mach number and the type of blading are the two strong governing factors in determining off-design losses at transonic speeds.

Data for $(i - i^*) < 0$ and $(i - i^*) > 0$ are treated separately. The available data for each inlet Mach number are used for least-squares fit to a function in the form $\bar{\omega}_T - \bar{\omega}_T^* = c_m(i - i^*)^n$. A large number of trials revealed that curves with exponent n equal to 2 give the best fit to the data points for all inlet Mach numbers at both sides of the origin. Thus $\bar{\omega}_T - \bar{\omega}_T^* = c_m(i - i^*)^2$ is chosen and values of c_m for all inlet Mach numbers are determined. The fitted curves are shown in Figures 3.13 and 3.14 for multiple circular arc and double circular arc blades respectively.

The relations between inlet Mach number and the coefficient c_m are given by Figures 3.15 and 3.16. Figure 3.15 shows the variation of c_m with inlet Mach number for MCA blade profiles. The variation can be approximated by a straight line. A straight line is fitted to the data points using least square curve fitting technique. The slope of the straight line for $(i - i^*) < 0$ is greater than that of $(i - i^*) > 0$. This means that for negative incidences the total loss increases faster with Mach number at off-design. The same trend can also be seen from Figure 3.16 for DCA blade profiles. Double circular arc profiles exhibit higher off-design losses at the same inlet Mach numbers compared to the MCA blades. Variation of c_m with inlet Mach number is given by the equations given in Table 1.

The equations in Table together with the modified NASA-2D correlation for minimum loss incidence and Koch & Smith design loss correlation may be used to predict the off-design loss performance of blade sections for design and performance prediction purposes. For calculating the total pressure loss coefficient for a given blade and cascade geometry, inlet flow direction and inlet Mach number one can proceed as follows:

Table 1 Variation of Coefficient c_m with inlet Mach Number
Base equation $\bar{\omega}_T - \bar{\omega}_T^* = c_m(i - i^*)^2$, $M_1 \geqslant 0.5$

Type of Blade Profile	$(i - i^*)$	Equation
MCA	< 0	$c_m = 0.02845M_1 - 0.01741$
	> 0	$c_m = 0.00363M_1 - 0.00065$
DCA	< 0	$c_m = 0.05336M_1 - 0.02937$
	> 0	$c_m = 0.00500M_1 - 0.00075$

1. Calculate the minimum (design) loss coefficient $\bar{\omega}_T^*$ using Koch & Smith [17] correlation.
2. Calculate minimum loss incidence i^* using modified NASA-2D correlation (see Section 3.3)
3. Calculate the value of coefficient c_m from the equations given in Table 1.
4. Calculate off-design loss-coefficient from

$$\bar{\omega}_T = \bar{\omega}_T^* + c_m(i - i^*)^2 .$$

Equation 3.3 can also be used to estimate stall and choke angle of incidences if they are taken as the incidences, where the losses are twice their minimum values. Equation 3.3 can now be written in the form

$$i_{st,ch} = i^* + \left(\frac{\bar{\omega}_T^*}{c_m}\right)^{1/2} \tag{3.4}$$

where c_m can be obtained from Table 1. The value of c_m for predicting stall incidence is obtained from equations given for $(i - i^*) > 0$, whereas for choke incidence, equations for $(i - i^*) < 0$ are used. The values of i^* and $\bar{\omega}_T^*$ are calculated from modified NASA-2D and Koch & Smith correlations.

3.6 Verification of the Total Loss Correlation Set

The four off-design correlations of Creveling et al. [19], Swan [16], Howell [20] and Jansen & Moffatt [18] are used to predict the off-design loss and the results are compared with the measured values of $(\bar{\omega}_T - \bar{\omega}_T^*)$. For these calculations samples are taken arbitrarily from different blade profiles, cascade geometry and upstream conditions. Figures 3.17 to 3.20 show these comparisons. From the figures it may be concluded that, although a slight under-prediction exists, the best prediction is made by Swan's off-design correlation. The large over predicted values by Howell's correlation are attributed to the wrong assessment of fluid angles at design and off-design operations, and to the lack of any corrections for Mach number effects. The overpredictions seen in Jansen & Moffatt off-design loss calculations are most probably due to the errors in assessing the stall and choke angle of incidences. Creveling's off-design loss prediction method is more successful compared to the above two. The discrepancies from the experimental values are attributed to the non-continuous variation off-design loss correction with inlet Mach number. Swan's correlation is more successful since it accounts for the momentum thickness change with the inlet Mach number.

Figure 3.21 shows a comparison of the experimental off-design loss and the off-design loss predicted by the new correlation. It is clearly seen that the new off-design correlation predicts the off design losses most satisfactorily. The results are condensed around the one to one correspondence line with a low degree of scatter.

Two other verification calculations are also performed by using the new loss correlation set. The loss coefficient, including design and off-design parts, is calculated for a number of blade and cascade geometries and inlet conditions. The calculated loss coefficients are then compared with the corresponding experimental values. The first comparison is given in Figure 3.22. This figure is obtained from sample operating conditions selected arbitrarily among the data used for obtaining the new correlation set. The figure shows the variation of percent deviation of the calculated value from that of the experimental, with inlet Mach number. It is clearly seen that there is no bias with regard to either inlet Mach number or the shape of the blade. All points fall inside ± 30% deviation from the experimental value. The range of incidence angles of the data points presented in Figure 3.22 is between − 3 and + 15 degrees. The second check for the new correlation set was made by utilising the unused data. Percent deviation of calculated loss coefficient from experimental value is plotted against inlet Mach number in Figure 3.23. A larger deviation is expected, since this data was not used in the correlation assessment work due to the large scatter. The data points with higher percent deviations mostly belong to the near stall operating conditions. The figure shows that about 60% of the data points fall inside the ± 30% deviation band.

3.7 Design Deviation Angle Correlation

The data available in references [1] to [8] were used for deviation angle correlation assessment. Measured deviations were plotted against angle of incidence for the prescribed inlet Mach number ranges. A large number of such plots were made for stators and rotors at various spanwise locations [40]. The result of careful inspection of all the plots showed that the effect of angle of incidence on deviation angle does not show any consistent trend. A sample plot is shown in Figure 3.24. No influence of the Mach number was also seen. For rotor blade elements a slightly increasing trend of deviation angle with positive incidence is detected in some of the tests. However, it was not possible to detect this rise for stator blade sections. Therefore, a single deviation angle was calculated from the arithmetic mean of the data points of different inlet Mach numbers and incidence angles of the known cascade geometry. It was then decided to compare these mean deviation angles with the deviation angles calculated from correlations [42]. Figure 3.25 shows the comparison of these mean measured deviation angles with the deviation angles calculated from Carter's rule. The figure implies that Carter's rule underestimates the deviation angle to some extent, especially at the higher deviation values. In Figure 3.26 a similar comparison for NASA/NACA deviation is given. This correlation is better in predicting the experimental deviations obtained from the compressor tests with a larger scatter. In Figures 3.25 and 3.26 data points for both MCA and DCA blades exist. Since a more consistent trend is observed in the discrepancy between measured and calculated values with Carter's rule, a correction to the Carter's rule is obtained by fitting a least square second order curve to the data points, as follows:

$$\delta^* = -1.099379 + 3.0186\delta^*_{CAR} - 0.1988\delta^{*2}_{CAR} \tag{3.5}$$

The discrepancy between δ^*_{CAR} and δ^*, and therefore the required correction can be attributed to the transonic and 3-D effects which can not be separated in the present analysis. The value of coefficient m in Carter's rule was obtained by assuming circular arc mean camber line. The comparison of modified Carter's rule and experimental mean deviations is shown in Figure 3.27.

3.8 Off-Design Deviation Angle Correlation

Since no consistent off-design deviation angle data could be extracted from the available compressor tests, it was decided to use throughflow calculations for the assessment of the best off-design deviation correlation. For this purpose, off-design deviation angle correlations proposed by Jansen & Moffatt [18], Swan [16], Creveling [19] and Howell [20] were evaluated. Systematic test runs were performed for determining the most successful off-design deviation calculation technique. As a result of these calculations Creveling's off-design evaluation method is found more successful than the others. It must be noted that some convergence problems were experienced during the computations performed by correlations other than Creveling's more detailed information with regard to the computations given in Section 4.

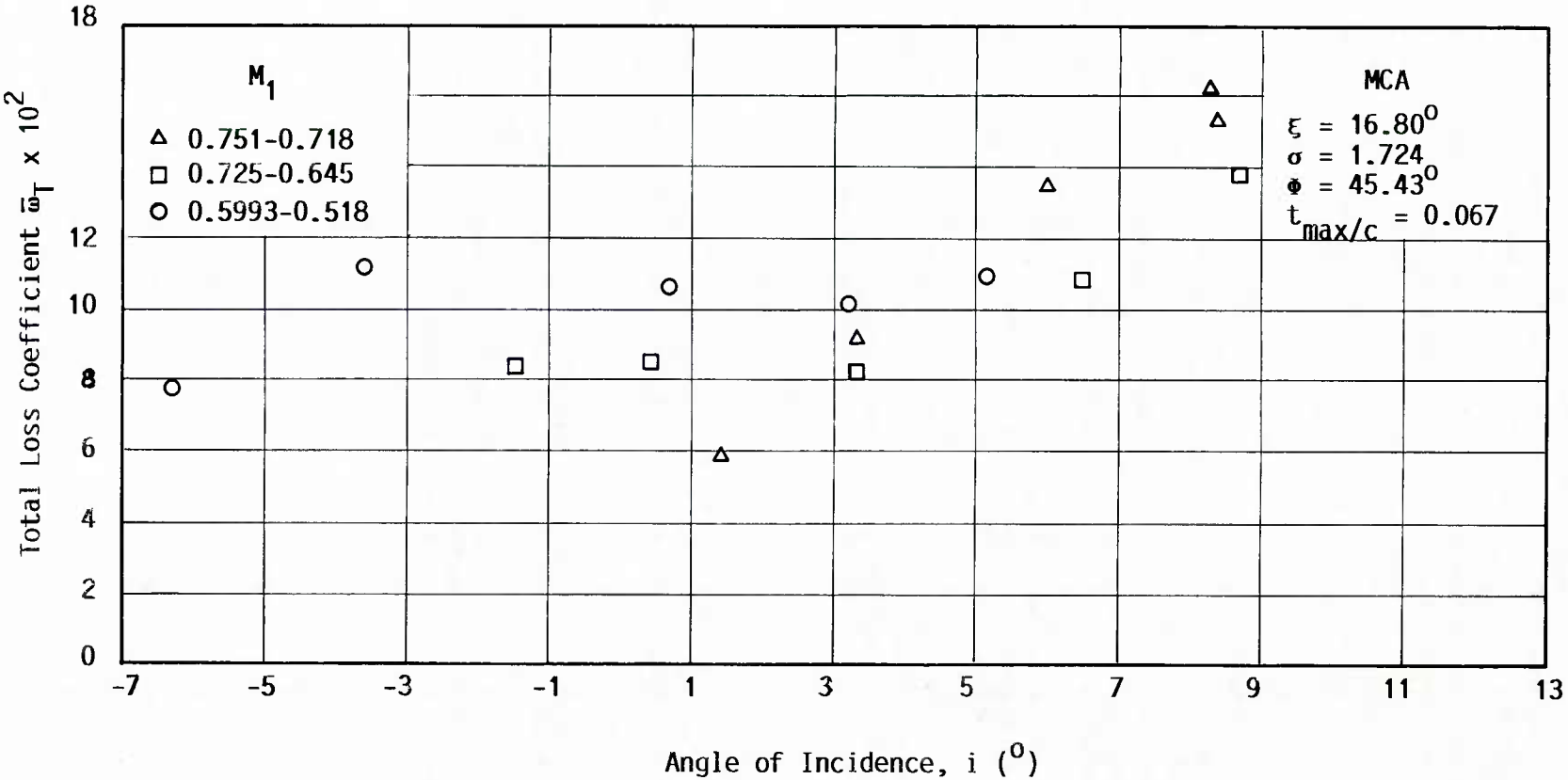

Figure 3.1 Loss Characteristic of a Sample Blade Element Section (70 % Span)

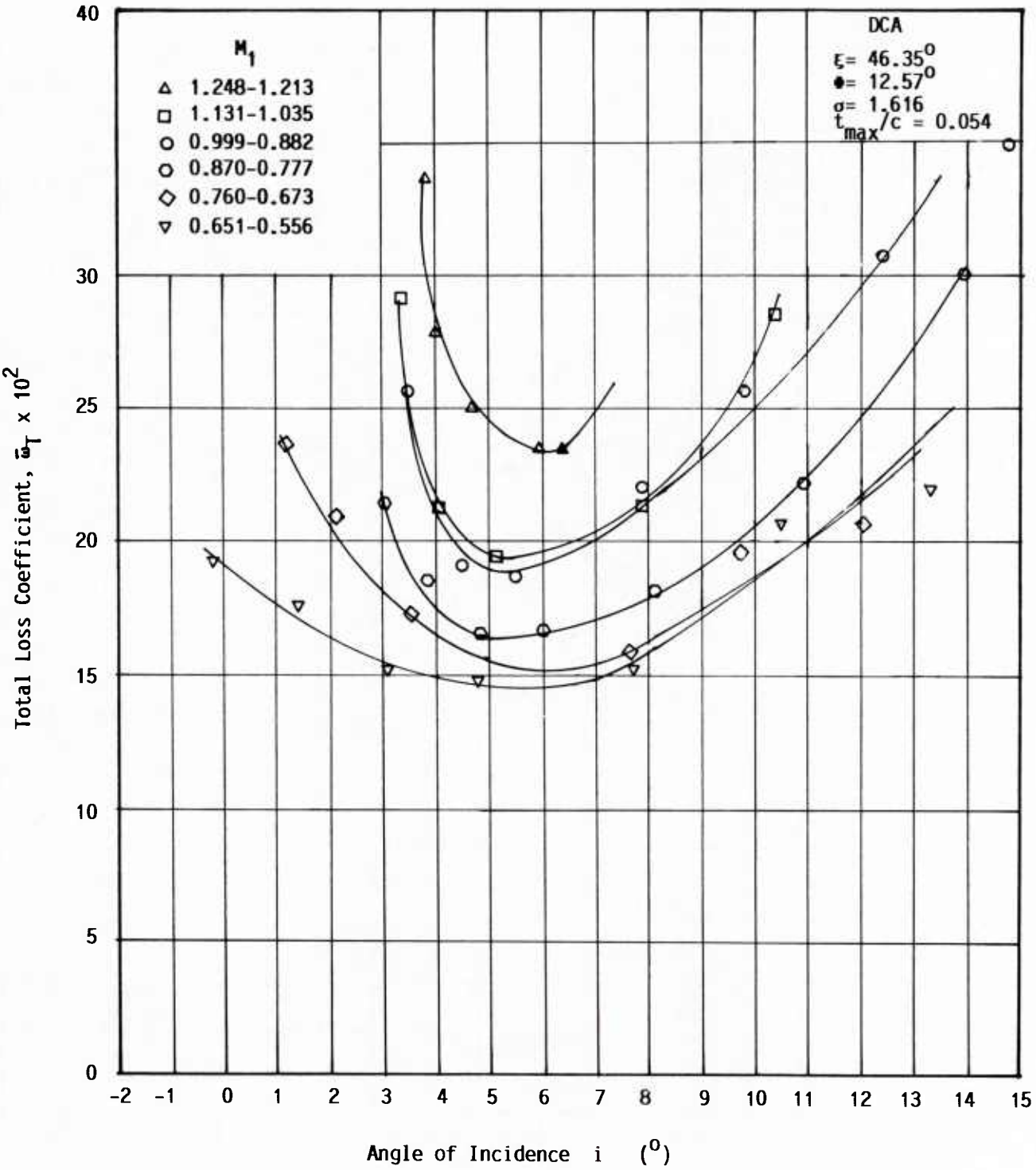

Figure 3.2 Variation of Total Losses with Incidence (42.5 % Span)

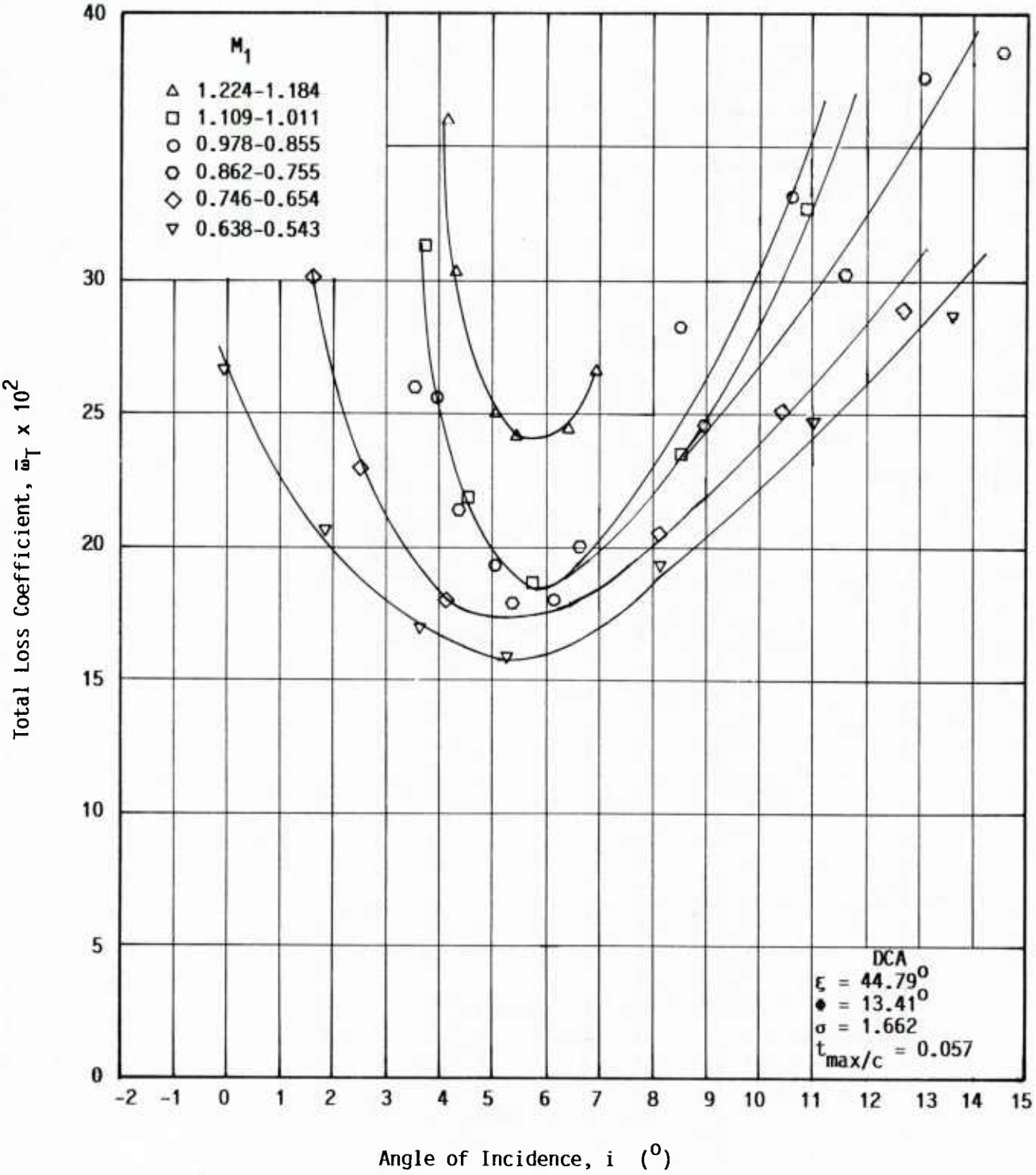

Figure 3.3 Variation of Total Losses with Incidence (47.5 % Span)

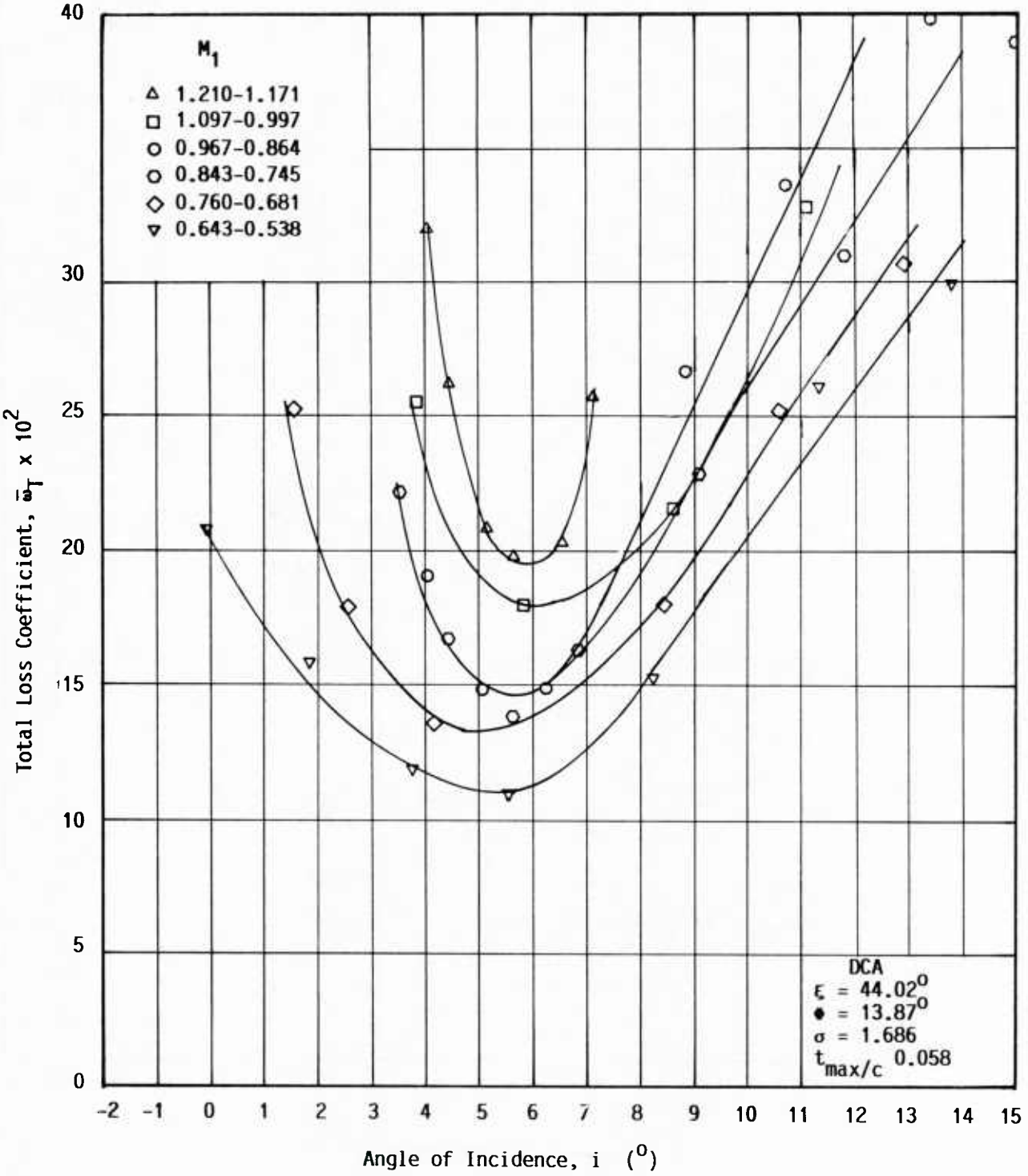

Figure 3.4 Variation of Total Losses with Incidence (50 % Span)

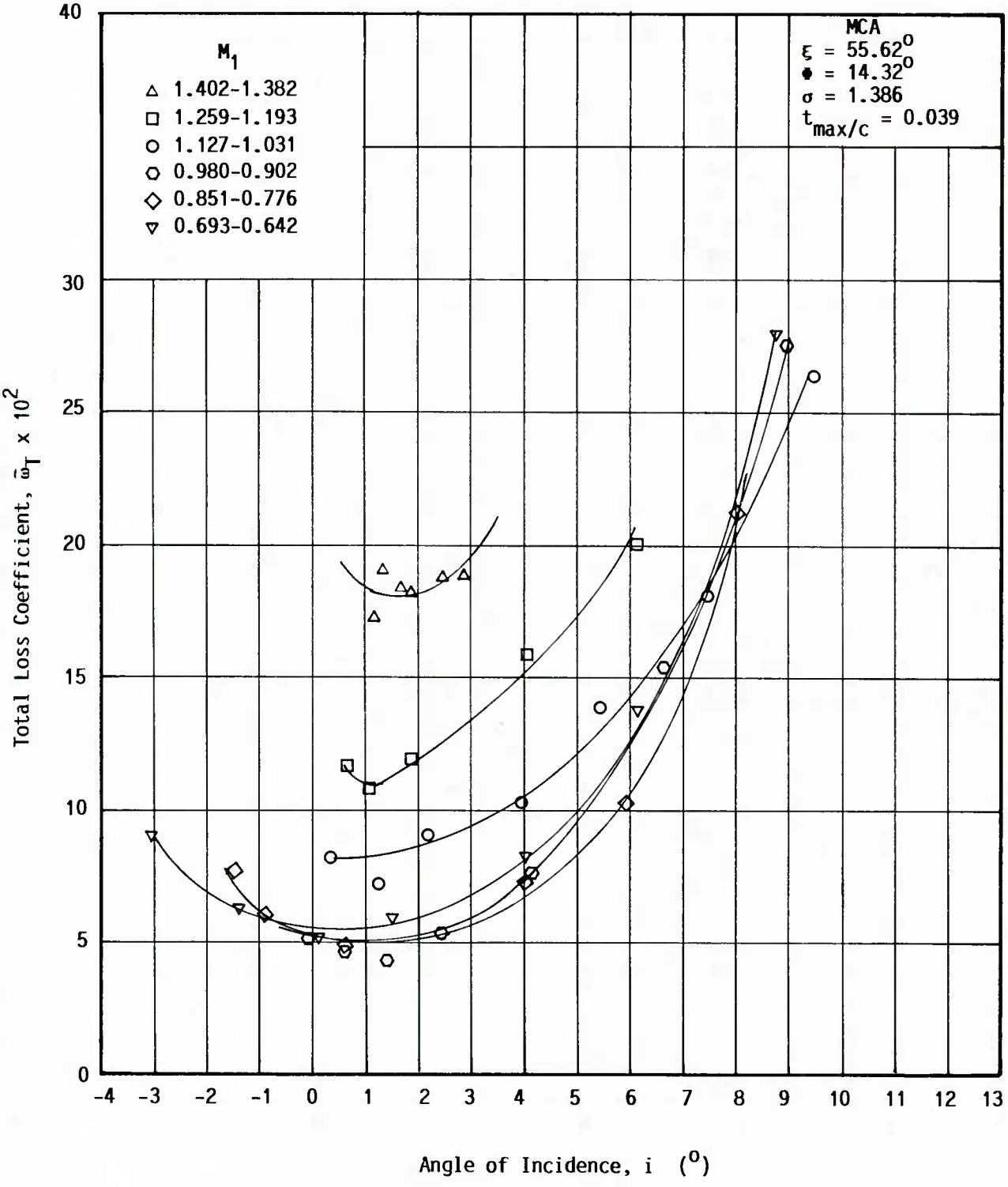

Figure 3.5 The Variation of Total Losses with Incidence (10 % Span)

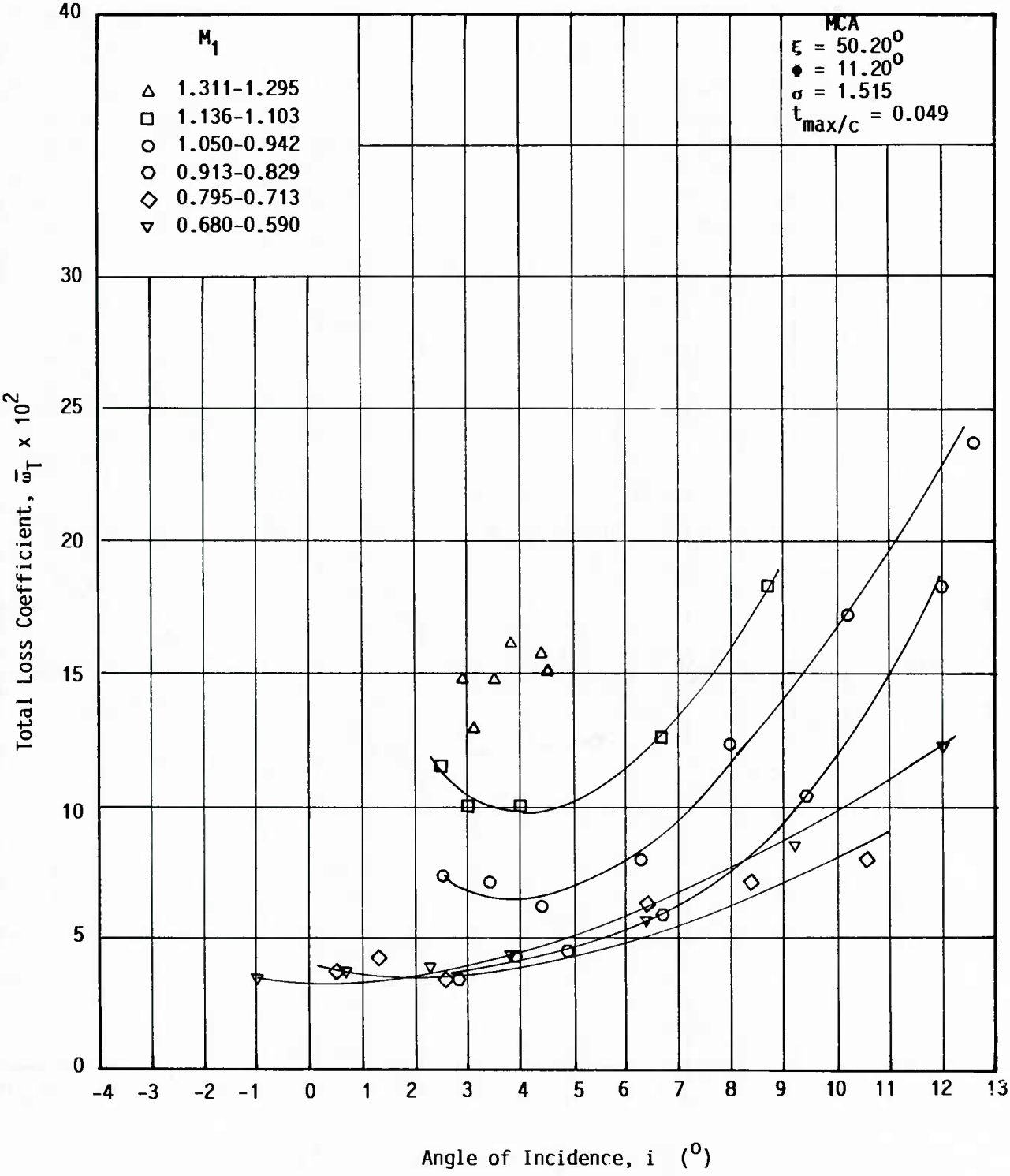

Figure 3.6 The Variation of Total Losses with Incidence (30 % Span)

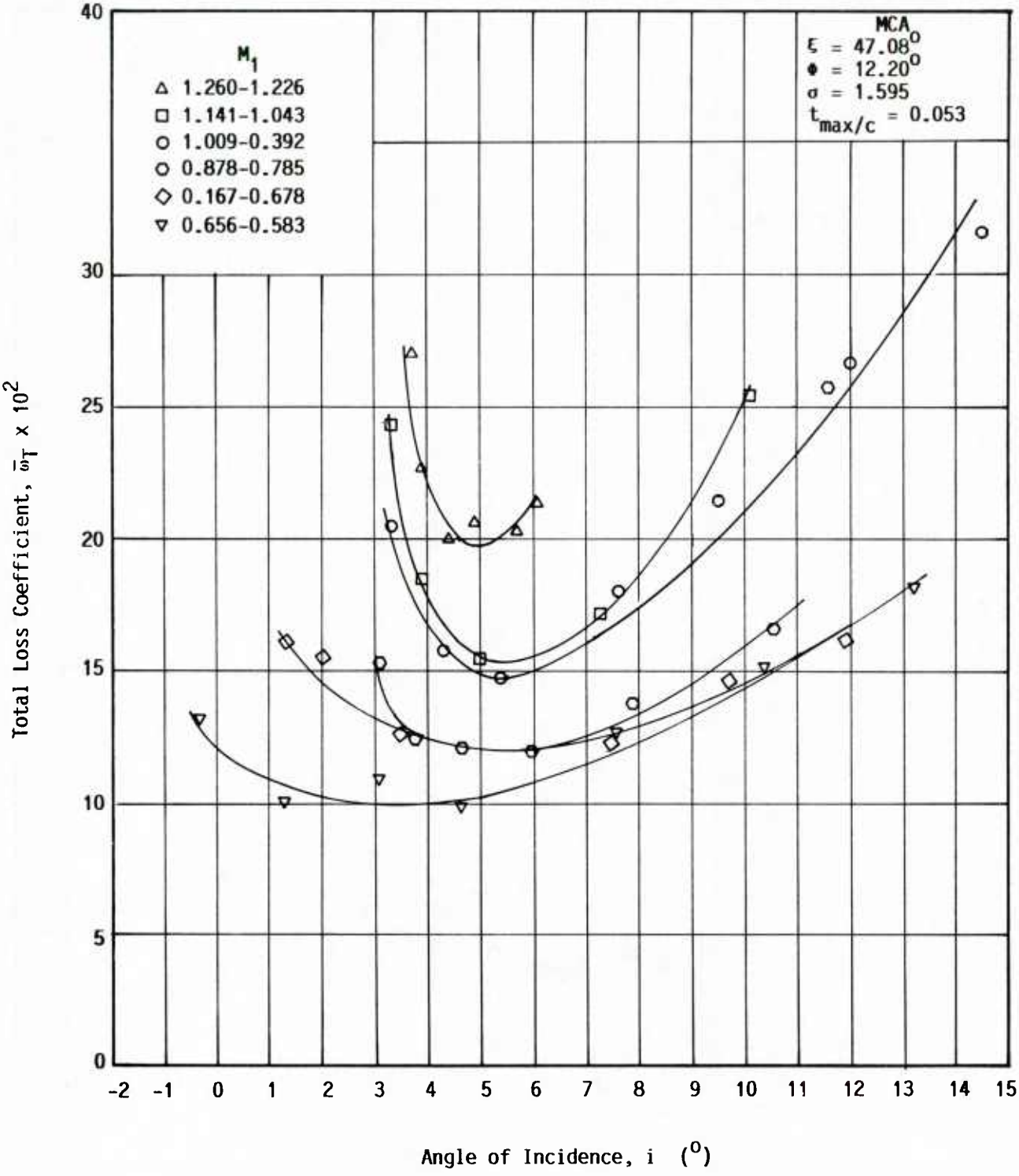

Figure 3.7 The Variation of Total Losses with Incidence (40 % Span)

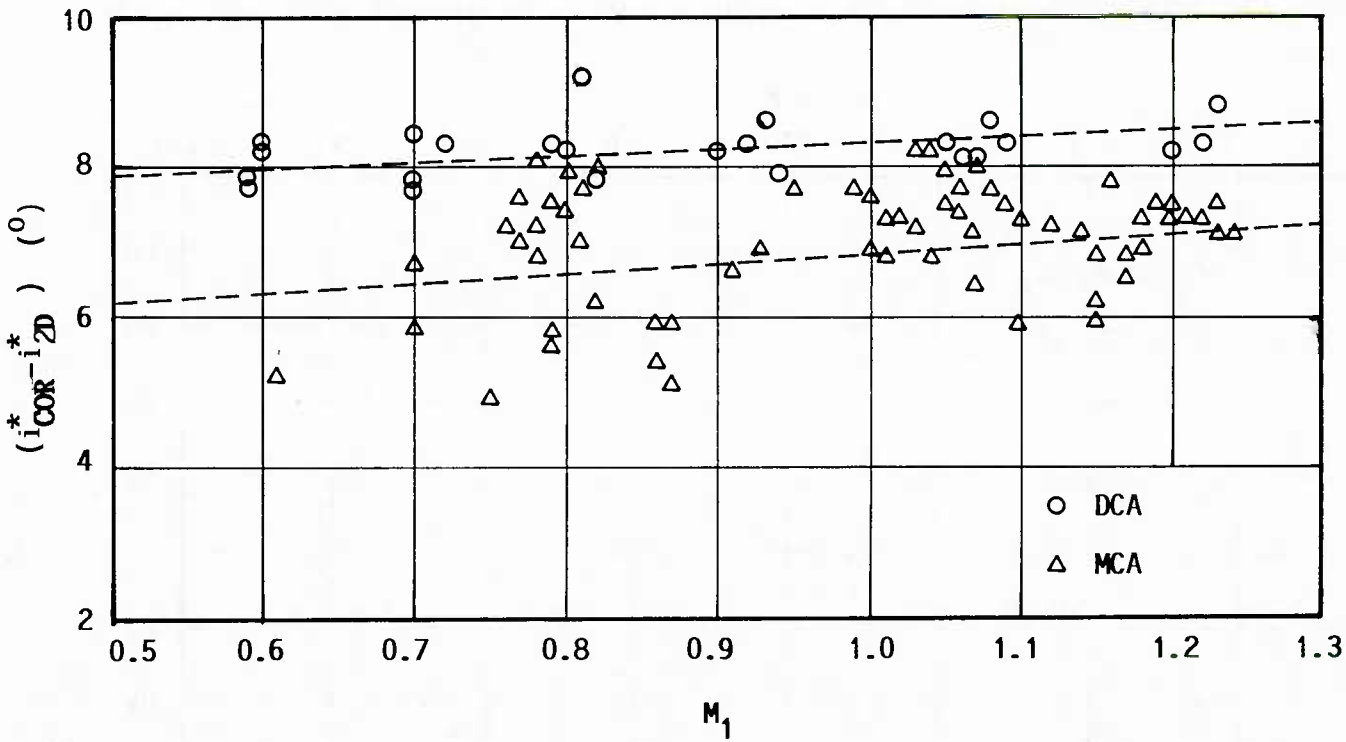

Figure 3.8 Deduced Variation of Transonic Rotor Design Incidence Angle Minus Low-Speed Two-Dimensional-Cascade-Rule Design Incidence Angle [9] with Relative Inlet Mach Number For DCA and MCA Profiles

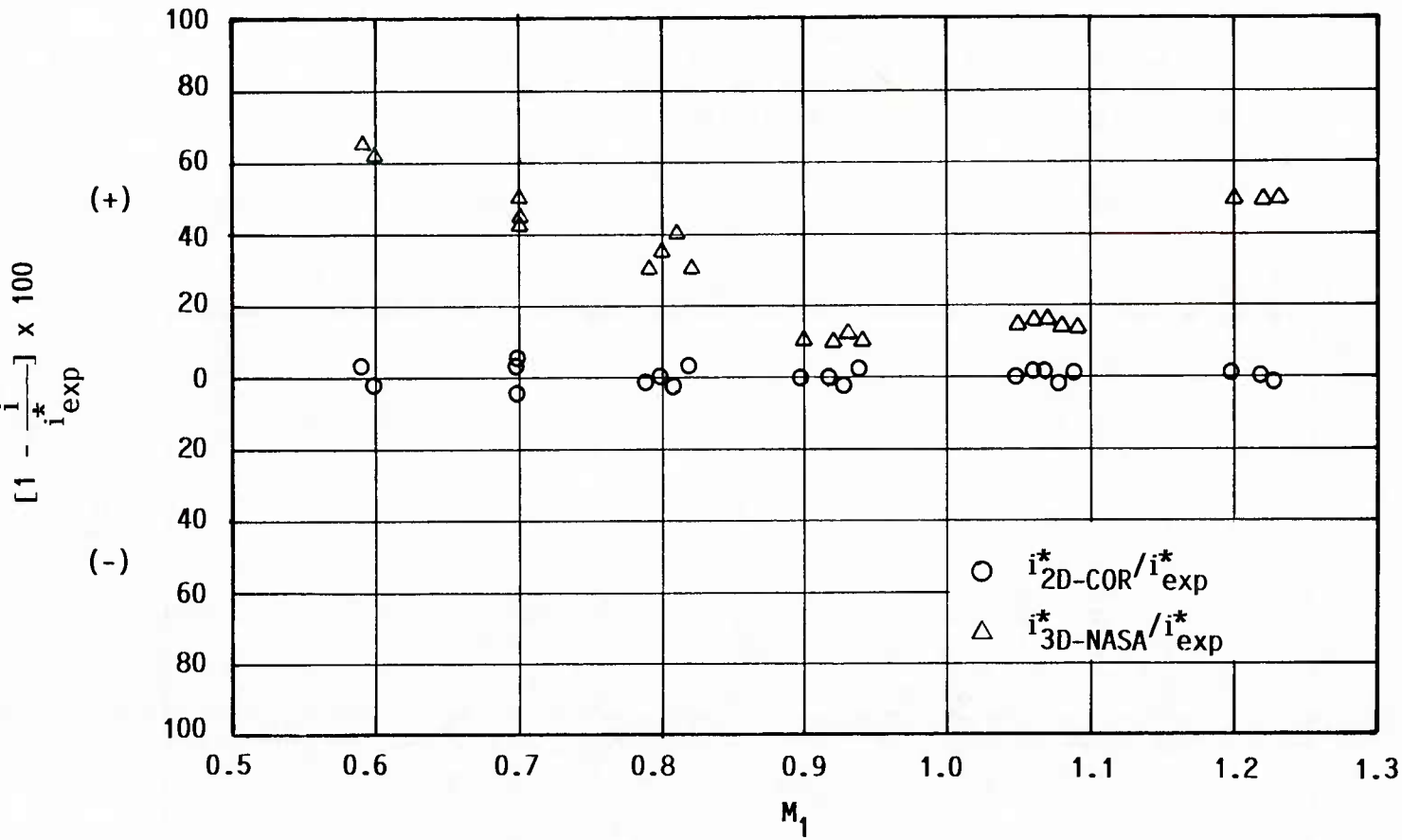

Figure 3.9 Comparison of Design Angle of Incidence Calculated by NASA-3D [9] and by NASA-2D with Modification for 3-D and Transonic Cascades

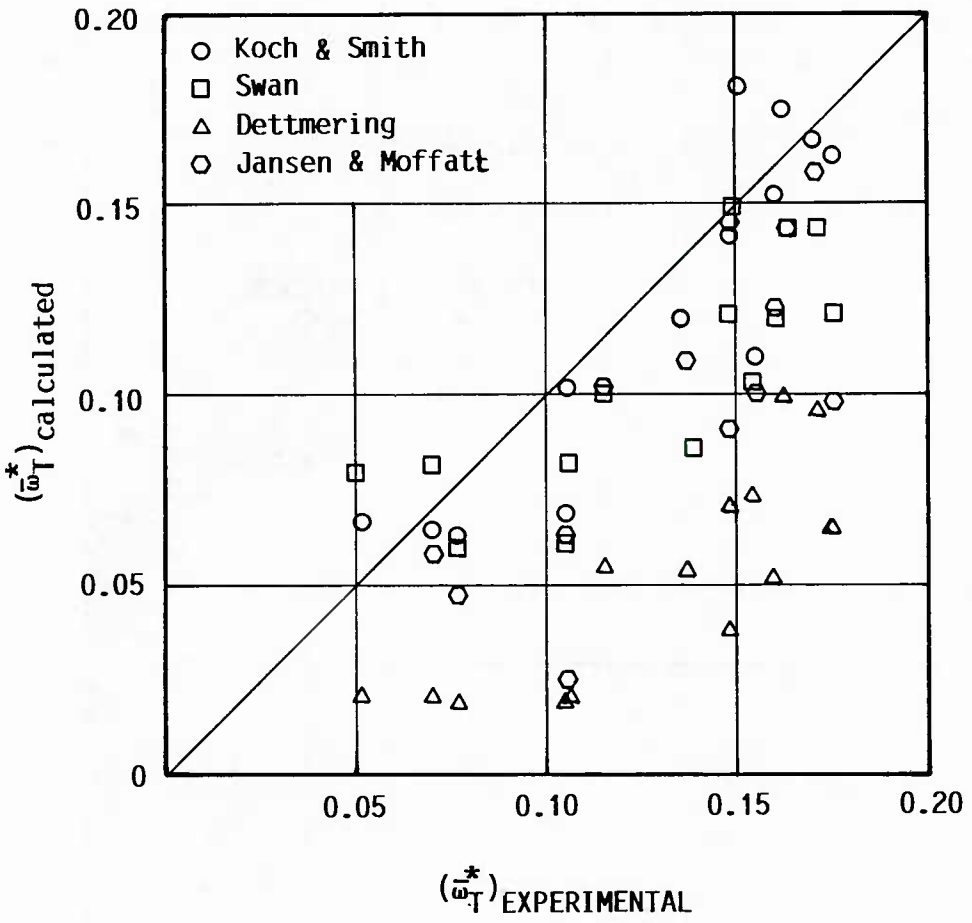

Figure 3.10 Comparison of Design-loss Coefficient Calculated by Various Correlations with Experimental Results

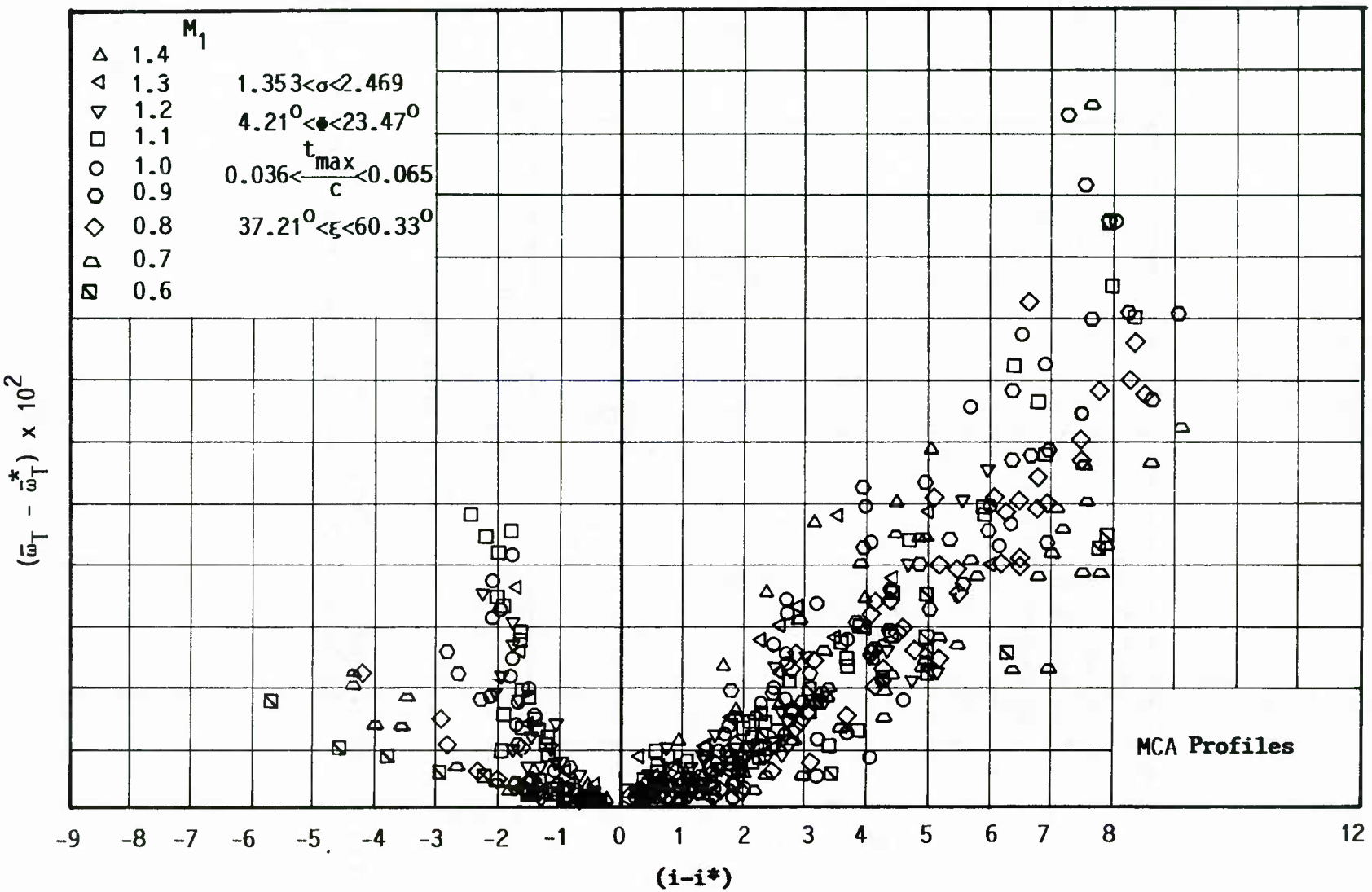

Figure 3.11 Variation of Off-Design Losses with Design Incidences

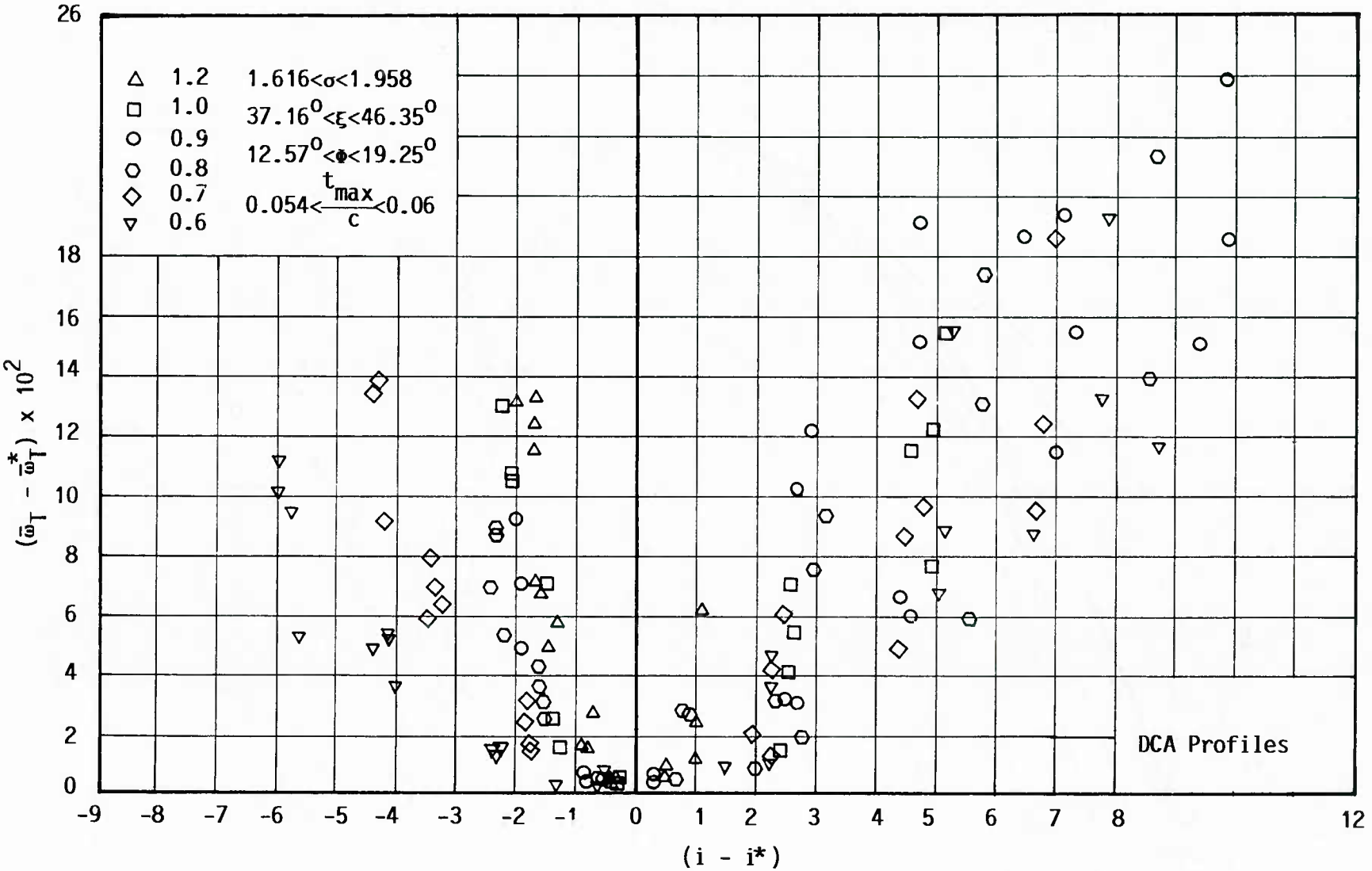

Figure 3.12 Variation of Off-Design Losses with Off-Design Incidences

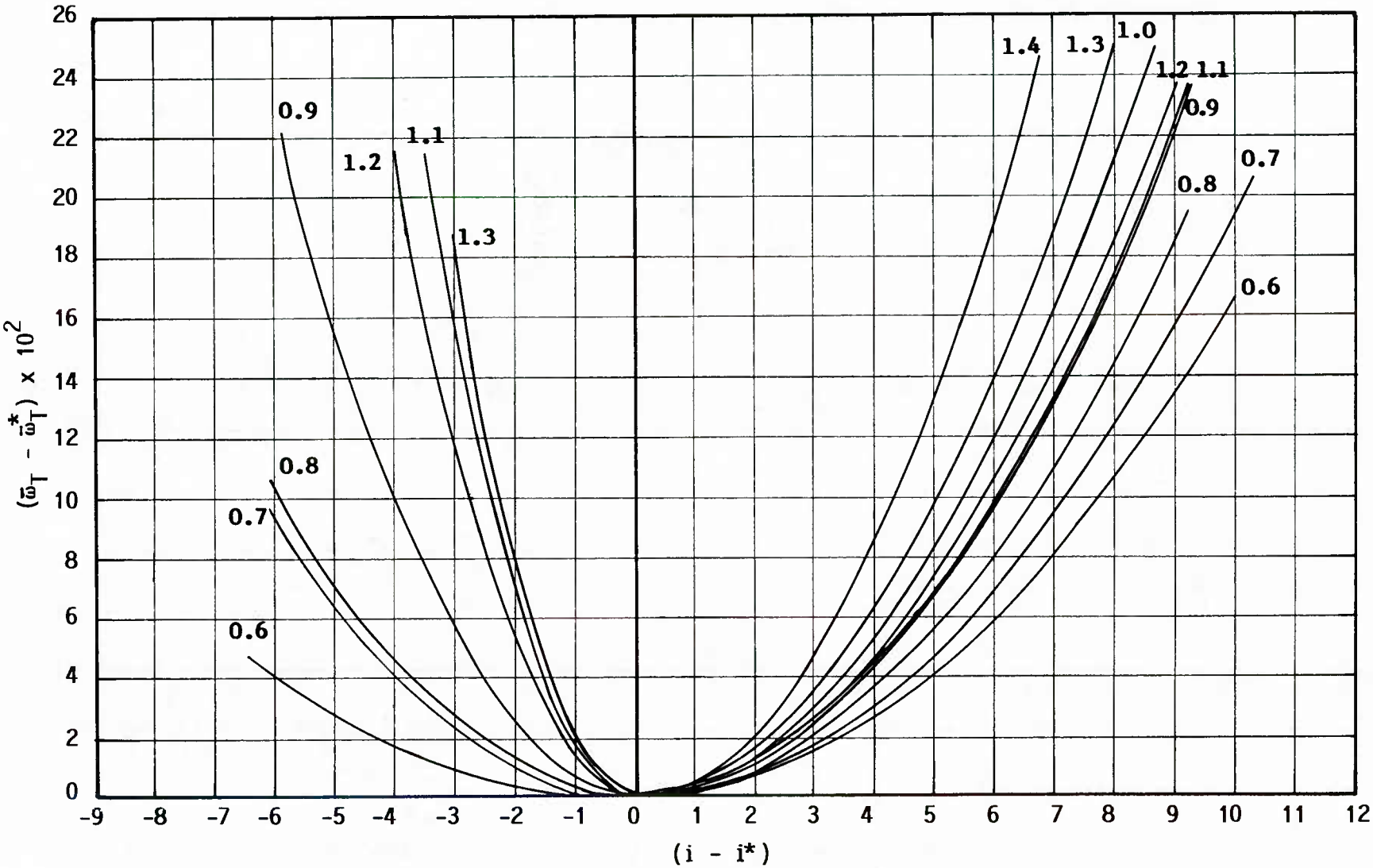

Figure 3.13 Curve fit through the Data Points of MCA Blade Profiles

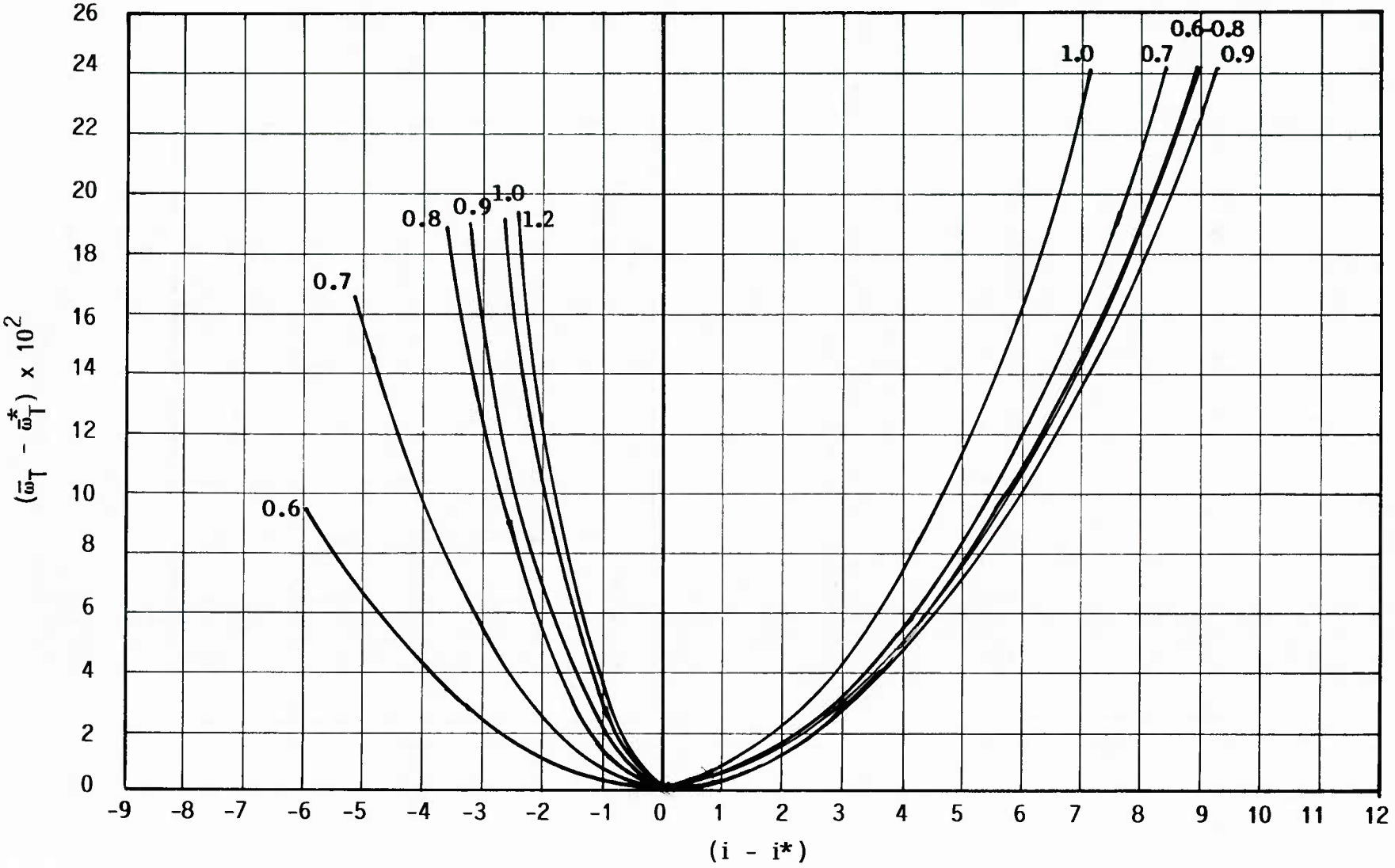

Figure 3.14 Curve fit Through the Data Points of DCA Blade Profiles

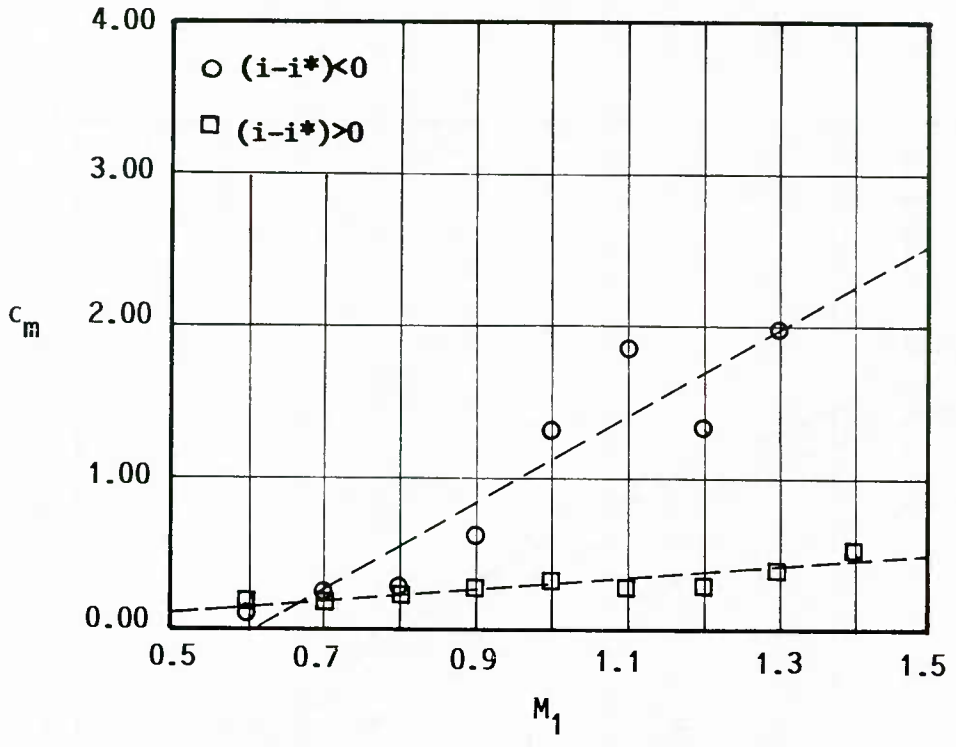

Figure 3.15 Variation of Coefficient c_m with Relative Inlet Mach Number (For MCA Blades)

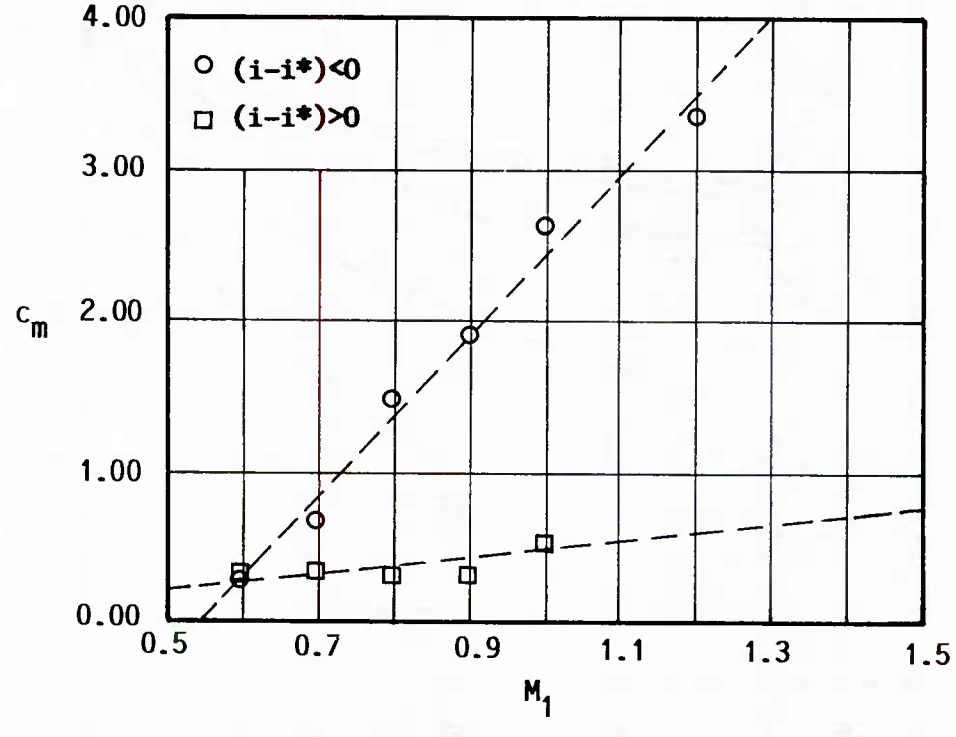

Figure 3.16 Variation of Coefficient c_m with Relative Inlet Mach Number (For DCA Blades)

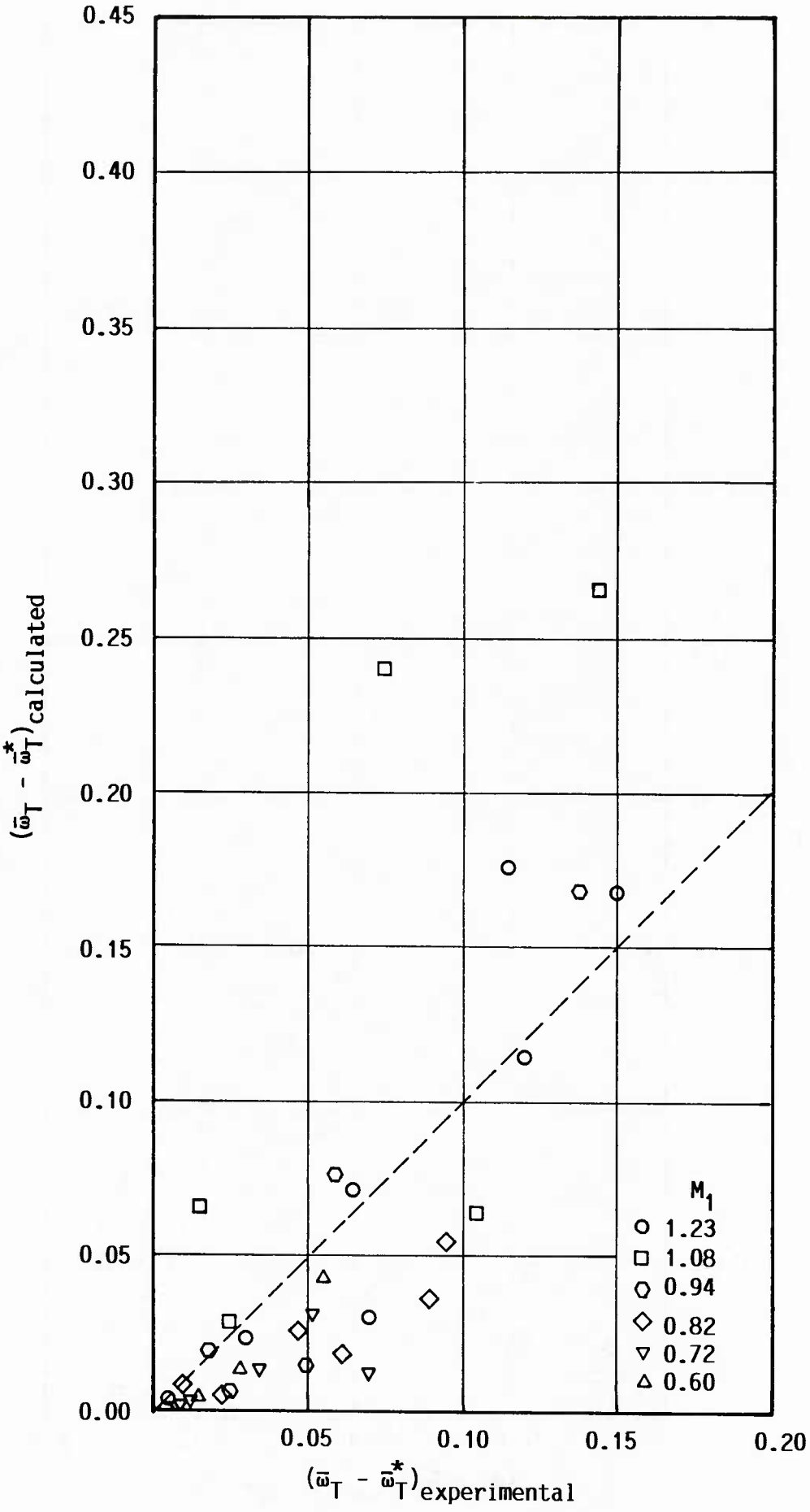

Figure 3.17 Comparison of Creveling's [19] Off-Design Loss Correlation with Experimental Results

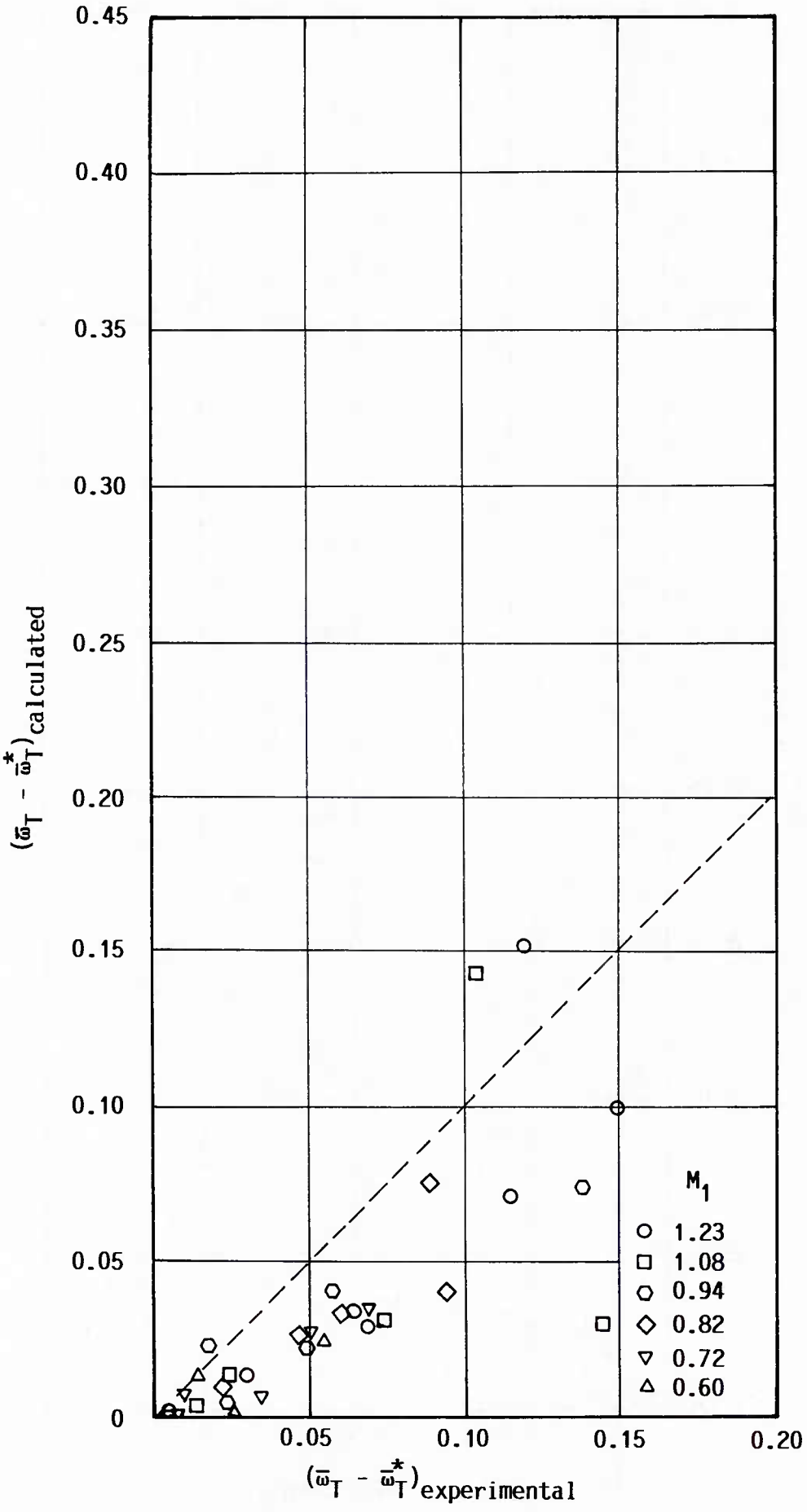

Figure 3.18 Comparison of Swan's [16] Off-Design Loss Correlation with Experimental Results

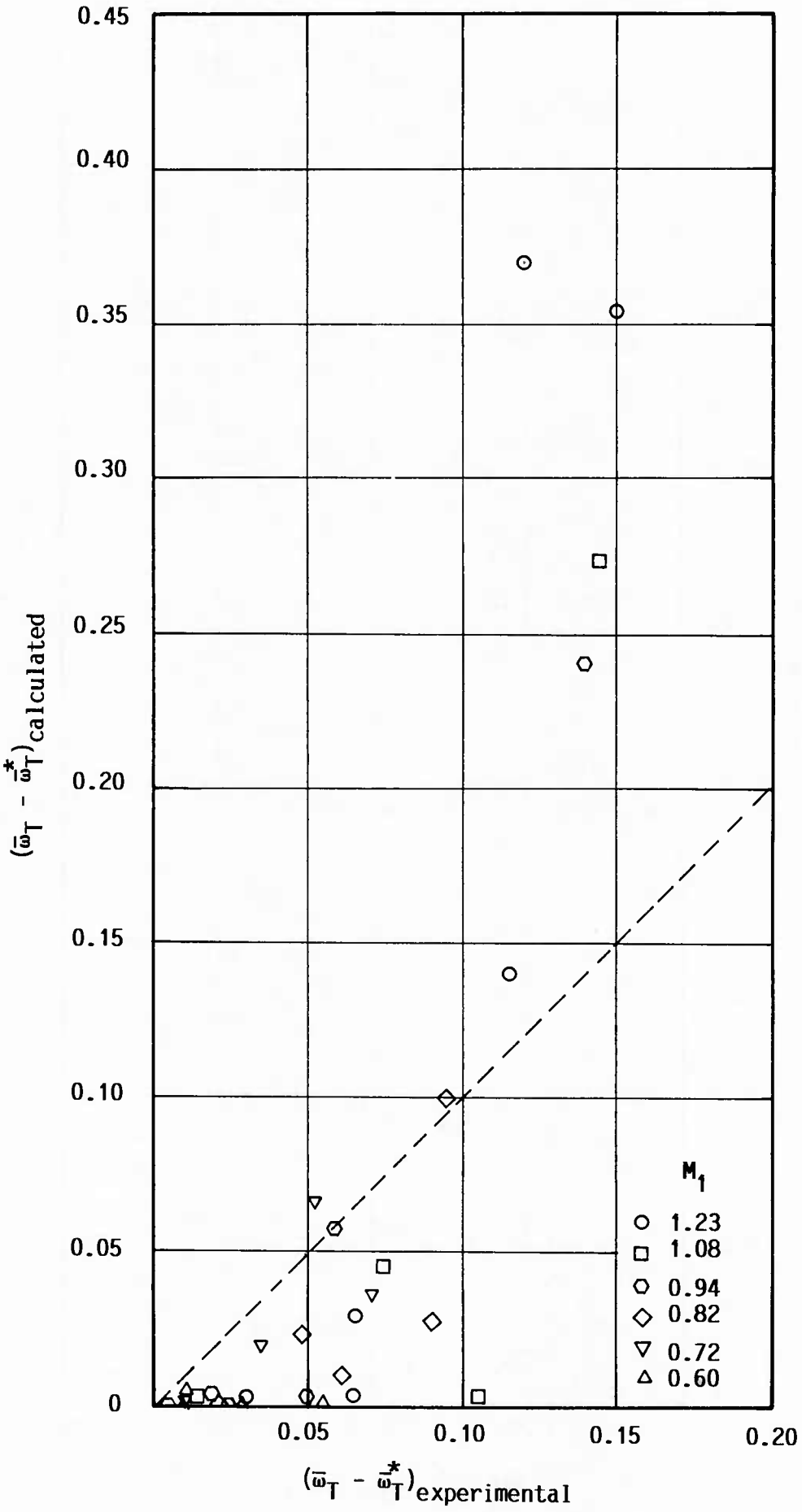

Figure 3.19 Comparison of Howell's [20] Off-Design Loss Correlation with Experimental Results

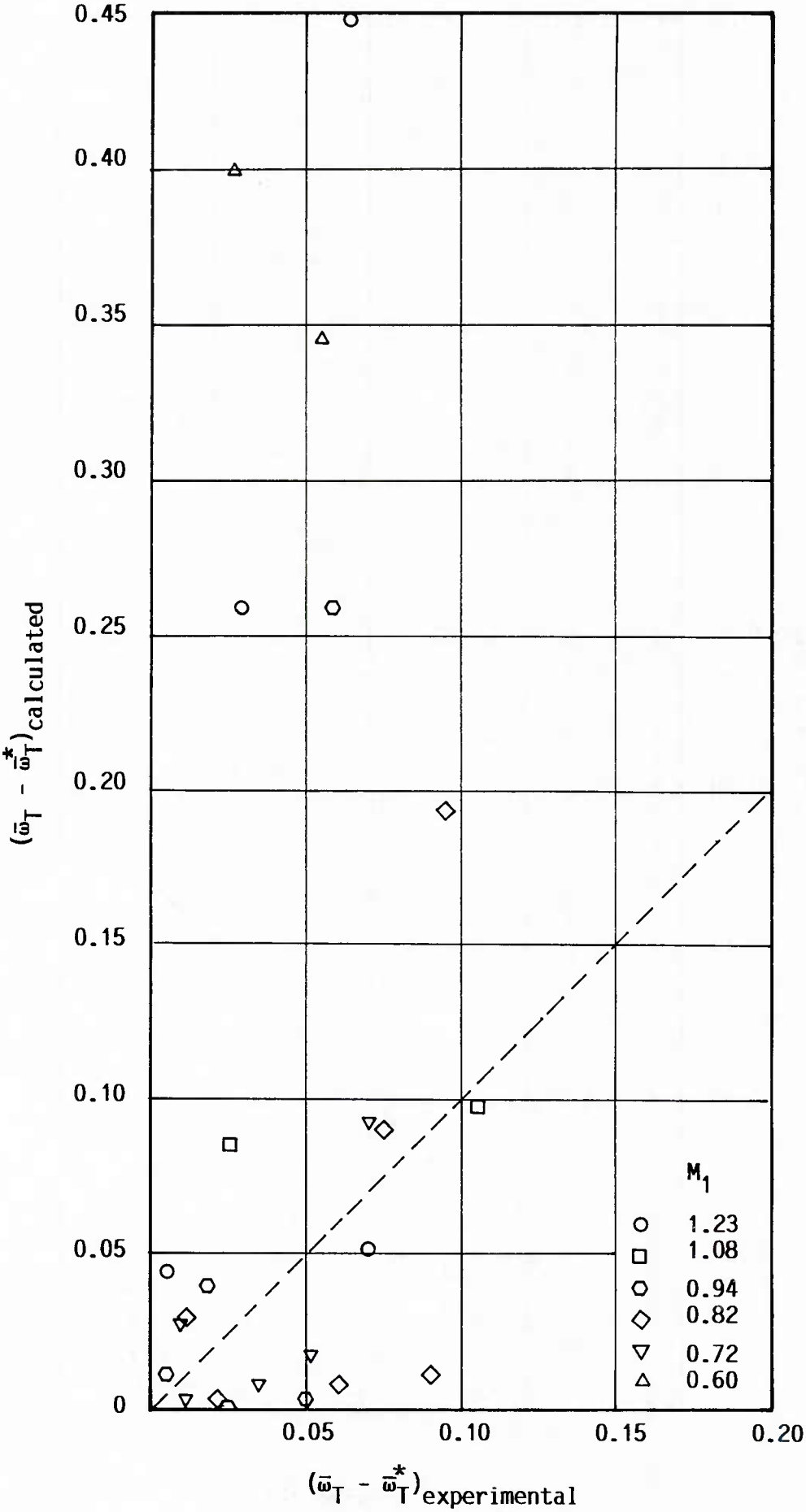

Figure 3.20 Comparison of Jansen & Moffatt's[18] Off-Design Loss Correlation with Experimental Results

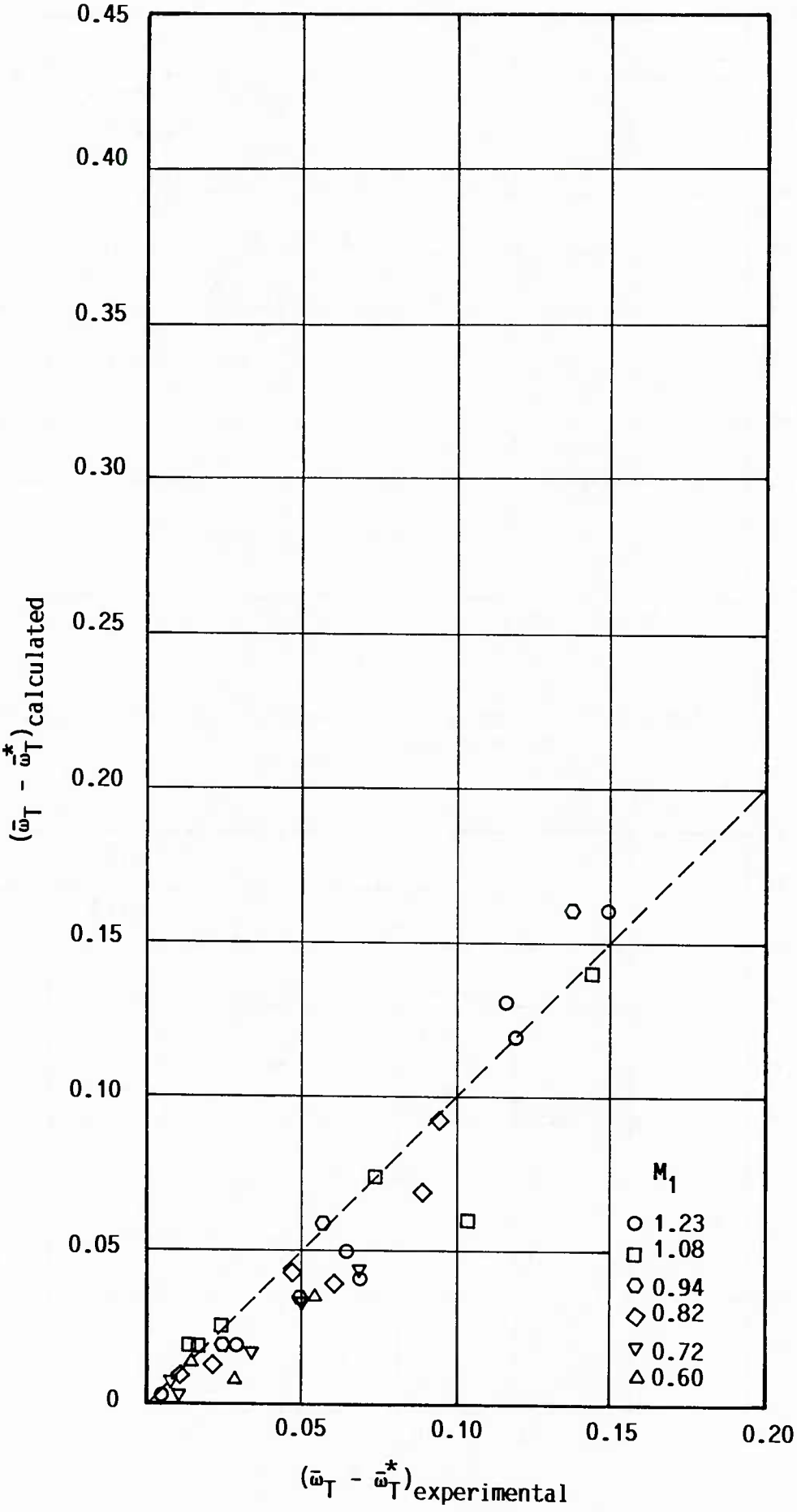

Figure 3.21 Comparison of The New Off-Design Loss Correlation with Experimental Results

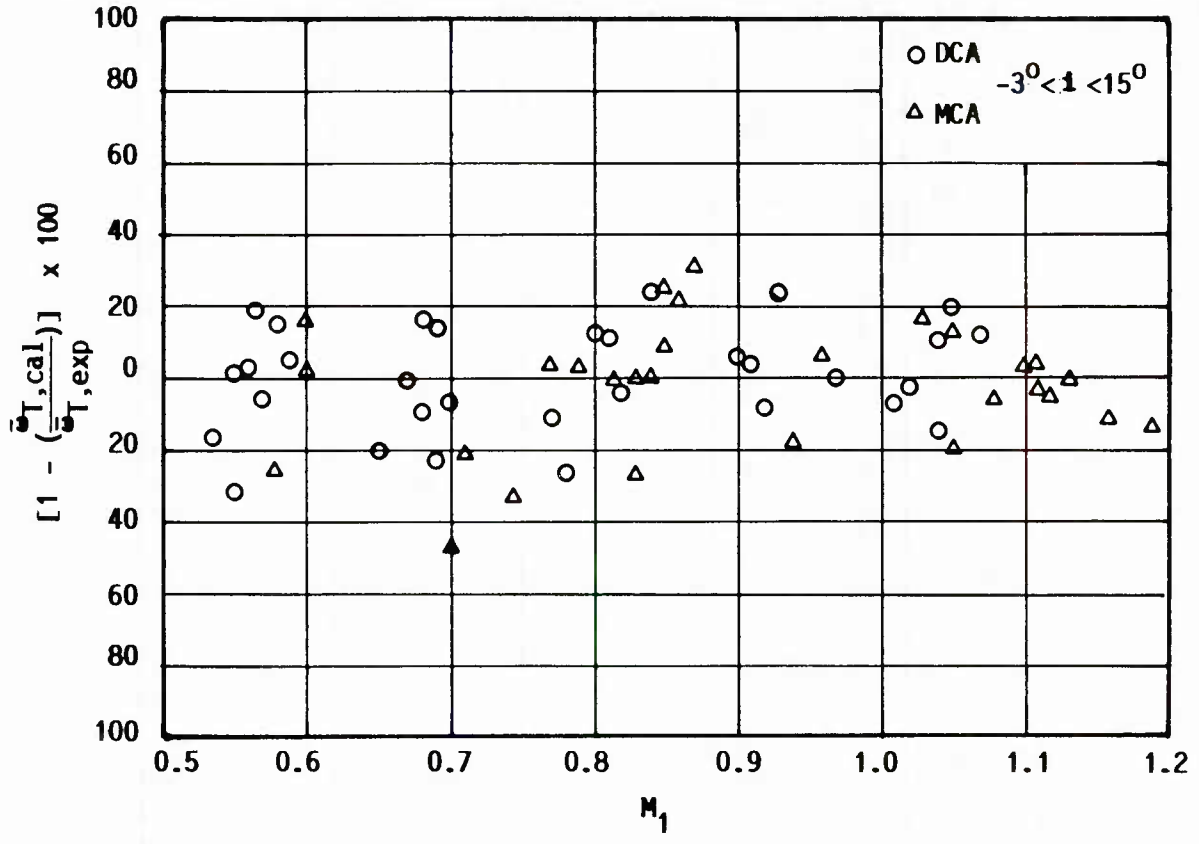

Figure 3.22 Percent Error in Prediction of Total Losses For Used Data

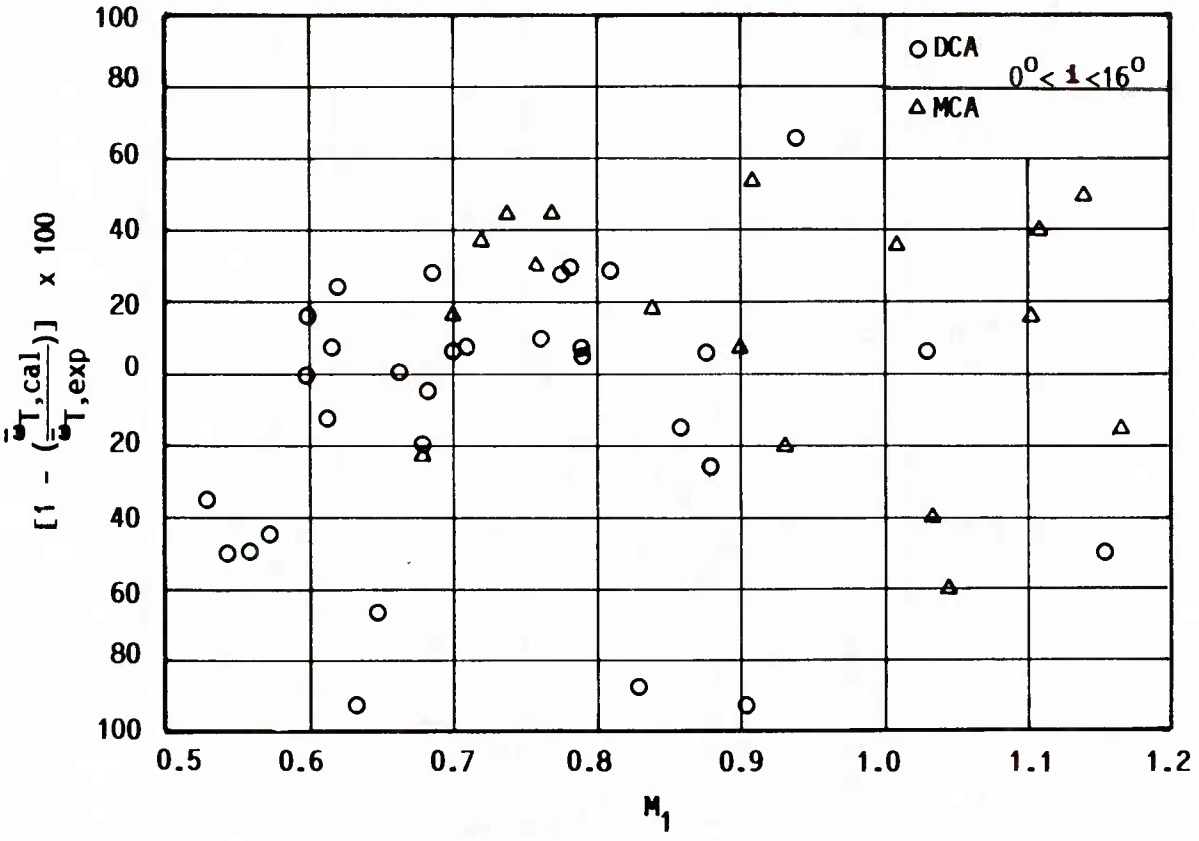

Figure 3.23 Percent Error in Prediction of Total Losses For Unused Data

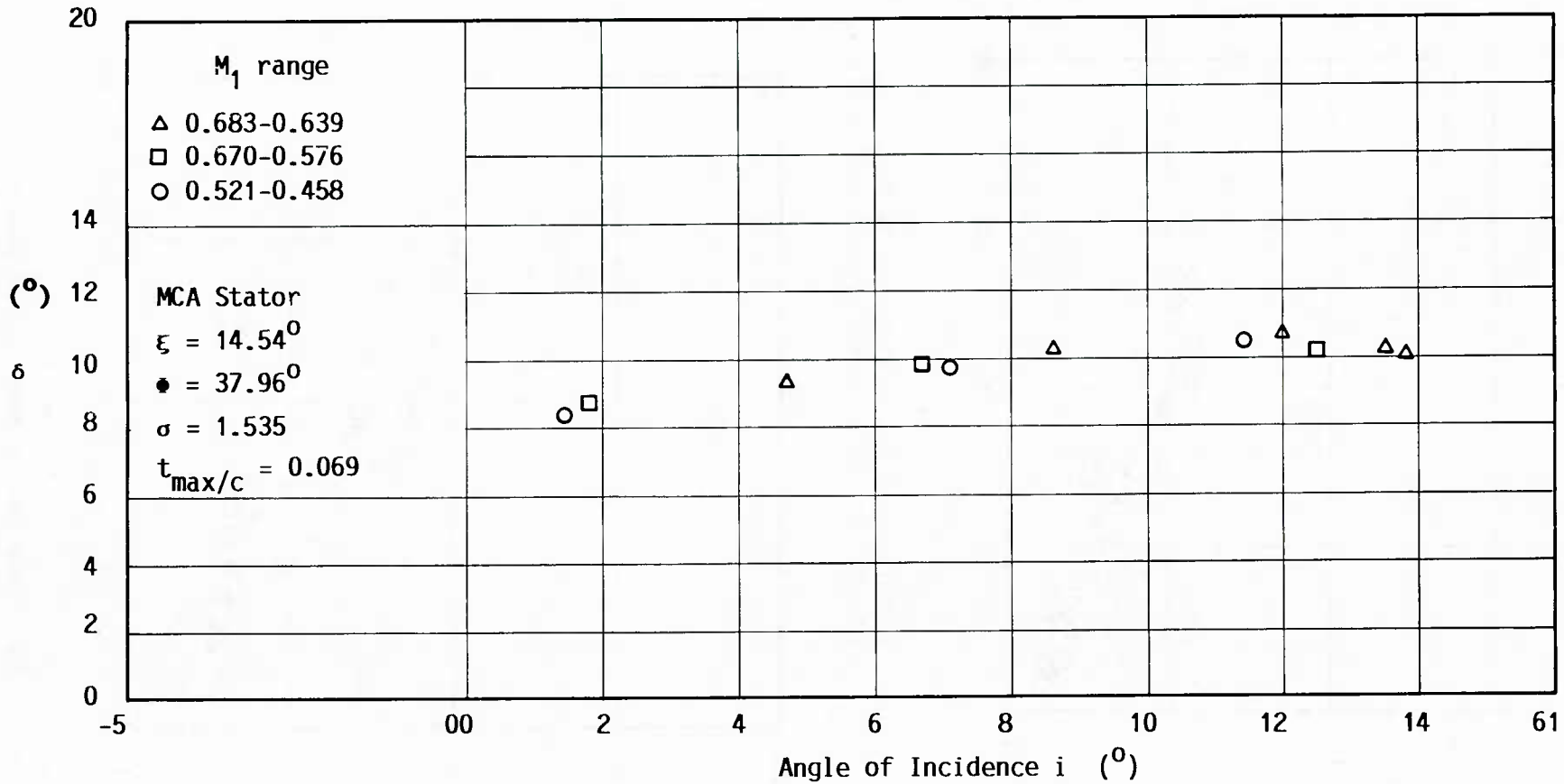

Figure 3.24 A Sample of Deviation Versus Angle of Incidence

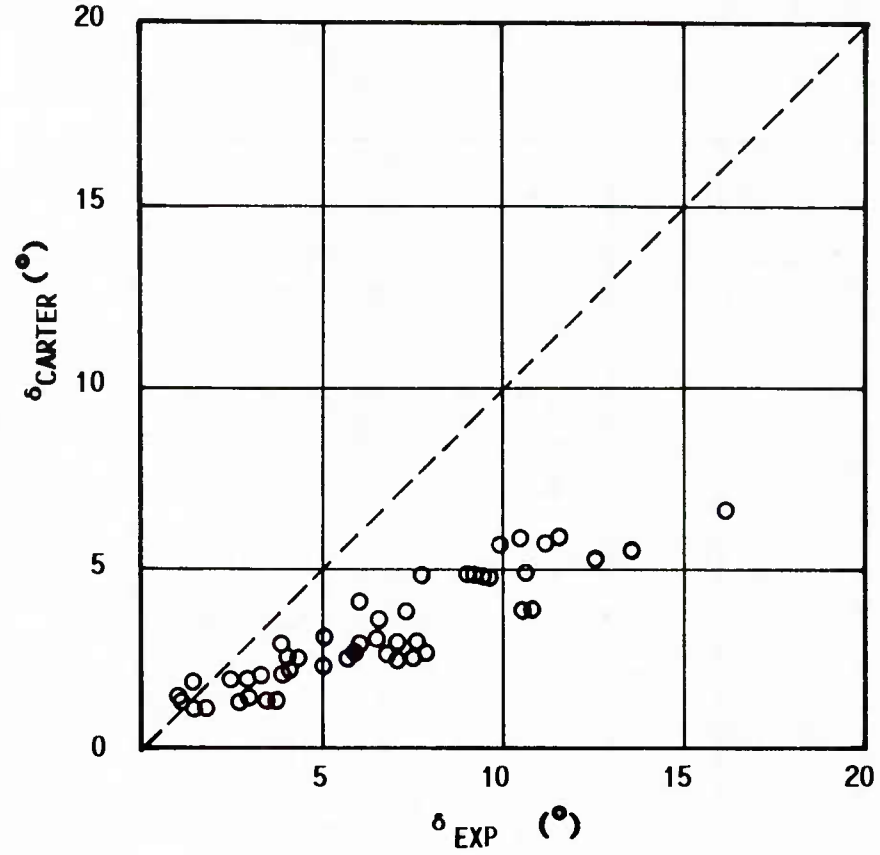

Figure 3.25 Comparison of Measured Deviation Angles with the Predictions of Carter's Correlation

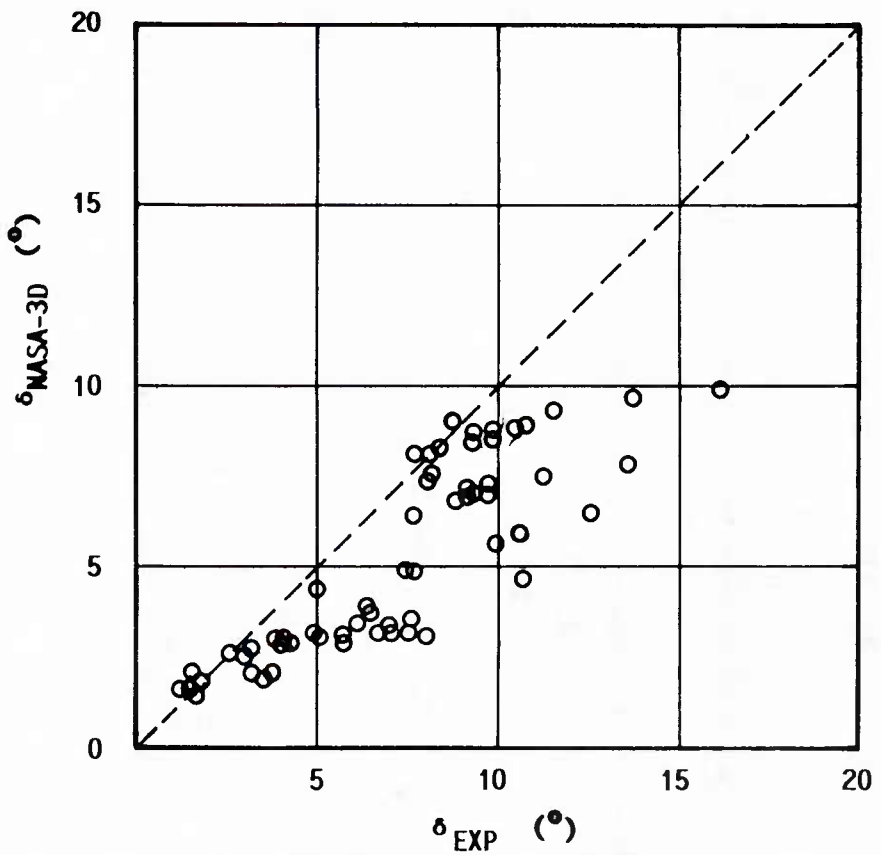

Figure 3.26 Comparison of Measured Deviation Angles with The Predictions of NASA-3D Correlation

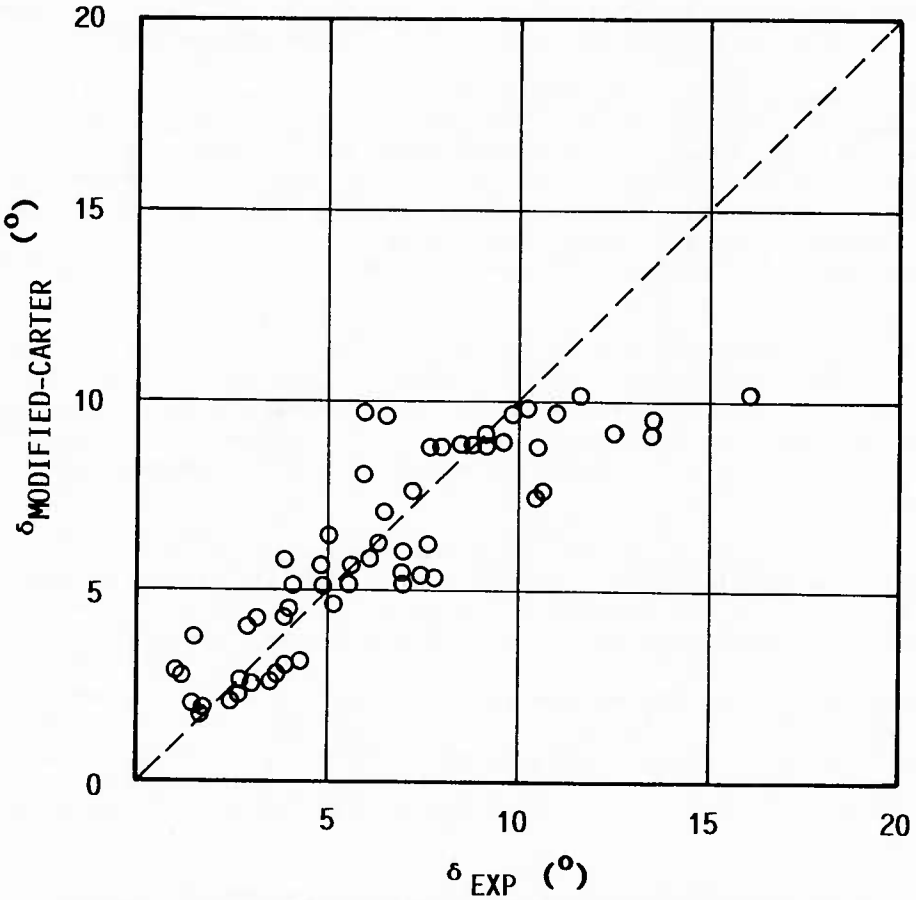

Figure 3.27 Comparison of Measured Deviation Angles with The Predictions of Modified Carter's Correlation (Sample points)

4. APPLICATION OF MODIFIED LOSS AND DEVIATION CORRELATION SET TO PERFORMANCE PREDICTION

As a result of the work explained in the last section a set of correlations were selected which may be used for performance prediction of transonic compressors. These are:

Minimum loss incidence angle:	Modified NASA-2D
Design total loss:	Koch and Smith
Off-design total loss:	New Correlation (Table 1)
Design deviation angle:	Modified Carter's rule
Off-design deviation angle:	Creveling

It should be noted that the design loss and deviation are the values which occur at the minimum-loss incidence angle. Therefore blade sections will be operating at off-design condition if $i^* \neq i$. This condition almost always occurs in performance prediction calculations because of the iterative procedures and inherent errors of the computational method. Especially during the convergence phase of the computation, the blade sections would be operating far from design. Therefore, some stops must be included in computer codes in order to control the loss and deviations when the blade rows either stall or choke prematurely.

The throughflow computer code used for performance prediction calculations was developed in the Mechanical Engineering Department of the Middle East Technical University [37]. The code uses a finite-element method for determining the flow on axisymmetric hub-to-shroud surfaces. The code requires empirical correlations for determining the losses and turning through the blade rows. Interblade calculation stations are allowed and blade blockage and lean angle are distributed to these locations from the geometrical data. Turning and loss are also estimated for the interblade nodes in the streamwise direction. In order not to complicate the problem by introducing additional unknowns, no end wall boundary layer calculation procedure is used. Instead, experimental values of the end wall boundary layer blockage are introduced. This is done by displacing the hub and tip walls.

A systematic investigation was performed on the influence of the streamwise inter-blade distribution of loss and deviation on flow properties. Both linear and exponential distributions of loss and deviation were evaluated. Different ways of distributing the loss and deviation to the inter-blade stations had a negligible effect on the calculated flow property distributions. Exponential distribution with the exponent less than one gave convergence problems. The exponent equal to two was successful with results almost the same as the linear distribution i.e., exponent equal to one. A linear distribution of loss and turning is preferred and used in the performance prediction calculations.

As the test geometry, a NASA two stage fan is used. This test case is well documented in references [26] and [41]. The fan has low aspect ratio blading particularly in the first rotor (aspect ratio being equal to 1.56). This test case is quite challenging with regard to performance prediction, especially off-design as illustrated in AGARD WG12 report [11]. The test case is one of the few well-documented two-stage compressor test cases, allowing comparisons for multiple blade rows.

As the first check of the computer code, calculations were performed at 70, 80, 90 and 100 percent design speeds using the measured total loss and deviations given in reference [26]. The axial velocity and density variations in the spanwise direction were found to be satisfactory at all speeds. Later computations were performed using measured turning angles and correlations for loss prediction. Computations were also performed using correlations for turning angle, and measured values of losses as input. These calculations showed that correct prediction of turning angle at design and off-design is more important than the correct prediction of losses.

For selection of the most suitable off-design deviation correlation, test computations were performed using measured total losses as input with the various off-design deviations mentioned in Section 3.8. As a result of these computations Creveling's off-design deviation correlation was found to be the most satisfactory one.

The experimental and predicted values given in Figures 4.1 to 4.4 are the results of the computations performed using the set of loss correlations recommended as a result of the work described in this report. The design and off-design correlations are used simultaneously in the calculations. The correlation sub-program is given in Appendix IV. The test point calculated is at 100% design speed. The comparisons of experimental and theoretical results of the first stage rotor, first stage stator, second stage rotor, and second stage stator are given in Figures 4.1, 4.2, 4.3 and 4.4 respectively. In each figure the variation of axial velocity and density with percent span is plotted both upstream and downstream of the blade row. On the same figure the variation of predicted loss and deviation with percent span is also displayed. Percent span indicated in the figures is measured from the hub. As expected, examination of the figures shows that the correlation set can not be regarded as very successful in predicting the details of flow near the hub and casing. Because no explicit spanwise treatment of the secondary flow losses exists this mis-prediction extends towards the mid-span especially in rotor blades. The discrepancies are greater at the tip of the rotor blades due to the complicated flow structure of leakage, end wall boundary layer and transonic flow effects which can not be completely accounted for in the predicted total loss coefficients. However, except at the end wall regions, deviation and loss predictions of stator blade rows are more accurate compared to the prediction of losses in the rotors. In all cases the deviations are predicted better than the losses. On the whole overall mid-span trends at almost all stations are predicted well. However, there are discrepancies between measured and calculated values. A careful examination of the development of flow through the blade rows shows that any errors in total loss and deviation distribution in the spanwise direction propagate downstream and can be detected in the spanwise property variations at the downstream stations.

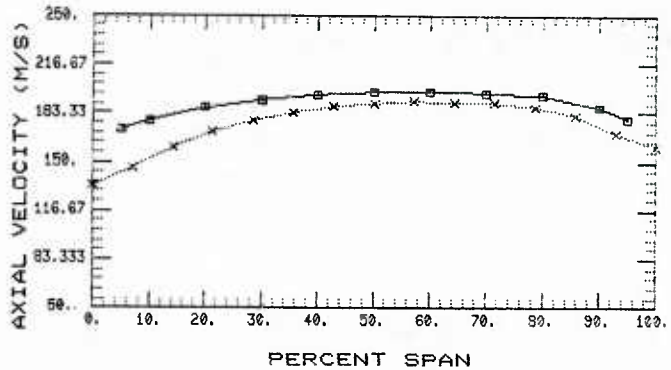

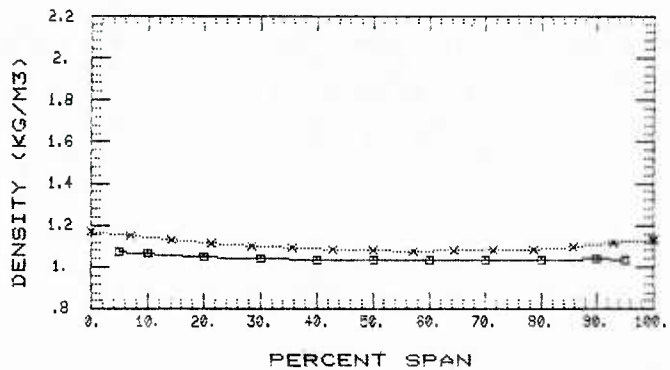

4.1a UPSTREAM

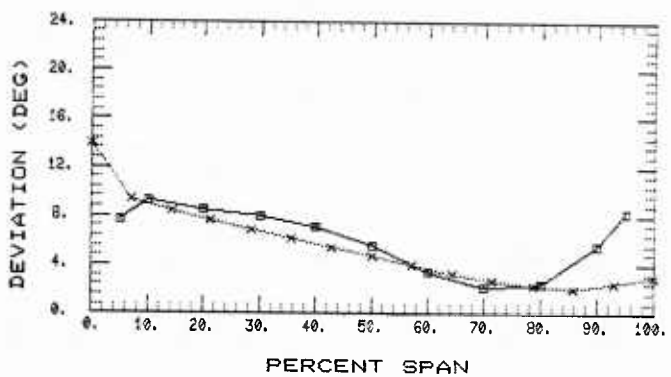

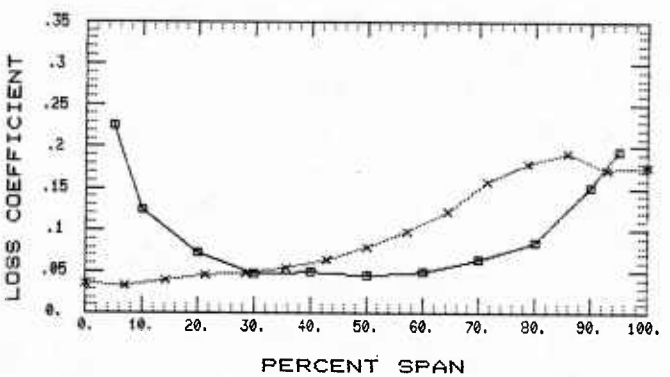

4.1b LOSS AND DEVIATION

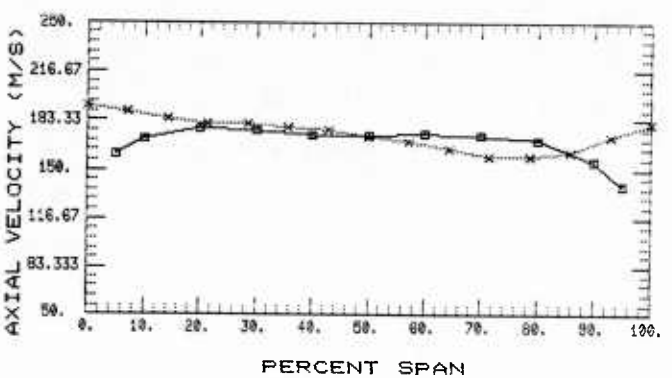

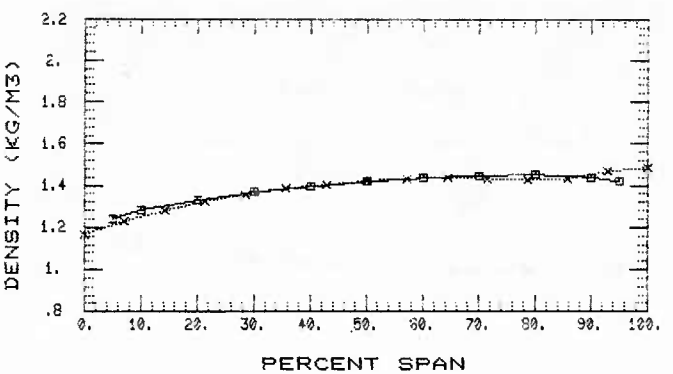

4.1c DOWNSTREAM

FIGURE 4.I F I R S T S T A G E R O T O R

PREDICTED MEASURED

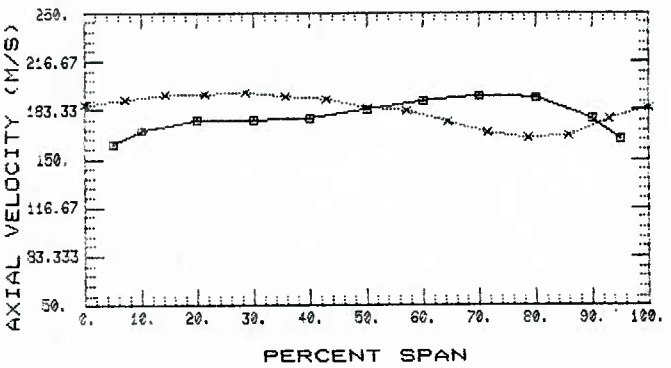

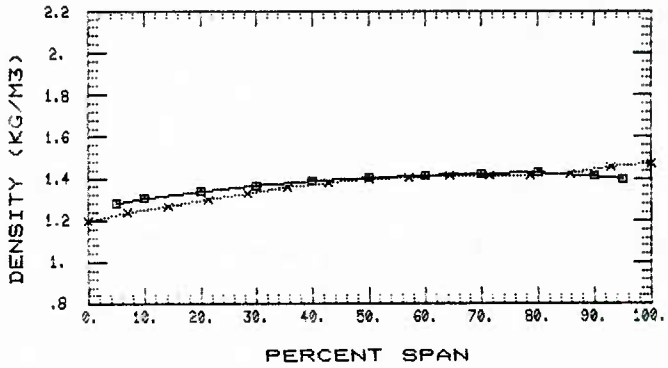

4.2a UPSTREAM

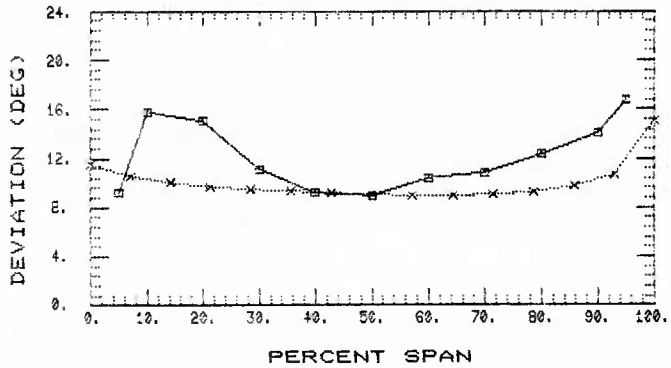

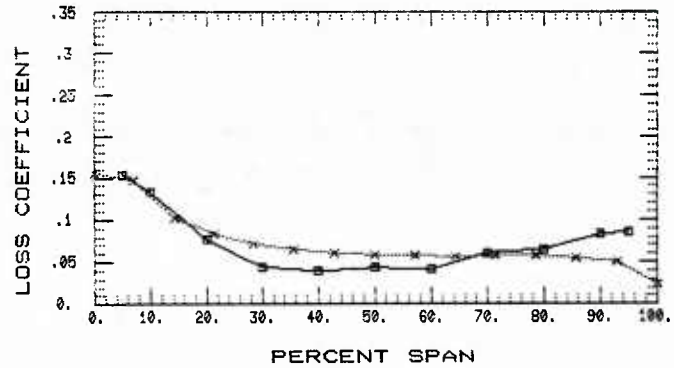

4.2b LOSS AND DEVIATION

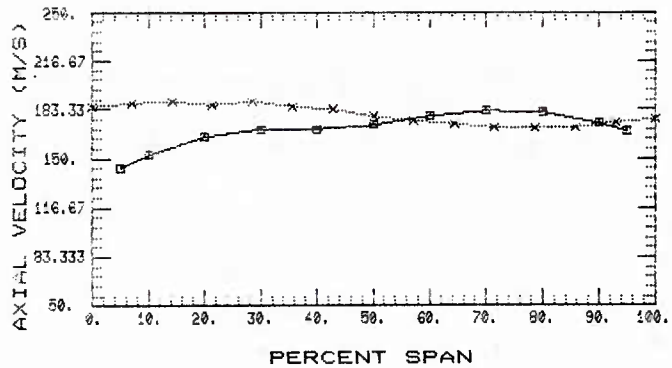

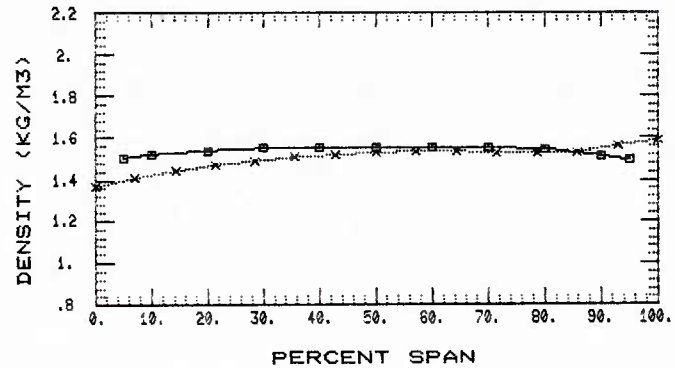

4.2c DOWNSTREAM

FIGURE 4.2 F I R S T S T A G E S T A T O R —×— PREDICTED —□— MEASURED

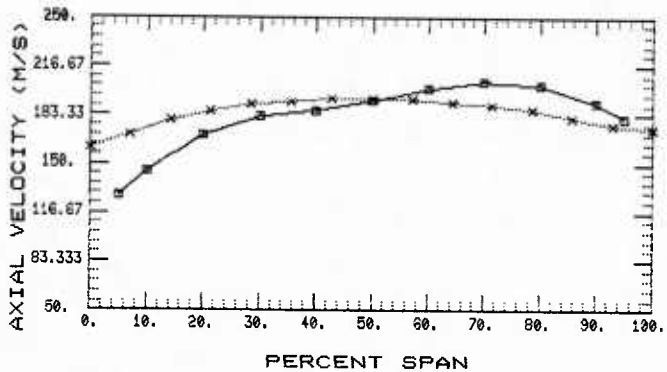

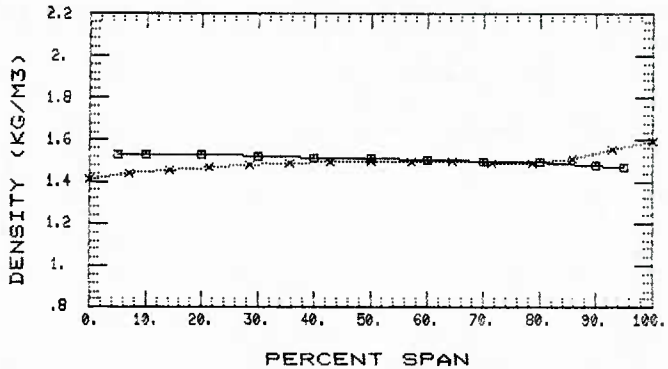

4.3a UPSTREAM

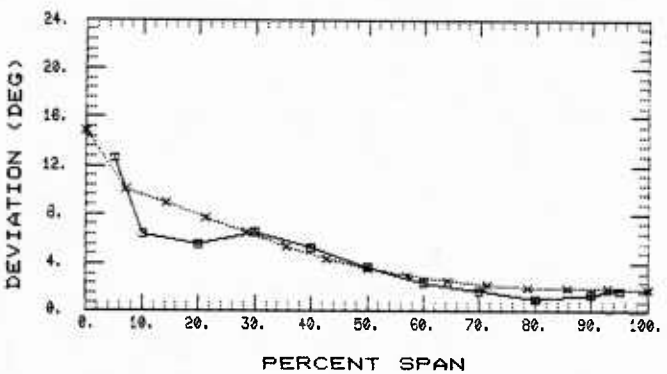

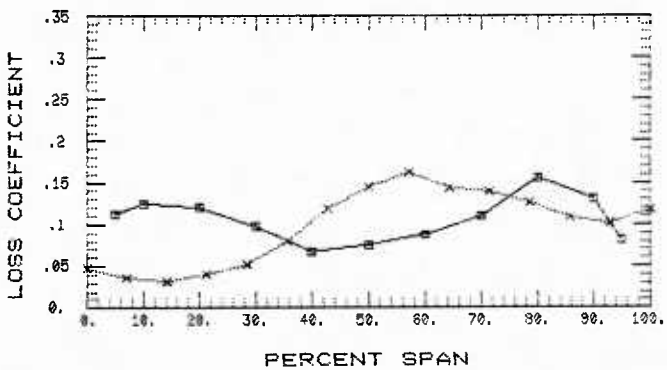

4.3b LOSS AND DEVIATION

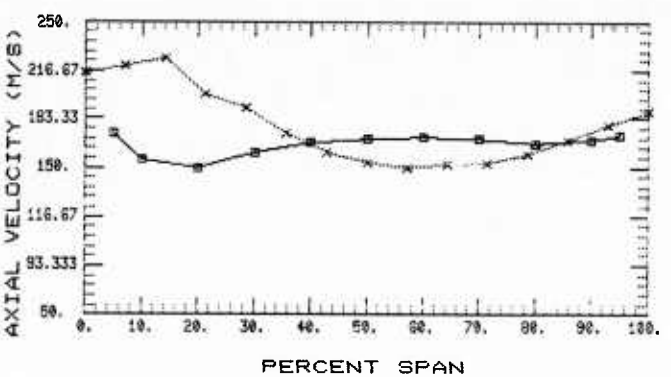

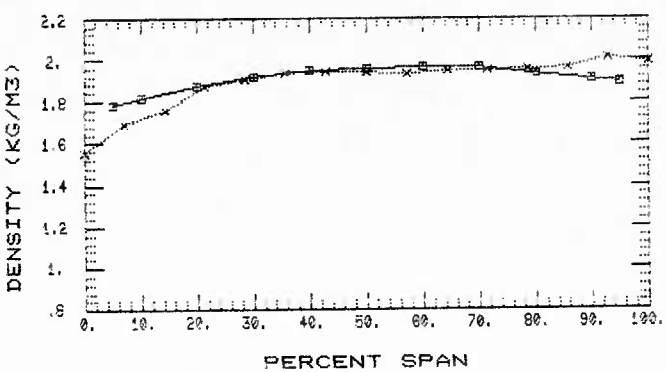

4.3c DOWNSTREAM

FIGURE 4.3 SECOND STAGE ROTOR ····×···· PREDICTED —□— MEASURED

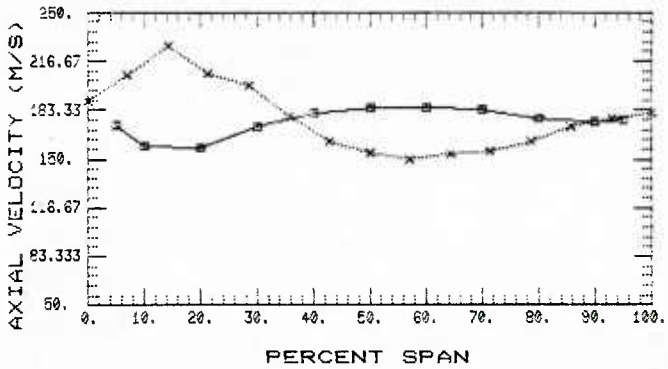

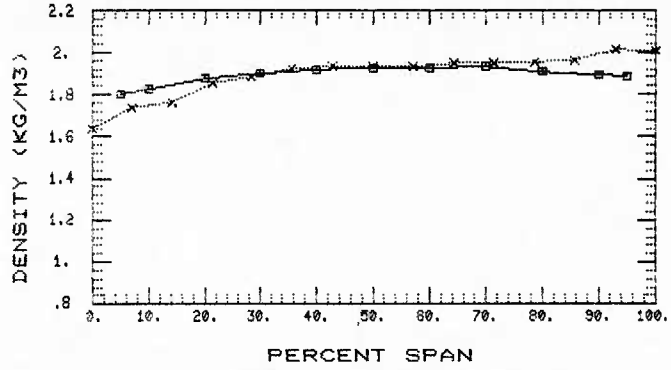

4.4a UPSTREAM

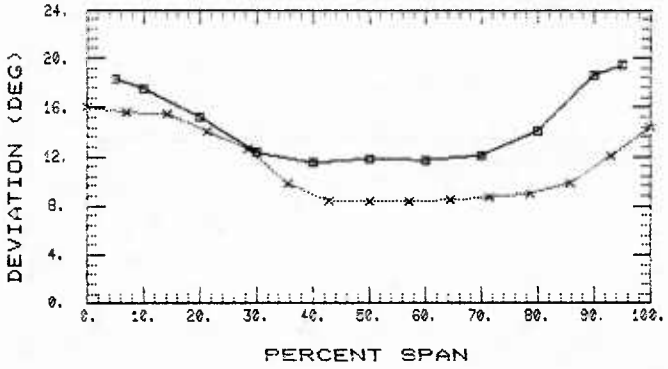

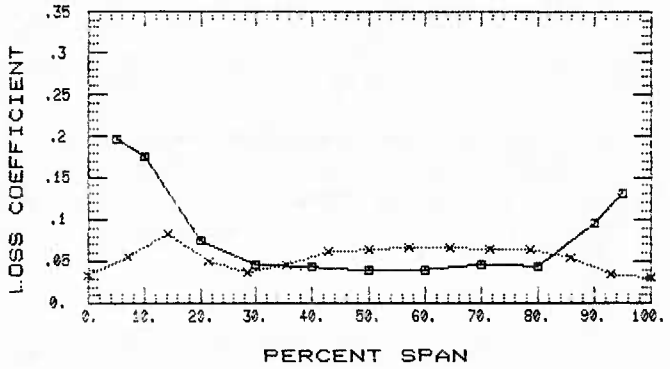

4.4b LOSS AND DEVIATION

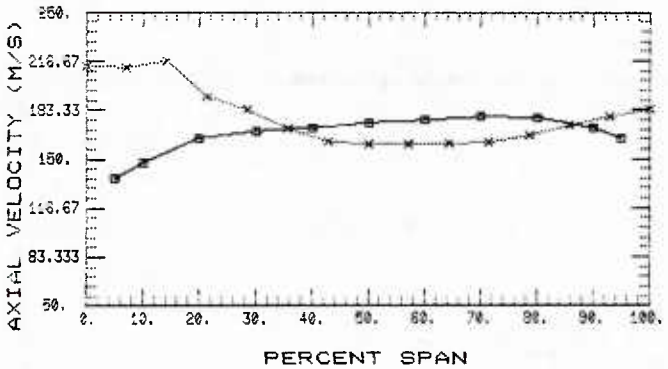

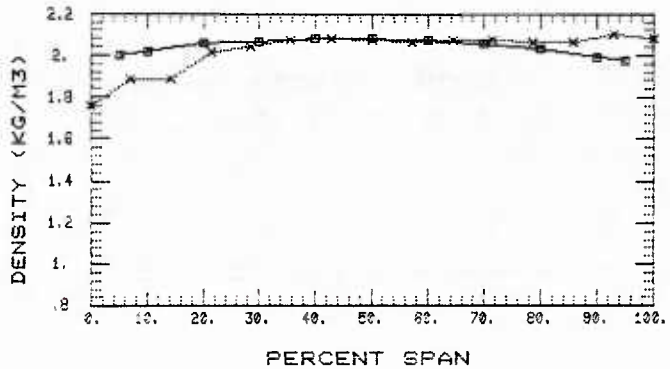

4.4c DOWNSTREAM

FIGURE 4.4 SECOND STAGE STATOR

PREDICTED MEASURED

5. CONCLUSIONS

The goal of this work was to analyse the transonic compressor tests available in the open literature and to propose possible improvements in total loss and turning correlations. As an outcome of the work the following conclusions are reached:

- The level of accuracy of deviation prediction should be greater than that of losses.
- The off-design deviation correlation which gives most consistent and successful results was found to be that of Creveling.
- The minimum loss incidence predicted by the NASA-2D correlation needs a modification separately for DCA and MCA blade profiles. This modification depends on the blade element geometry and accounts for the transonic and 3-D effects which can not be separated in the present investigation.
- The design deviation angle correlation of Carter needs a correction for taking into account the transonic and 3-D effects which are not separable in the analysed data.
- The off-design transonic loss correlation developed in this work compares quite favourably with the other available off-design correlations in terms of overall performance prediction.
- Koch and Smith [17] minimum loss correlation is the most accurate design loss prediction method available in the open literature.

The comparison of the experimental results of a 2-stage compressor with the computed results using the new correlation set, revealed that the new set can be regarded as satisfactory in giving the overall trends in deviation, losses and fluid properties except at the end walls. A consistent end-wall boundary layer and secondary loss calculation method is necessary for more accurate predictions. The loss and deviation predictions across the stators are more accurate compared to the predictions of losses across the rotors. For more accurate predictions of the flow in multi-stage machines spanwise loss mixing procedures must be used. Especially for off-design predictions the minimum loss incidence of the blade row together with the flow direction of the flow ahead of the blade row should be correct. Small errors in the incidence obviously increases in a cumulative way through the compressor in the case of multi-stage machines.

6. LIST OF REFERENCES

1. Hager, R.D. Janetzke, C.D. Reid, L. — *Performance of a 1380 Ft/sec. Tip. Speed Axial-Flow Compressor Rotor with a Blade Tip Solidity of 1.3*, NASA TM X-2448, 1972.

2. Urasek, D.C. Moore, R.D. Osborn, W.M. — *Performance of a Single-Stage Transonic Compressor with a Blade Tip Solidity of 1.3*, NASA TM X-2645, 1972.

3. Moore, R.D. Reid, L. — *Performance of a Single Stage Axial Flow Transonic Compressor with Blade Tip Solidity of 1.7*, NASA TM X-2658, 1972.

4. Kovich, G. Moore, R.D. Urasek, D.C. — *Performance of Transonic Fan Stage with Weight Flow per Unit Annulus Area of 198 Kilograms per Second per Square Meter*, NASA TM X-2905, 1973.

5. Moore, R.D. et al. — *Performance of Transonic Fan Stage with Weight Flow per Unit Annulus Area of 178 Kilograms per Second per Square Meter*, NASA TM X-2904, 1973.

6. Ruggeri, R.S. et al. — *Performance of a Highly Loaded Two Stage Axial-Flow Fan*, NASA TM X-3076, 1974.

7. Sulam, D.H. et al. — *Single-Stage Evaluation of Highly-Loaded High-Mach-Number Compressor Stages. 2: Data and Performance, Multiple-Circular-Arc rotor*, NASA CR-72694, 1972.

8. Harley, K.G. et al. — *High-Loading Low-Speed Fan Study. 3: Data and Performance Slotted Blades and Vanes and Rotor Tip Treatment*, NASA Cr-72895, 1971.

9. — — *Aerodynamic Design of Axial-Flow Compressor*, NASA SP-36, 1965.

10. Scholz, N. — *Aerodynamics of Cascades*, AGARD-AG-220, 1965.

11. — — AGARD/PEP Working Group 12, *Through Flow Calculations in Axial Flow Turbomachines*, AGARD-AR-175, 1981.

12. — — *Advanced Compressors*, AGARD-LS-39.70, 1970.

13. Lieblein, S. — *Analysis of Experimental Low-Speed Loss and Stall Characteristics of Two-Dimensional Compressor Blade Cascades*, NASA RM E 57A28, 1957.

14. Lieblein, S. — *Loss and Stall Analysis of Compressor Cascades*, Trans of the ASME, Journal of Eng. for Power, pp.387-400, 1959.

15. Lieblein, S. Johnston, I. — *Resume of Transonic Compressor Research at NASA-Lewis Laboratory*, Trans. of the ASME, Journal of Eng. for Power, p.322, 1961.

16. Swan, W.C. — *A Practical Method of Predicting Transonic Compressor Performance*, Trans. of the ASME, Journal of Eng. for Power, pp.322-330, 1961.

17. Koch, C.C. Smith, L.H. — *Loss Sources and Magnitudes in Axial-Flow Compressors*, Trans. of the ASME, Journal of Eng. for Power, p.411, 1976.

18. Jansen, W. Moffatt, W.C. — *The Off-Design Analysis of Axial-Flow Compressors*, Trans. of the ASME, Journal of Eng. for Power, pp.453-462, 1967.

19. Creveling, H.F. — *Axial-Flow Compressor Computer Program for Calculating Off-Design Performance*, NASA CR 72472, 1968.

20. Howell, A.R. — *Development of the British Gas Turbine Unit*, Lecture: Fluid Dynamics of Axial Compressors, ASME Reprint, 1947.

21. Lieblein, S. Roudebush, W.H. — *Theoretical Loss Relations for Low-Speed Two-Dimensional-Cascade Flow*, NASA TH-3662, 1956.

22. Miller, G.R. Lewis, G.W. Harmann, M.J. — *Shock Losses in Transonic Compressor Blade Rows*, Trans. of the ASME, Journal of Eng. for Power, p.235, 1961.

23. Schrieber, H.A.
Starken, H.
Experimental Cascade Analysis of Transonic Compressor Rotor Blade Section, ASME, 83-GT-209, 1983.

24. Bullock, R.O.
Critical High Lights in the Development of The Transonic Compressor, Trans of the ASME, Journal of Eng. for Power, p.243, 1961.

25. Horlock, J.H.
Shaw, R.
Pallard, D.
Lewkowicz, A.
Reynolds Number Effects in Cascades and Axial-Flow Compressors, Trans of the ASME, Journal of Eng. for Power, p.236, 1964.

26. Urasek, D.C.
Gorrell, W.T.
Cunnan, W.S.
Performance of Two-Stage Fan Having Low-Aspect-Ratio, First-Stage Rotor Blading, NASA TR-78-49, NASA TP-1493, 1979.

27. Koch, C.C.
Bilwakesh, K.R.
Doyle, V.L.
Evaluation of Range and Distortion Tolerance for High Mach Number Transonic Fan Stages, NASA CR-72964, 1971.

28. Wennerstrom, A.J.
De Rose, R.D.
Law, C.H.
Investigation of A 1500 Ft/sec., Transonic, High-Through-Flow, Single-Stage Axial Flow Compressor With Low Hub/Tip Ratio, AFAPL-TR-76-92, 1983.

29. Monsarrat, N.T.
Design Report Single Stage Evaluation of Highly Loaded High-Mach-Number Compressor stages, NASA N 69-30869, 1969.

30. Fottner, L.
Answer to Questionnaire on Compressor Loss and Deviation Angle Correlations, AGARD-PEP WG 12, 1972.

31. Carter, A.D.S.
Hughes, H.P.
A Theoretical Investigation into the Effect of Profile Shape on the Performance of Aerofoils in Cascade, ARC Rep. and Memo. 2384, 1950.

32. Carter, A.D.S.
The Low Speed Performance of Related Aerofoils in Cascades, ARC CP 29, 1950.

33. Crouse, J.E.
Computer Program for Definition of Transonic Axial Flow Compressor Blade Rows, NASA TN-D-7345, 1974.

34. Dettmering, W.
Machzahleinfluss auf die Verdichterscharakteristik, Z.Flujwiss., 19, pp.145-50, 1971.

35. Strinning, P.
Dunker, R.
Grundlagen des Auslegungsverfahrens und Vergleich Messung/Rechnung, Forschungs-berichte Verbiennungsskreftmaschinen, Heft 235, 1977.

36. Chauvin, J.
Sieverding, C.
Gripentrog, H.
Flow in Cascades with A Transonic Regime, Flow Research on Blading, Elsevier Publishing Company, 1979.

37. Üçer, A.Ş.
Yeğen, İ.
Durmaz, T.
A Quasi-Three-Dimensional Finite Element Solution for Steady Compressible Flow Through Turbomachines, Trans. of the ASME, Journal of Eng. for Power, pp.536-542, 1983.

38. Wu, C.H.
A General Theory of Three-Dimensional Flow in Subsonic and Supersonic Turbomachines of Axial, Radial and Mixed Flow Types, US NASA TN 2604, 1952.

39. Serovy, G.K.
Deviation Angle/Turning Angle Prediction for Advanced Axial-Flow Compressor Blade Row Geometries, AFAPL-TR-77, 1977.

40. Çetin, M.
An Investigation on Losses and Deviations in Axial Flow Compressors, M.Sc. Thesis METU, 1985.

41. Calvin, L.B.
et al.
End Wall Boundary Layer Measurements in a Two-Stage Fan, AGARD CP 351, 1983.

42. Abernethy, R.B.
Fluid Flow Measurement Uncertainty, ISO Draft, ISO TC 30 SC9, 1981.

APPENDIX I

NOTATION AND CASCADE TERMINOLOGY

A_a	Annulus area of the streamtube
A_p	Annulus area contraction ratio
c	Chord length
C_D	Drag coefficient
C_f	Skin friction coefficient
C_{p_1}	Local static pressure coefficient
D	Diffusion ratio
h	Blade height
H	Form factor (δ^*/θ)
i	Angle of incidence (^{o})
La	Laval number
m	Correction factor for deviation
M	Mach number
r	Radius
p	Pressure
R	Gas constant for air
Re	Reynolds number
R_u	Suction surface radius of curvature
s	Pitch length
S	Entropy
t	Blade thickness
V	Velocity relative to blade row
V_{max}	Maximum suction surface velocity
W_m	Meridional velocity

Greek Letters

α	Angle of attack (^{o})
β	Fluid angle (^{o})
γ	Ratio of specific heats
δ	Deviation angle (^{o})
δ^{*}	Displacement thickness , **Design deviation**
Γ	Circulation parameter
ϵ	Deflection angle (^{o})
θ	Momentum thickness
θ_{PM}	Prandtl-Meyer expansion angle (^{o})
κ	Blade angle (^{o})
ν	Prandtl-Meyer angle (^{o})
ξ	Stagger angle (^{o})
ρ	Density
σ	Solidity
Φ	Camber angle (^{o})
$\bar{\omega}$	Loss coefficient
ω	Rotational speed (rad/sec)

Subscripts

1	Inlet condition
2	Outlet condition
1s	Upstream of shock wave
2s	Downstream of shock wave
a	Sonic condition
c	Based on chord length
ch	Choke condition
cl	Clearance
com	Compressible
COR	Corrected value
CR	Critical condition

eq	Equivalent
inc	Incompressible
LE	Leading edge
m	Average (based on mean velocity vector or at mean radius)
md	Modified
min	Minimum
p	Profile
ref	Reference
s	Shock
st	Stall
T	Total
TE	Trailing edge
thr	Throat
z	Axial direction
θ	Tangential direction

Superscripts

*	Design condition
"	Corrected values
-	Arithmetic average
Λ	Pitch average

BLADE AND CASCADE TERMINOLOGY

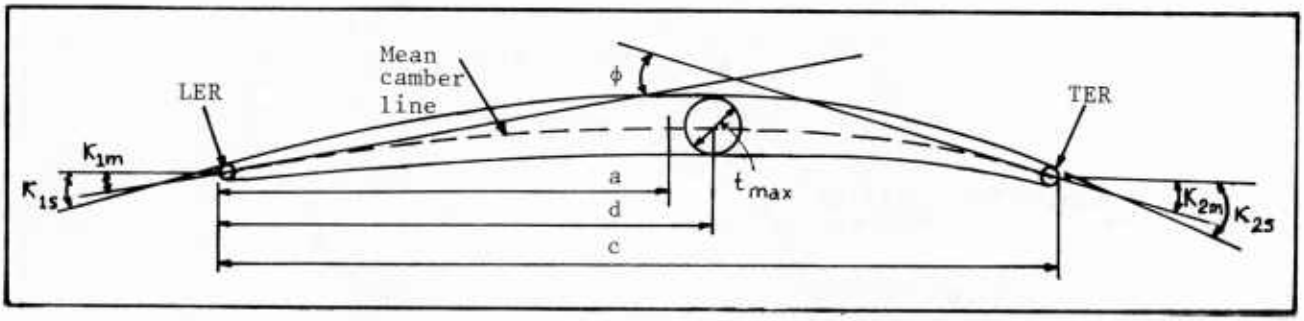

Fig.I.1 Blade Section Profile Terminology

a	Location of maximum camber
d	Location of maximum thickness
c	Chord Length
κ_{1S}	Angle between blade-element suction-surface leading edge tangent line on conical surface and meridional plane referenced to leading edge
κ_{2S}	Angle between blade-element suction-surface trailing edge tangent line on conical surface and meridional plane, referred to trailing edge
κ_{1m}	Angle between blade-element mean camber line on the conical surface and meridional plane, referred to leading edge
κ_{2m}	Angle between blade-element mean camber line on the conical surface and meridional plane, referred to trailing edge
Φ	Total Camber Angle
t_{max}	Maximum blade thickness
LER	Leading edge radius
TER	Trailing edge radius

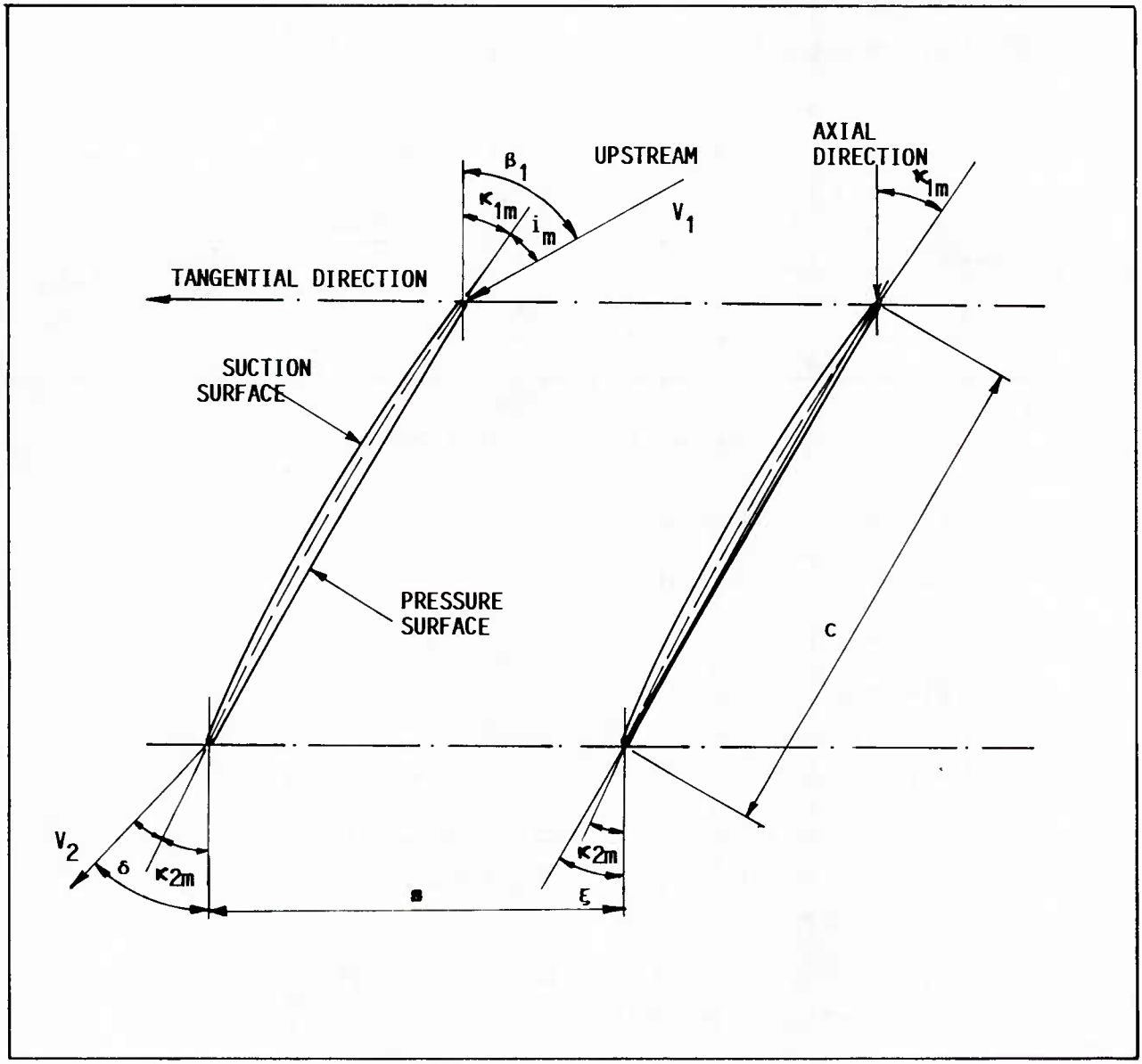

Fig. I.2 Cascade Terminology

s	Pitch length
V_1	Air inlet velocity
V_2	Air outlet velocity
β_1	Air inlet angle
β_2	Air outlet angle
ξ	Stagger (setting) angle
σ	Solidity (chord length/pitch length)
ϵ	Deflection, difference between air inlet angle and air outlet angle

i_m,i Mean incidence angle, angle between inlet-air direction and line tangent to blade mean camber line at leading edge

δ Deviation angle, angle between exit-air direction and tangent to blade mean camber line at trailing edge

The dependent parameters, listed above, may also be expressed in arithmetical form;

$$\Phi = \kappa_{1m} - \kappa_{2m}$$

$$\sigma = \frac{C}{S}$$

$$\varepsilon = \beta_1 - \beta_2$$

$$\delta = \beta_2 - \kappa_{2m}$$

$$i_m = \beta_1 - \kappa_{1m}$$

Sometimes it is convenient to define incidence angle with respect to suction surface. As shown in the magnified form of the leading edge (Figure I.3). Suction-surface incidence angle is denoted as the angle between inlet-air direction and the line tangent to the blade-suction-surface. The relation between i_{ss} and i_m is given as

$$i_m = i_{ss} + (\kappa_{1S} - \kappa_{1m})$$

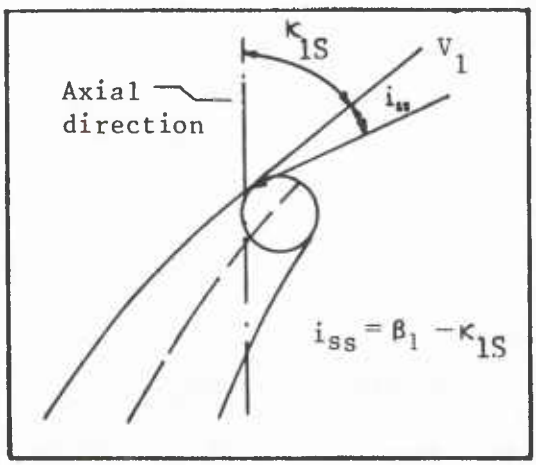

Fig. I.3 Definition of Suction-Surface Incidence Angle

APPENDIX II

CORRELATIONS AND CALCULATION PROCEDURE

The table of correlations given in the following pages are complied from the relevant references on design and off-design loss and deviation correlations present in the open literature. The first column of the table gives the references from which the correlations are taken. The second column containes the equation numbers. Since some of the equations are repeated in the different correlations, such equations are referred to by the equation numbers. The third column gives the correlation formulea together with the calculation procedure. The sequence of computation is indicated by giving each step a number. In most cases, for obtaining the required result from a correlation several empirical coefficients are needed. These coefficients in most of the cases are given in a graphical form. The figure numbers in column 3 of the table are the figure numbers of the original publications (references in column 1). The last column under the heading "remarks" include information with regard to the applicability of the correlations to different flow conditions and blade geometry.

TABLE OF CORRELATIONS

Ref.	Eq'n No	CORRELATION FORMULAE & PROCEDURE	REMARKS
[9]		PROFILE LOSSES	
	(1)	1) Calculate, $D = 1 - \frac{V_2}{V_1} + \frac{\lvert\Delta V_\theta\rvert}{2\sigma V_1}$	Blading NACA65 Series Low speed application. Correction for Re & M. Reasonable results up to $Re_c < 2.5\times10^5$. Design only.
		2) $(\frac{\theta}{c})^* = f(D^*)$ (Fig.148, p.204) and H = 1.1	
	(2)	3) $\bar{\omega} = 2(\frac{\theta}{c})\frac{\sigma}{\cos\beta_2}(\frac{\cos\beta_1}{\cos\beta_2})^2 . \{\frac{\frac{2H}{3H-1}}{\left[1-(\frac{\theta}{c})\frac{\sigma H}{\cos\beta_2}\right]^3}\}$	
		4) Correct, $\bar{\omega} = f(Re_c, \text{Blade})$ (Fig.152, p.206) $\bar{\omega} = k_c\bar{\omega}$, $k_c = f(M_2, H_{inc})$ (Fig.156)	
[13]	(3)	1) Calculate, $D_{eq} = \left[1.12+a(\alpha-\alpha^*)^{1.43}+0.61\frac{\cos^2\beta_1}{\sigma}(\tan\beta_1-\tan\beta_2)\right]\frac{\cos\beta_2}{\cos\beta_1}$	Incompressible. a = 0.0117 (for 65-series) a = 0.007 (for C.4 series) Design & off-design.
		2) $(\frac{\theta}{c}) = f(D_{eq})$ (Fig.15) and H = 1.08	
		3) Substitute into eq'n(2) for $\bar{\omega}$	
[14]	(4)	1) $(\frac{\theta}{c}) = \frac{C_f'}{1-k_s \ln(\frac{V_{max}}{V_2})}$	Incompressible. V_{max} occurs near the leading edge.
		2) The values of k_s & C_f' from Table 2, H = 1.08	
		3) Substitute into eq'n(2)for $\bar{\omega}$	
[16]	(5)	1) Calculate, $D_{eq} = \frac{\cos\beta_2}{\cos\beta_1}\left[\frac{V_{z1}}{V_{z2}}\right. 1.12+a(\alpha-\alpha^*)^{1.43}+0.61\frac{\cos^2\beta_2}{\sigma} . .(\tan\beta_1-\frac{r_2V_{z2}}{r_1V_{z1}}\tan\beta_2-\frac{r_1\omega}{V_z}(1-\frac{r_2^2}{r_1^2}))\left.\right]$ For design $(\alpha-\alpha^*) = 0$ and $D_{eq} = D_{eq}^*$	NACA65 and C.4 series. Design & off-design. For transonic case off-design depends on M. Spanwise correction for $(\frac{\theta}{c})$ Leakage & secondary losses partly taken into account. a = 0.017 (65 series) a = 0.007 (C.4 series)
		2) Correct, $(\frac{\theta}{c})^* = f(D_{eq}^*, \text{radial pos.})$ (Fig.2)	
	(6)	3) $\bar{\omega} = 2(\frac{\theta}{c})\cdot\frac{\sigma}{\cos\beta_2}\cdot(\frac{\cos\beta_1}{\cos\beta_2})^2$	
		Off-design: $(\frac{\theta}{c})-(\frac{\theta}{c})^* = (0.827M_1-2.692M_1^2+2.675M_1^3)(D_{eq}-D_{eq}^*)^2$, $D_{eq}>D_{eq}^*$	
		$(\frac{\theta}{c})-(\frac{\theta}{c})^* = (2.80M_1-8.71M_1^2+9.36M_1^3)(D_{eq}-D_{eq}^*)^2$, $D_{eq}<D_{eq}^*$	

Ref.	Eq'n No	CORRELATION FORMULAE & PROCEDURE	REMARKS
[29]	(7)	1) Calculate, $D^* = 1 - \frac{V_2}{V_1} + \frac{r_1 V_{\theta 1} - r_2 V_{\theta 2}}{(r_1+r_2)V_1\sigma}$	Tip clearance, secondary, end-wall B.L losses partly included.
		2) $(\frac{\theta}{c})^* = f(D^*, \%\ \text{SPAN})$ for rotors (fig.6)	
		$(\frac{\theta}{c})^* = f(D^*, \%\ \text{SPAN})$ for stators (fig.7)	
	(8)	3) $\bar{\omega}^*_{inc} = \frac{2\sigma}{\cos\beta_2^*}(\frac{\theta}{c})^*$	Desing only.
	(9)	1) Calculate, $D^* = 1 - \frac{V_2}{V} + \frac{\Delta V_\theta}{2\sigma V_1}$	
	(10)	2) $(\frac{\theta}{c})^* = 0.003 + 0.02375\ D^* - 0.05\ D^{*2} + 0.125\ D^{*3}$	
		3) Use eq'n (6) for $\bar{\omega}^*$	
[18]		Off-design :	
	(11)	1) Determine M_{1CR}, $(\frac{V_{max}}{V_1})^2 - 1 = \frac{1-(\frac{2}{\gamma+1} + \frac{\gamma-1}{\gamma+1} M_{ICR})^{\gamma/\gamma-1}}{(1+\frac{\gamma-1}{2} M^2_{ICR})^{\gamma/\gamma-1} - 1}$ where,	NACA 65 series, DCA, PCA For Transonic Flows. Design & Off-design. M_{1CR} can be approximated as, $M_{1CR} \cong 0.7$
	(12)	$\frac{V_{max}}{V_1} = 1 + (0.4 + \frac{t}{c})(\frac{\Delta V_\theta}{\sigma V_1}) + 0.03 + 0.7\frac{t}{c}$	
	(13)	2) If $M_1 > M_{1CR}$, correct $\bar{\omega}^*$ as, $\bar{\omega}^*_{COR} = \bar{\omega}^*[2(M_1 - M_{1CR}) + 1]$	For off-design operation, a parabolic variation of loss with incidence is assumed.
	(14)	3) Correct flow angles (if $M_1 > M_{1CR}$) $\beta''_{1st} = \beta_{1st}$; $\beta''_{1ch} = \beta_{1ch} + 1.5\,\Delta\beta$; $\beta_1{}^{*''} = \beta_1{}^* + \Delta\beta$ where, $\Delta\beta = 10.M_1 - 7.$	Choke and stall conditions are reached when, $\bar{\omega} = 2.\bar{\omega}^*$
	(15)	4) Then, off-design losses, $\bar{\omega} = \bar{\omega}^{*''}.(0.8333\ \bar{s}^2 + 0.1667\ \bar{s} + 1.0)$ where, $\bar{s} = \frac{\beta_1 - \beta_1{}^*}{\beta_{1ch} - \beta_1{}^*}$ for $\beta_1 < \beta_1{}^*$; $\bar{s} = \frac{\beta_1 - \beta_1{}^*}{\beta_{1st} - \beta_1{}^*}$ for $\beta_1 > \beta_1{}^*$	
[30]	(16)	1) Calculate, $D^* = \frac{V_{max} - V_2}{V_1}$ where,	Incompressible.
	(17)	$\frac{V_{max}}{V_1} = 1.03 + (0.4 + \frac{t}{c})\frac{1}{\sigma}\frac{\Delta V_\theta}{V_1} + 0.7\frac{t}{c}$	Blade thickness arbitrarily specified.
	(18)	2) $(\frac{\theta}{c})^* = (6.6\frac{t}{c} + 0.34)(0.0088 + 0.0107D^* - 0.052D^{*2} + 0.116D^{*3})$	
		3) Use eq'n (6) for $\bar{\omega}^*_{inc}$	Design.
		4) For off-design, follow the eq'ns. (11), (12), (13), (14) but use a factor of 1.8 instead of 2.0 in eq'n.(13)	

Ref.	Eq'n No	CORRELATION FORMULAE & PROCEDURE	REMARKS
[35]		For $M_1 < 1$,	
	(19)	1) $D_{com} = (\frac{V_{max}}{V_1})_{com} - \frac{V_2}{V_1}$	Design only.
		where,	Covers up to $M_1 = 1.4$
	(20)	$(\frac{V_{max}}{V_1})_{com} = \frac{1}{M_1}\sqrt{\frac{\gamma+1}{\gamma-1}\left\{1-\left[1-(\frac{V_{max}}{V_1})^2_{inc}\,(1-(1-\frac{\gamma-1}{\gamma+1}M_1^2)^{\gamma/\gamma-1})\right]^{\gamma-1/\gamma}\right\}}$	At supersonic inlet flow, D is calculated assuming an equivalent subsonic flow ahead of the shock that leads to the same Mach number at the position just downstream of the shock.
		use eq'n.(17) for $(\frac{V_{max}}{V_1})_{inc}$	
		2) for $(\frac{\theta}{c})^*$ and $\bar{\omega}^*$ use eq'ns.(18)&(6) respectively.	
		For $M_1 > 1$,	
	(21)	1) $V_1'' = \frac{V_1}{M_1^2}$	
		2) $(\frac{\Delta V_\theta}{V})'' = \frac{V_{\theta 1} - V_{\theta 2} \cdot M_1^2}{V_1}$	
		3) Substitute the corrected values into eq'ns.(17)&(20)	
	(22)	4) $D_{com} = (\frac{V_{max}}{V_1})''_{com} - \frac{V_2}{V_1''}$	
		5) for $(\frac{\theta}{c})^*$ and $\bar{\omega}^*$, use eq'ns.(18)&(6) respectively.	
[17]		1) Calculate,	
	(23)	$D^*_{eq} = \frac{V_1}{V_2}\left[(\sin\beta_1 - K_1\sigma\Gamma^*)^2 + (\frac{\cos\beta_1}{A_p^*\,\rho^*})^2\right]^{1/2}(1+K_3\,\frac{t}{c}+K_4\Gamma^*)$	
		where,	
	(24)	$\Gamma^* = \frac{r_1 V_{\theta 1} - r_2 V_{\theta 2}}{(\frac{r_1+r_2}{2})\,\sigma\,V_1}$, $\rho^* = 1 - \frac{M_{z_1}^2}{1-M_{z_1}^2}(1-A_p^* - K_1\,\frac{\tan\beta_1}{\cos\beta_1}\,\sigma\Gamma^*)$	Desing only.
	(25)	$A_p^* = (1-\frac{K_2\sigma\frac{t}{c}}{\cos\bar{\beta}})(1-\frac{A_{a_1}-A_{a_2}}{3A_{a_1}})$, $\bar{\beta} = \frac{\beta_1+\beta_2}{2}$	Compressibility, M, Re, streamtube contraction are taken into account.
		2) $D^*_{eq} \xrightarrow{\text{Fig.2a-b}} (\frac{\theta}{c})$, H_{TE}	
		3) D^*_{eq}, $M_1 \xrightarrow{\text{Fig.3}} (\frac{\theta}{c})$, H (correction for M_1)	
		4) D^*_{eq}, $\frac{h_1}{h_2} \xrightarrow{\text{Fig.4a-b}} (\frac{\theta}{c})$, H (correction for streamtube height variations)	$K_1 = 0.2445$
		5) If $Re_c > 10^6$, a final correction for Re_c	$K_2 = 0.4458$
		- Obtain k_s from Appendix 2.	$K_3 = 0.7688$
		- Enter Fig.5 with k_s & Re_c and correct $(\frac{\theta}{c})$	$K_4 = 0.6024$
		6) Use eq'n(2) for calculating $\bar{\omega}^*$.	

Ref.	Eq'n No	CORRELATION FORMULAE & PROCEDURE	REMARKS
[20]		For $\frac{i-i^*}{\Delta\beta^*} < 0$	
	(26)	1) $\bar{\omega}_T = \frac{\sigma\cos^2\beta_1}{\cos^3(\frac{\beta_1+\beta_2}{2})} \left[0.017+0.91 \left\|\frac{i-i^*}{\Delta\beta^*}\right\|^{4.23}\right]$	Off-design only.
		For $\frac{i-i^*}{\Delta\beta^*} \geq 0$	
	(27)	2) $\bar{\omega}_T = \frac{\sigma\cos^2\beta_1}{\cos^3(\frac{\beta_1+\beta_2}{2})} \left[0.017+0.423 \left(\frac{i-i^*}{\Delta\beta^*}\right)^{3.5}\right]$	
[19]		1) Calculate $\bar{\omega}_T^*$ from any of design loss correlations (the method described in reference [17] is recommended)	
		2) For $M_1 < 0.6$	
	(28)	$\bar{\omega}_T = \bar{\omega}_T^* + 0.0005\ (i-i^*)^2$	Off-design.
		3) For $0.6 \leq M_1 \leq 0.95$	
	(29)	$\bar{\omega}_T = \bar{\omega}_T^* + (-0.0055+0.01\ M_1)\ (i-i^*)^2$	
		4) For $M_1 > 0.95$	
	(30)	$\bar{\omega}_T = \bar{\omega}_T^* + (-0.0594+0.0667\ M_1)\ (i-i^*)^2$	
		SHOCK LOSSES	
	(31)	1) $La_{1CR} = \sqrt{\frac{\gamma+1}{\gamma-1}\left\{1-\left[\frac{(\frac{2}{\gamma+1})^{\gamma/\gamma-1}\ (Cp_1)_{min}}{1-(Cp_1)_{min}}\right]^{\gamma-1/\gamma}\right\}}$	
	(32)	2) $(Cp_1)_{min} = 1 - (\frac{V_{max}}{V_1})_{inc}$ where,	
[18]	(33)	$(\frac{V_{max}}{V_1})_{inc} = 1.03 + (\frac{t}{c} + 0.4)\ \sigma\frac{\Delta V_\theta}{V_1} + 0.7\ \frac{t}{c}$	
[17]	(34)	or, $\frac{V_{max}}{V_1} \simeq \frac{V_{max}}{V_{thr}} = 1+0.7688\ \frac{t}{c} + 0.6024\ \sigma\ \frac{\Delta V_\theta}{V_1}$	
	(35)	3) $M_{1CR} = \frac{La_{1CR}}{\sqrt{0.5\left[1+\gamma-(\gamma-1)\ La_{1CR}^2\right]}}$	
[18]	(36)	<u>Supercritical subsonic inlet conditions</u>: 4) $\bar{\omega}_T = \bar{\omega}_p + \bar{\omega}_s = \bar{\omega}_{p,inc}\left[2.0\ (M_1-M_{1CR})+1\right]$	Taking into account the compressibility effect on $\bar{\omega}_p$ as well as the losses due to local shocks.

Ref.	Eq'n No	CORRELATION FORMULAE & PROCEDURE	REMARKS
[34]	(37)	4) $\bar{\omega}_T = \bar{\omega}_p + \bar{\omega}_s = \bar{\omega}_{p,inc} \left\{ 1.4 \left[M_1 - (M_{1CR} - 0.4)^3 \right] + 1 \right\}$	For DCA profiles $\bar{\omega}_{p,inc}$ is given in eq'n.8
	(38)	1) $\bar{M}_{1s} = \frac{1}{2} (M_{1s} + 1.0)$	
	(39)	2) $(1 - \frac{P_{02s}}{P_{01}}) = \bar{La}_{1s} \left[\frac{1 - \frac{\gamma-1}{\gamma+1} La_{1s}^2}{1 - \frac{\gamma-1}{\gamma+1} \frac{1}{La_{1s}^2}} \right]^{1/\gamma-1}$	The shock losses are calculated from the pressure distribution.
[11]		where La is calculated using (31), but using the values at shock location instead of minimum ones,	
	(40)	$\bar{La}_{1s} = \frac{1}{2} (La_{1s} + 1)$	
	(41)	3) Pitch averaged total pressure at the exit of the cascade,	
	(42)	$\frac{\hat{P}_{02}}{P_{01}} = 1 - \frac{M_{1s} - 1}{M_{1s} - M_1} \left(1 - \frac{P_{02s}}{P_{01}} \right)$	
		Supersonic inlet conditions:	
	(43)	1) $Ru = \frac{t_{LE}}{2} + \left[\frac{\{ \frac{t_{max}}{2} - \frac{t_{LE}}{2} + \left[\frac{c}{2} - \frac{t_{LE}}{2} \right] \tan(\frac{\theta}{4}) \}^2 + \{ \frac{c}{2} - \frac{t_{LE}}{2} \}^2}{2\{ \left[\frac{c}{2} - \frac{t_{LE}}{2} \right] \tan(\frac{\theta}{4}) + \frac{t_{max}}{2} - \frac{t_{LE}}{2} \}} \right]$	
	(44)	2) The Prandtl-Meyer expansion angle is, $\theta_{PM} = \tan^{-1} \left[\frac{s.\sin\beta_1}{s.\cos\beta_1 + Ru} \right]$	
[16]	(45)	3) The Prandtl-Meyer angle is, $\nu_1 = \frac{\gamma+1}{\gamma-1} \{ \tan^{-1} \frac{\gamma-1}{\gamma+1} (M_1^2 - 1)^{1/2} \} - \tan^{-1} (M_1^2 - 1)^{1/2}$	
	(46)	4) After the wave, the Mach number is given by, $M_{1s} = f(\nu_1 + \theta_{PM}) = f(\nu_{1s})$	
		or,	
	(47)	$M_{1s} \tilde{=} 1.0 + (0.0432)\, \nu_{1s}$	
	(48)	5) The normal shock entry Mach number is, $\bar{M}_{1s} = \frac{1}{2} (M_1 + M_{1s})$	
	(49)	6) From normal shock tables, with $\bar{M}_{1s}$, find the value of P_{02s}/P_{01s} $\bar{\omega}_s = \frac{P_{01s} - P_{02s}}{P_{01s} - P_1} = \frac{1 - P_{02s}/P_{01s}}{1 - P_1/P_{01s}}$	

Ref.	Eq'n No	CORRELATION FORMULA & PROCEDURE	REMARKS
[17]	(50)	1) Losses due to leading edge bluntness is given in terms of entropy rise, $\frac{\Delta S}{R} = -\ln\{1-t_{LE}/(s.\cos\beta_1).[1.28(M_1-1)+0.96(M_1-1)^2]\}$ 2) Shock losses due to normal and oblique shocks are given in figure 7.	There exist 3 types of shock losses, 1- Due to leading edge bluntness 2- Due to normal passage shock 3- Due to oblique shock.
		DEVIATION	
[32]	(51)	1) Base equation is given as $\delta^* = m\phi\sqrt{\frac{s}{c}}$ 2) m = m (profile shape, ξ) Fig. A.3 in [11] or Ref. [32]	
[29]	(52)	1) Modified base equation is given as $\delta^*_{md} = \frac{(\varepsilon-i)\, m_{md}\sqrt{\frac{s}{c}}}{1 - m_{md}\sqrt{\frac{s}{c}}}$ 2) $m_{md} = 0.92\,(\frac{a}{c})^2 + 0.002\,\bar{\beta}_2$ or,	ε fluid turning angle degrees. $\bar{\beta}_2$ average fluid angle at cascade exit measured from axial direction, degrees.
[33]	(53)	$m_{md} = (0.219 + 0.0008916\,\xi + 0.00002708\,\xi^2).$ $.(\frac{2a}{c})^{2.175-0.03552\xi + 0.0001917\xi^2}$	
[9]	(54) (55) (56)	1) Base equation is given as, $\delta^o_{ref} = \delta^o_o + \frac{m_{\sigma=1}}{\sigma^6}\phi$ 2) $\delta^o_o = (K_\delta)_{sh}\,(K_\delta)_t\,(\delta^o_o)_{10}$ 3) For off-design $\delta^o = \delta^o_{ref} + (i-i_{ref})(\frac{d\delta}{di})_{ref}$	$(\delta^o_o)_{10}$= f(β,σ)(Fig.161,SP-36) $m_{\sigma=1}$= f(β_1) (Fig.163,SP-36) b = f(β_1) (Fig.164, SP-36) $(K_\delta)_t$= f($\frac{t}{c}$) (Fig.172, SP-36) $(K_\delta)_{sh}$= f(Blade shape)(SP-36) = 1.1 (for C series) $(\frac{d\delta}{di})_{ref}$=f($\beta_1$,σ)(Fig.177,SP-36)
[11]	(57) (58) (59) (60) (61) (62)	1) Base equation is given as $\varepsilon = K_1.K_2\left[\frac{K_3\phi}{1000} + B\right]$ where, $K_3 = (5-2\,\frac{s}{c})\sqrt{\xi^2-1000\,\frac{s}{c}} + 100\,(5.5 - 2.6\,\frac{s}{c})$ $B = 8\,(\frac{s}{c})^2 - 17\,\frac{s}{c} + 16$ $K_1 = 1-0.28\,(\bar{x}_c - 0.40)$ for $\bar{x}_c$ = 0.3 to 1.0 $K_2 = 1-0.016\,(10-\bar{c})$ for $\bar{c}$ = 1.25 to 12.5% at base incidence $i_o = \kappa_{1m,\theta} - \sin^{-1}\frac{F\Gamma}{s}$	$\bar{c} = \frac{\text{Maximum thickness}}{\text{Length of camberline}}$ $\bar{x}_c = \frac{\text{Location of max.thickness}}{\text{Lenth of camberline}}$ $\kappa_{1m,\theta}$= Blade angle at LE (measured from tangential direction) F_Γ = minimum flow blade passage width (throat)

Ref.	Eq'n No	CORRELATION FORMULAE & PROCEDURE	REMARKS
[18]		1) Correct design air inlet angle for Mach number,	For off-design. The method suggested by Lieblein [13] is used with corrections applied for M_1, streamline slope and axial velocity. α = streamline slope.
	(63)	$(\beta_1^*)' = \beta_1^* + 10\,M_1 - 7.0$ for $M_1 > 0.7$	
	(64)	$(\beta_1^*)' = \beta_1^*$ for $M_1 \leq 0.7$	
		2) Corrections for streamline slope & axial velocity variation are applied as,	
	(65)	$\tan(\beta^*_{i_{cor}}) = \dfrac{2\tan\left[(\beta_1^*)'/\cos\alpha\right]}{(1+\frac{W_{m_2}}{W_{m_1}})}$	
		3) Assuming the air turning angle varies linearly with incidence in minimum-loss region,	
	(66)	$\beta_{2_e} = \beta_1 - \Delta\beta = \beta_1 - \{\Delta\beta^* + \left[\frac{d(\Delta\beta)}{di}\right]^* (i-i^*)\}$	
		where, $\Delta\beta^* = \phi - \delta^* + i^*$	
	(67)	$\left[\frac{d(\Delta\beta)}{di}\right]^* = 0.4805 + (0.00407 - 1.38\times10^{-4})\beta_{1_{COR}}^* + (0.698 - 0.005\,\beta^*_{i_{COR}} + 1.51\times10^{-4}\,\beta^{*2}_{i_{COR}})\sigma + (-0.226 + 0.00152\,\beta^*_{i_{COR}} - 0.431\times10^{-4}\,\beta^{*2}_{i_{COR}})\sigma^2$	
	(68)	4) $\tan\beta_2 = \frac{1}{2}\{\frac{1}{W_{m_2}/W_{m_1}} + 1\}\tan(\beta_{2_e}\cos\alpha)$	
	(69)	5) $\delta = \beta_2 - (\kappa_1 - \phi)$	
[16]	(70)	1) $\delta = \delta^* + \left[6.40 - 9.45\,(M_1 - 0.6)\right](D_{eq} - D^*_{eq})$	For off-design. For DCA Blading δ^* may be obtained from either [9] or [32]
[19]	(71)	1) $\frac{\delta-\delta^*}{\Delta\beta^*} = f(x)$	For off-design.
		2) for $x \geq 0$	
	(72)	$f(x) = -0.809\times10^{-3} + 0.5588x - 0.2928x^2$	
		for $x < 0$	
	(73)	$f(x) = 0.1191\times10^{-3} + 0.480x + 0.3452x^2$	
		where,	
	(74)	$x = \frac{i-i^*}{\Delta\beta^*}$	
[20]	(75)	1) $\beta_2 = \beta_1 - \Delta\beta^*\{f(x)\}$	For off-design.
		2) for $x \geq 0$,	
	(76)	$f(x) = 1.0 + 0.86x - 1.36\,x^2$	
		for $x < 0$,	
	(77)	$f(x) = 1.0 + 0.86x - 0.35\,x^2$	
		3) where x is defined by equation (74)	

APPENDIX III

DATA UNCERTAINTY

Table III.1 lists the precision errors given in the reports on which the work explained in this report is based on. It was not possible to apply uncertainty analysis to the averaging procedures due to the lack of relevant data. However, the uncertainty limits given in the table is propagated through the equation 2.2, (Section 2) which is used for loss coefficient calculations. The precision index for the loss coefficient (S_{ω_T}) is calculated using Taylor series expansion [43]

$$S_{\bar{\omega}_T} = \sqrt{\left(\frac{\partial \bar{\omega}_T}{\partial po_1} S_{po_1}\right)^2 + \left(\frac{\partial \bar{\omega}_T}{\partial po_2} S_{po_2}\right)^2 + \left(\frac{\partial \bar{\omega}_T}{\partial \omega} S_{\omega}\right)^2 + \left(\frac{\partial \bar{\omega}_T}{\partial T_{01}} S_{T_{01}}\right)^2 + \left(\frac{\partial \bar{\omega}_T}{\partial r_2} Sr_2\right)^2 + \left(\frac{\partial \bar{\omega}_T}{\partial r_1} Sr_1\right)^2} \qquad \text{(III.1)}$$

The partial derivatives in the above equation are evaluated from equation 2.2 and precision index of the loss coefficient is calculated for 197 sample points of reference [1]. If was found out that the maximum occurance is at the precision error of $\pm$ 1.78 % on the total loss. In this calculation the precision error of r_1 and r_2 are taken as $\pm$ 0.33 mm.

For analysing the effect of mislocating the streamline, a single operating point is chosen and it is assumed that the upstream location of the streamline is correct. The downstream radius is then changed between $\pm$ 0.5 cm along the span. For each downstream spanwise streamline location, thermodynamic quantities measured at the corresponding location are taken. The precision errors on the measured quantities and on r_2 are then used in Equation III.1. The change of uncertainty interval due to the mislocation of the downstream point of the streamline can be seen in Figure III.1. The figure shows that the precision index $S_{\bar{\omega}_T}$ reduces $\pm$ 0.04 % when the streamline position is misplaced by 0.5 cm towards the bub of the blade. If the streamline is misplaced by 0.5 cm towards the tip of the blade the precision index on $\bar{\omega}_T$ increases by

APPENDIX IV

SUBROUTINE FOR THE NEW LOSS AND DEVIATION SET

The following subroutine is prepared in FORTRAN IV language and used in the throughflow computer code for performance prediction.

```
      SUBROUTINE CASCADE(AA1,AA2,ALPA,CAM,CODE,CORD,ET1,ET2,
     1GM,H1H2,LER,MIN,OMEGA,PH1,PH2,P1,PO1,R1,R2,RO1,SOL,T1X,
     2TRAT,WM1,WM2,WZ1,WZ2,XBET1,XKAP1,DEV,PLOD)
      IMPLICIT REAL*8(A-H,O-Z)
      DIMENSION HOHM(4),TOTM(4),DFACT(4),HOHH(4)
      REAL*8  MIN,KAP1,INCH
C-------------------------------------------------------------C
C     FOLLOWING DATA SHOULD BE SUPPLIED TO SUBROUTINE CASCADE  C
C                                                              C
C       AA1    : ANNULUS AREA AT THE INLET                     C
C       AA2    : ANNULUS AREA AT THE EXIT                      C
C       ALPA   : STREAMLINE SLOPE                              C
C       CAM    : CAMBER ANGLE                                  C
C       CODE   : 1 SPECIFIES ROTORS ; 2 SPECIFIES STATORS      C
C       CORD   : CHORD LENGTH                                  C
C       ET1    : DIMENSIONLESS RADIUS AT THE INLET             C
C       ET2    : DIMENSIONLESS RADIUS AT THE EXIT              C
C       GM     : RATIO OF SPECIFIC HEATS                       C
C       H1H2   : STREAMTUBE HEIGHT RATIO                       C
C       LER    : BLADE LEADING-EDGE RADIUS                     C
C       MIN    : RELATIVE INLET MACH NUMBER                    C
C       OMEGA  : ANGULAR SPEED                                 C
C       PH1    : FLOW COEFFICIENT AT THE INLET                 C
C       PH2    : FLOW COEFFICIENT AT THE EXIT                  C
C       P1     : INLET STATIC PRESSURE                         C
C       PO1    : INLET TOTAL PRESSURE                          C
C       R1     : RADIUS AT THE INLET                           C
C       R2     : RADIUS AT THE EXIT                            C
C       RO1    : INLET DENSITY                                 C
C       SOL    : SOLIDITY                                      C
C       T1X    : INLET TEMPERATURE                             C
C       TRAT   : BLADE THICKNESS TO CHORD RATIO                C
C       WM1    : MERIDIONAL VELOCITY AT THE INLET              C
C       WM2    : MERIDIONAL VELOCITY AT THE EXIT               C
C       WZ1    : AXIAL VELOCITY AT THE INLET                   C
C       WZ2    : AXIAL VELOCITY AT THE EXIT                    C
C       XBET1  : AIR ANGLE AT THE INLET                        C
C       XKAP1  : BLADE ANGLE AT THE INLET                      C
C                                                              C
C-------------------------------------------------------------C
C                                                              C
C                          OUTPUTS ARE ;                       C
C       DEV    : OFF-DESIGN DEVIATION ANGLE                    C
C       PLOD   : OFF-DESIGN LOSS COEFFICIENT                   C
C                                                              C
C-------------------------------------------------------------C
C                                                              C
C    KOUT SPECIFIES OFF-DESIGN DEVIATION ANGLE CALCULATION METHOD C
C       KOUT=1 MOFFAT(LIEBLEIN+CORRECTIONS)                    C
C       KOUT=2 SWAN                                            C
C       KOUT=3 CREVELING                                       C
C       KOUT=4 HOWELL                                          C
C                                                              C
C-------------------------------------------------------------C
C                                                              C
C    KSER SPECIFIES THE TYPE OF PROFILE                        C
C      KSER=1  DCA PROFILES                                    C
C      KSER=2  MCA PROFILES                                    C
C                                                              C
C-------------------------------------------------------------C
```

```
C*************************************************************************
C********************** PRELIMINARIES ************************************
C*************************************************************************
C
      PI=3.141592
      DEG=PI/180.
      INCH=100./2.54
      KOUT=2
      KSER=2
      SH=0.7
      EQ=0.007
      BET1=DABS(XBET1)
      KAP1=DABS(XKAP1)
      STG=DABS(KAP1-CAM/2.)
      ACIN=XBET1-XKAP1
      XKS=0.0001*INCH
      CORD=CORD*INCH
      RTIP1=R1/ET1
      RTIP2=R2/ET2
C
C*************************************************************************
C********************** DESIGN INCIDENCE---AIN****************************
C*************************************************************************
C
C----------------- SP-36 DESIGN INCIDENCE (MODIFIED)
      B1M=KAP1
      SLP=(-.063+.02274*SOL)+(-.0035+.0029*SOL)*B1M+(-.379E-4-1.11E-5*
     1SOL)*B1M**2
      ZCI=(.0325-.0674*SOL)+(-.2364E-2+.0913*SOL)*B1M
     1+(1.64E-5-2.38E-4*SOL)*B1M**2
      COR=-6.19E-3+13.64*TRAT-93.7*TRAT**2+274.3*TRAT**3
      AIN=COR*SH*ZCI+SLP*CAM
      GO TO (100,200) KSER
  100 AIN=AIN+0.7238*MIN+7.5481
      GO TO 300
  200 AIN=AIN+1.3016*MIN+5.7380
  300 B1M=KAP1+AIN
C
C*************************************************************************
C********************** DESIGN DEVIATION---DEVM **************************
C*************************************************************************
C
C----------------- CARTERS DEVIATION RULE (MODIFIED)
      SC=0.216+9.72E-4*STG+2.38E-5*STG**2
      DEVM=SC*CAM/DSQRT(SOL)
      DEVM=-.1988183*DEVM**2+3.0186*DEVM-1.099379
C
C*************************************************************************
C*************************** PRELIMINARIES *******************************
C*************************************************************************
C
C ---COMPUTE THE FOLLOWING DESIGN PARAMETERS---
C       B1*, B2*, DELB*, DEG*
      DELBM=CAM-DEVM+AIN
      B2M=B1M-DELBM
      B1R=B1M*DEG
      B2R=B2M*DEG
      B1=BET1*DEG
      CSB1=DCOS(B1R)
      TNB1=DTAN(B1R)
```

```
      CSB2=DCOS(B2R)
      TNB2=DTAN(B2R)
C ---MINIMUM LOSS DIFFUSION FACTORS---
      AK1=ET2*PH2/(ET1*PH1)
C ---CORIOLLIS TERM---
      AK2=ET1/PH1*(1.0-(ET2/ET1)**2)
      IF(CODE.EQ.2) AK2=0.0
      AK3=EQ*(DABS(ACIN-AIN))*1.43
      V1V2=PH1*CSB2/(PH2*CSB1)
C
C*************************************************************************
C************ DESIGN TOTAL PRESSURE LOSS COEFFICIENT*********************
C*************************************************************************
C
C ---KOCH & SMITHS CORRELATION TO COMPUTE DESIGN LOSS---
      IF(CODE.EQ.2) OMEGA=0.0
      VTET2=OMEGA*R2-WM2*DTAN(B2R)
      VTET1=OMEGA*R1-WM1*DTAN(B1R)
      V1=DSQRT(VTET1**2+WM1**2)
      IF(CODE.EQ.1) V1=DSQRT((WM1*DTAN(B1R))**2+WM1**2)
C ---CALCULATE BLADE CIRCULATION PARAMETER---
      RAVE=(R1+R2)/2
      CIRC=(R1*VTET1-R2*VTET2)/(SOL*RAVE*V1)
      BETAV=(B1M+B2M)/2.0
      BETAVR=BETAV*DEG
      XMZ1=WZ1/DSQRT(GM*287.05*T1X)
C ---CALCULATE ANNULUS AREA CONTRACTION RATIO---
      AACR=(1.0-0.4458*SOL*TRAT/DCOS(BETAVR))*(1.0-((AA1-AA2)/
     1(3.0*AA1)))
      ROPRO1=1.-(XMZ1**2/(1.-XMZ1**2))*(1.-AACR-.2445*(DTAN(B1R)/
     1DCOS(B1R))*SOL*CIRC)
      VMAXVP=1.0+0.7688*TRAT+0.6024*CIRC
      VPV1=((DSIN(B1R)-0.2445*SOL*CIRC)**2+(DCOS(B1R)/(AACR*ROPRO1))**2
     +)**0.5
C ---CALCULATE DESIGN DIFFUSION FACTOR---
      DEQM=VPV1*VMAXVP*V1V2
      IF(DEQM.GT.2.) DEQM=2.0
C ---CALCULATE DESIGN MOMENTUM THICKNESS---
      DMTU=0.0216*DEQM**2-0.0557*DEQM+0.0406+0.0025
C ---CALCULATE FORM FACTOR---
      HTEU=2.047628*DEQM**2-4.902983*DEQM+4.2060615
      IF(DEQM.GE.2.) HTEU=2.6
C ---CORRECT DMT & HTE FOR INLET MACH NUMBER---
      HOHM(1)=0.297619*MIN**2+0.109226*MIN+0.99
      HOHM(2)=0.188988*MIN**2+0.069702*MIN+0.994
      HOHM(3)=0.140557*MIN**2+0.039275*MIN+0.9992
      HOHM(4)=0.088474*MIN**2+0.035108*MIN+0.9984
C
      TOTM(1)=-0.045103*MIN**2-0.018419*MIN+1.0035
      TOTM(2)=-0.08846*MIN**2-0.01967*MIN+1.004
      TOTM(3)=-0.110173*MIN**2-0.033056*MIN+1.004
      TOTM(4)=-0.120996*MIN**2-0.065324*MIN+1.006
C
      DFACT(1)=1.0
      DFACT(2)=1.3
      DFACT(3)=1.5
      DFACT(4)=1.7
C
      CALL INTERP(DFACT,HOHM,DEQM,HOHMX,4)
      CALL INTERP(DFACT,TOTM,DEQM,TOTMX,4)
```

```
C
      IF(DEQM.GT.1.7) HOHMX=1.0
      HTE=HTEU*HOHMX
      DMT=DMTU*TOTMX
C ---CORRECT DMT & HTE FOR STREAMTUBE CONTRACTION(H1H2)---
      DMT=DMT*(0.588235*H1H2+0.411765)
      HOHH(1)=-0.02143*H1H2+1.02143
      HOHH(2)=-0.00714*H1H2+1.00714
      HOHH(3)=0.04524*H1H2+0.95476
      HOHH(4)=0.15714*H1H2+0.84286
      CALL INTERP(DFACT,HOHH,DEQM,HOHHX,4)
      HTE=HTE*HOHHX
C ---CORRECT DMT FOR REYNOLDS NUMBER---
      XMU1=0.00001*(0.0045833*T1X+0.468751)
      XNU1=XMU1/RO1
      REX=(V1*CORD/INCH)/XNU1
      RROUGH=XKS/CORD
      IF(RROUGH.NE.0.) GO TO 222
 548  IF(REX.LE.200000.) TOTR=589.6*REX**(-0.5)
      IF(REX.GT.200000.) TOTR=10.0*REX**(-0.166)
      GO TO 333
 222  CONTINUE
      IF(RROUGH.GE.0.005) GO TO 111
      IF(RROUGH.GE.0.001) GO TO 544
      IF(RROUGH.GE.0.0005) GO TO 545
      IF(RROUGH.GE.0.0001) GO TO 546
      IF(RROUGH.GE.0.00005) GO TO 547
 547  THTH=((RROUGH-0.001)/0.004)*0.115+0.915
      IF(REX.LT.1800000.) GO TO 548
      TOTR=THTH
      GO TO 333
 546  THTH=((RROUGH-0.001)/0.004)*0.36+1.03
      IF(REX.LT.900000.) GO TO 548
      TOTR=THTH
      GO TO 333
 545  THTH=((RROUGH-0.001)/0.004)*0.58+1.39
      IF(REX.LT.108000.) GO TO 548
      TOTR=THTH
      GO TO 333
 544  THTH=((RROUGH-0..001)/0.004)*2.33+1.97
      IF(REX.LT.90000.) GO TO 548
      TOTR=THTH
      GO TO 333
 111  IF(REX.LT.18000.) TOTR=10.0*REX**(-.166)
      IF(REX.GE.18000.) TOTR=4.3
 333  CONTINUE
C ---CORRECT HTE FOR REYNOLDS NUMBER---
      HOHR=2.29087*REX**(-0.06)
      DMT=DMT*TOTR
      HTE=HTE*HOHR
C ---CALCULATE PLM---
      AA=((2.*HTE)/(3.*HTE-1.))/((1.-DMT*SOL*HTE/DCOS(B2R))**3)
      PLM=2.*DMT*(SOL/DCOS(B2R))*((DCOS(B1R)/DCOS(B2R))**2)*AA
C ---CALCULATE SHOCK LOSS---
      PLS=(PO1/(PO1-P1))*((2*SOL*LER/CORD*DCOS(BIM))*(1.28(MIN-
     11.)+0.96(MIN-1.)**2))
      PLM=PLM+PLS
C     CORRECT B1* FOR MACH NO
      IF(MIN.LE.0.7) GO TO 10
      DB=10.*MIN-7.
```

```
      BIM=BIM+DB
   10 CONTINUE
C
C*************************************************************************
C********************** OFF-DESIGN  DEVIATION ****************************
C*************************************************************************
C
      GO TO (485,486,487,488),KOUT
  485 CONTINUE
C
C ---LIEBLEINS OFF-DESIGN DEVIATION CORRELATION---
C -------CORRECT FOR AXIAL VELOCITY VARIATION AND SLOPE(MOFFAT)---
      B1E=B1M/DCOS(ALPA*DEG)
      VRAT=WM2/WM1
      B1E=DATAN(2.*DTAN(B1E*DEG)/(1.+VRAT))/DEG
      DBDI=0.4805+(0.00407-0.000138*B1E)*B1E+(0.698+(-0.005+
     10.000151*B1E)*B1E)*SOL+(-0.226+(0.00152-0.431E-4*B1E)*B1E)*SOL**2
      ZI=ACIN-AIN
      B2E=BET1-(DELBM+DBDI*ZI)
      BET2=DATAN(0.5*(1.+1./VRAT)*DTAN(B2E*DEG*DCOS(ALPA*DEG)))/DEG
      GO TO 489
  486 CONTINUE
C
C ---SWANS OFF-DESIGN DEVIATION CORRELATION---
      BET2=DEVM+(KAP1-CAM)
      KNT=1
  250 CONTINUE
      B2=BET2*DEG
      VRM=1.12+AK3+0.61*DCOS(B1)**2*(DTAN(B1)-AK1*DTAN(B2)-AK2)/SOL
      V1V2=PH1*DCOS(B2)/(PH2*DCOS(B1))
      DEQ=VRM*V1V2
C
C ------------IF FLOW SEPARATES,USE A LIMITING VALUE OF DEQ---
      IF(DEQ.GT.2.2) DEQ=2.2
      DIFF=DEQ-DEQM
      AM=MIN
      IF(AM.LT.0.65) AM=0.65
      DF=(6.4-9.45*(AM-0.6))*DIFF
      DEV=DF+DEVM
      BET2=DEV+(KAP1-CAM)
      IF(KNT.EQ.2) GO TO 260
      KNT=KNT+1
      B2=BET2*DEG
      GO TO 250
  260 CONTINUE
      GO TO 489
  487 CONTINUE
C
C ---CREVELINGS OFF-DESIGN DEVIATION CORRELATION---
      X=(ACIN-AIN)/DELBM
      IF(X.GE.0.0) F=0.809E-3+(.5588-.2928*X)*X
      IF(X.LT.0.0) F=0.1191E-3+(.48+0.3452*X)*X
      DEV=DELBM*F+DEVM
      BET2=DEV+KAP1-CAM
      GO TO 489
  488 CONTINUE
C
C ---HOWELLS OFF-DESIGN DEVIATION CORRELATION --
      X=(ACIN-AIN)/DELBM
      F1=1.36
```

```
      IF(X.LT.0.0) F1=0.35
      F=1.0+0.86*X-F1*X**2
      BET2=-DELBM*F+BET1
      DEV=BET2-KAP1+CAM
 489  CONTINUE
      COB1=DCOS(B1)
      TAB1=DTAN(B1)
      B2=BET2*DEG
      COB2=DCOS(B2)
      TAB2=DTAN(B2)
      DEV=BET2-(KAP1-CAM)
C
C*****************************************************************
C***************** OFF-DESIGN LOSS COEFFICIENT *******************
C*****************************************************************
C
C ---THE NEW OFF-DESIGN LOSS CORRELATION---
      AX=ACIN-AIN
      GO TO (450,500) KSER
  450 IF(MIN.LT.0.56) GO TO 451
      IF(AX.LT.0.) AEX=0.05336*MIN-0.02937
      GO TO 452
  451 AEX=0.
  452 IF(AX.GE.0.) AEX=0.00500*MIN-0.00075
      GO TO 550
  500 IF(MIN.LT.0.62) GO TO 501
      IF(AX.LT.0.) AEX=0.02845*MIN-0.01741
      GO TO 502
  501 AEX=0.
  502 IF(AX.GE.0.) AEX=0.00363*MIN-0.00065
  550 PLOD=AEX*AX**2+PLM
C
      RETURN
      END
C
C-------- SUBROUTINE INTERP INTERPOLATES THE PARAMETERS --------
C
      SUBROUTINE INTERP(PSI,PROP,PSIX,PROPX,NYY)
      IMPLICIT REAL*8(A-H,O-Z)
      DIMENSION PSI(NYY),PROP(NYY)
      NYNY=NYY-1
    1 IF(PSIX.LT.PSI(1)) GO TO 3
      IF(PSIX.GT.PSI(NYY)) GO TO 4
      DO 5 I=1,NYNY
      IF(PSIX.GE.PSI(I).AND.PSIX.LE.PSI(I+1)) GO TO 6
    5 CONTINUE
    3 PROPX=PROP(1)
      RETURN
    4 PROPX=PROP(NYY)
      RETURN
    6 PROPX=(PSIX-PSI(I+1))/(PSI(I)-PSI(I+1))*PROP(I)
      PROPX=PROPX+(PSIX-PSI(I))/(PSI(I+1)-PSI(I))*PROP(I+1)
      RETURN
      END
 F
```

AGARD
NATO OTAN
7 rue Ancelle · 92200 NEUILLY-SUR-SEINE
FRANCE
Telephone (1)47.38.57.00 · Telex 610 176

DISTRIBUTION OF UNCLASSIFIED AGARD PUBLICATIONS

AGARD does NOT hold stocks of AGARD publications at the above address for general distribution. Initial distribution of AGARD publications is made to AGARD Member Nations through the following National Distribution Centres.Further copies are sometimes available from these Centres, but if not may be purchased in Microfiche or Photocopy form from the Purchase Agencies listed below.

NATIONAL DISTRIBUTION CENTRES

BELGIUM
Coordonnateur AGARD — VSL
Etat-Major de la Force Aérienne
Quartier Reine Elisabeth
Rue d'Evere, 1140 Bruxelles

CANADA
Defence Scientific Information Services
Dept of National Defence
Ottawa, Ontario K1A 0K2

DENMARK
Danish Defence Research Board
Ved Idraetsparken 4
2100 Copenhagen Ø

FRANCE
O.N.E.R.A. (Direction)
29 Avenue de la Division Leclerc
92320 Châtillon

GERMANY
Fachinformationszentrum Energie,
Physik, Mathematik GmbH
Kernforschungszentrum
D-7514 Eggenstein-Leopoldshafen

GREECE
Hellenic Air Force General Staff
Research and Development Directorate
Holargos, Athens

ICELAND
Director of Aviation
c/o Flugrad
Reyjavik

ITALY
Aeronautica Militare
Ufficio del Delegato Nazionale all'AGARD
3 Piazzale Adenauer
00144 Roma/EUR

LUXEMBOURG
See Belgium

NETHERLANDS
Netherlands Delegation to AGARD
National Aerospace Laboratory, NLR
P.O. Box 126
2600 AC Delft

NORWAY
Norwegian Defence Research Establishment
Attn: Biblioteket
P.O. Box 25
N-2007 Kjeller

PORTUGAL
Portuguese National Coordinator to AGARD
Gabinete de Estudos e Programas
CLAFA
Base de Alfragide
Alfragide
2700 Amadora

TURKEY
Millî Savunma Bakanlığı
ARGE Daire Başkanlığı
Ankara

UNITED KINGDOM
Defence Research Information Centre
Kentigern House
65 Brown Street
Glasgow G2 8EX

UNITED STATES
National Aeronautics and Space Administration (NASA)
Langley Research Center
M/S 180
Hampton, Virginia 23665

THE UNITED STATES NATIONAL DISTRIBUTION CENTRE (NASA) DOES NOT HOLD STOCKS OF AGARD PUBLICATIONS, AND APPLICATIONS FOR COPIES SHOULD BE MADE DIRECT TO THE NATIONAL TECHNICAL INFORMATION SERVICE (NTIS) AT THE ADDRESS BELOW.

PURCHASE AGENCIES

National Technical
Information Service (NTIS)
5285 Port Royal Road
Springfield
Virginia 22161, USA

ESA/Information Retrieval Service
European Space Agency
10, rue Mario Nikis
75015 Paris, France

The British Library
Document Supply Division
Boston Spa, Wetherby
West Yorkshire LS23 7BQ
England

Requests for microfiche or photocopies of AGARD documents should include the AGARD serial number, title, author or editor, and publication date. Requests to NTIS should include the NASA accession report number. Full bibliographical references and abstracts of AGARD publications are given in the following journals:

Scientific and Technical Aerospace Reports (STAR)
published by NASA Scientific and Technical
Information Branch
NASA Headquarters (NIT-40)
Washington D.C. 20546, USA

Government Reports Announcements (GRA)
published by the National Technical
Information Services, Springfield
Virginia 22161, USA

Printed by Specialised Printing Services Limited
40 Chigwell Lane, Loughton, Essex IG10 3TZ

ISBN 92-835-0346-4